SOME DYNAMICAL PROBLEMS IN ELASTIC CONTINUA WITH MICROSTRUCTURES

A

Thesis

submitted in fulfillment of the requirement

for the award of degree

of

Doctor of Philosophy

in

Mathematics

Submitted by

Vikas Sharma

(Registration Number - 951211002)

SCHOOL OF MATHEMATICS

THAPAR UNIVERSITY, PATIALA-147004

PUNJAB, INDIA

May, 2016

DEDICATED TO

GOD

&

MY FAMILY

CERTIFICATE

This is to certify that the work presented in the thesis entitled, "***Some Dynamical Problems in Elastic Continua with Microstructures***", submitted by Mr. Vikas Sharma in the fulfillment of the requirement for the award of the degree of Doctor of Philosophy in School of Mathematics, Thapar University, Patiala, is a record of candidate's own work carried out by him under my supervision and guidance.

The matter presented in this thesis has not been submitted in part or full for the award of any degree in any other university or institute.

Attestation by supervisor

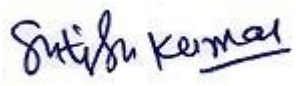

Dr. Satish Kumar

Assistant Professor,

School of Mathematics,

Thapar University,

Patiala, Punjab

India

DECLARATION

I hereby declare that the research work presented in this thesis entitled, "***Some Dynamical Problems in Elastic Continua with Microstructures***", submitted for the award of the degree of Doctor of Philosophy in School of Mathematics, Thapar University, Patiala is an authenticated record of my own research work carried out under the supervision of Dr. Satish Kumar (School of Mathematics) and refers other researcher's work are duly listed in the bibliography section.

The matter embodied in this thesis has not been submitted in part or full to any other university or institute for the award of any degree.

Vikas Sharma

Attestation by supervisor

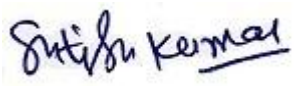

Dr. Satish Kumar

Assistant Professor,

School of Mathematics,

Thapar University,

Patiala, Punjab

India

ACKNOWLEDGEMENTS

Firstly, I would like to express my deepest gratitude to my Ph.D. supervisor, Dr. Satish Kumar, Assistant Professor, school of mathematics, Thapar university, Patiala (India) for giving me a chance to work under his guidance. He has been a constant source of support and encouragement throughout my Ph.D. work. I would not have been able to complete this research work without his constant guidance and cooperation.

I am highly thankful to Dr. A.K. Lal, head of the school of mathematics, for giving constant motivation and valuable inputs, especially during presentations of progress reports of the research work. I want to thank Dr. S.S. Bhatia, dean of academic affairs and former head of the school (SMCA), Thapar University, who gave me opportunity to start my research work during his tenure as head of the school and for always encouraging me at different phases of my research work. I also want to thank Dr. Rajesh Kumar, former head of the school (SMCA) for their cooperation and help during this research work. I also impart my thanks to Dr. Parkash Gopalan, Director, Thapar university, for providing necessary infrastructure and resources to accomplish my research work. I am also indebted to Dr. O.P. Pandey, dean of research and sponsored project, for his never ending motivation that was of immense value in the completion of this thesis. I want to express my gratitude to Late Dr. J.N. Sharma for their valuable inputs in the initial phase of my research work. Finally I want to thank whole faculty, administrative and technical staff of school of mathematics, Thapar university for their cooperation.

I also want to thank my colleagues and friends working in department of mathematics, Lovely Professional University, Phagwara, Punjab (India) who always supported me during my research work.

I sincerely want to thank my parents for providing me moral support throughout my life. It would not have been possible for me to reach this goal without their blessings and good wishes. I also want to thank my younger brother and my elder sister for always being supportive and for encouraging me. Finally at last but not the least, I want to thank my wife Smt. Jeevan Jyoti for her cooperation, patience and support during this whole period of research work. I want to apologies to my two daughters Sanvi and Amaira for missing few memorable moments of their life due to my constant engagement in this project for the past few years.

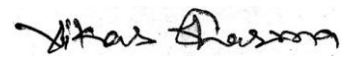

Date: **Vikas Sharma**

ABSTRACT

Chapter 1 contains the introduction of basic laws of classical theory of elasticity, short comings of classical elasticity and evolution of microcontinuum theories including consistent couple stress theory. Basic governing equation of motion and constitutive relations of couple stress theory are given in this chapter. It also contains discussion on various types of waves in elastic medium like body and surface waves, including their literature. Basics of viscoelastic materials with their applications are also discussed in this chapter.

Chapter 2 deals with the propagation of Lamb waves in a stress/couple stress free elastic plate. Profiles of Lamb waves are studied using consistent couple stress theory to capture the effects of a microstructural parameter called characteristic length involved in the theory. The governing equation of motion of couple stress theory and constitutive relations involving stresses and couple stresses are solved using various boundary conditions to find dispersion relation of Lamb waves propagating in a plate. Effects of varying characteristic length as compared to cell size have been observed. Phase velocity profiles for different Lamb wave modes are modified under the effect of couple stress theory. Results obtained under couple stress theory are compared graphically with the results of classical theory of elasticity. Since bones have an internal microstructure, so the study has been carried out for a cortical bone type material and this work will be quite useful for evaluation of characteristics of bones and the material exhibiting microstructures. This study may also find possible applications in the fields of non destructive testing techniques.

Chapter 3 is an extension of chapter 2 and it contains the study of propagation of Lamb waves in a plate with internal microstructure and loaded with an inviscid liquid on both sides using consistent couple stress theory. Lamb waves are guided waves, propagating in a traction free plate surface, however if the surface of the plate is in contact with the fluid or liquid, a part of energy will leak into the liquid. The dynamical characteristics of a structure get affected when it is surrounded by a fluid or liquid. Dispersion equation of Lamb waves propagating in an elastic plate loaded with a layer of an inviscid liquid of finite thickness is derived. The impact of liquid loadings is studied on the propagation of Lamb waves. Effect of

characteristic length (l) is also studied on the phase velocity of Lamb waves in plate for various modes in the presence of liquid loadings. Three different cases for the thickness of liquid loaded on both side of the plate are considered. It is observed that with the increase in the thickness of the loadings the phase velocity tends to decrease. Here, three different values of characteristic length are considered, which are comparable with the internal cell size of the material and their effect is studied on the phase velocity of the Lamb waves. It is observed that with the increase in the value of this parameter the phase velocity of Lamb wave also increases. The considered solid plate has material properties similar to cortical bone, so it also enhances the applicability of this model in the characterisation of the properties of bones loaded with different type of fluids. As the physical model of the problem consists of thin plate loaded with inviscid liquid on both sides, it is of practical use in ultrasonic immersion testing of plates.

Chapter 4 contains investigation of propagation of shear horizontal wave (SH) in a layered structure. The propagation of SH waves is studied in viscoelastic layer overlying a couple stress elastic half space. As theory of seismic wave propagation was developed within the frame work of linear elasticity, but later developments showed that earth should be more correctly regarded as a dissipative medium. To encounter dissipation of energy considerations and to overcome the shortcomings of linear elasticity the near sub surface of earth is modelled as linearly viscoelastic material. The geological evidence of heterogeneity within the earth are provided by the wide variations of rocks erupted from volcanoes. The scattering of high frequency seismic waves also support the existence of small scale heterogeneity in the earth lithosphere. Hence, for characterising the internal microstructure of solid earth, heterogeneity and viscoelasticity of the material composition of the earth subsurface has to be taken into account. In this problem, we have investigated shear horizontal wave propagation in a layered structure, consisting of granular macromorphic rock (Dionysos Marble) substrate underlying a viscoelastic layer of finite thickness. Dionysos Marble is a white fine-grained metamorphic marble with a saccharoidal microstructure. SH wave characteristics are affected by the material properties of both underlying substrate and the coating. Dispersion equation for propagation of SH waves using consistent couple stress theory is derived. The effects of microstructural parameter characteristic length of the substrate, along with heterogeneity, internal friction and thickness of viscoelastic layer are studied on the dispersion curves. Real and damping phase velocities of SH waves are studied against dimensionless wave number,

for different combinations of various parameters involved in the problem and it is observed that these parameters have significant effects on the propagation of SH waves. The numerical results are also presented graphically for various combinations of parameters involved in the problem. The theoretical consideration of study concerning microstructural effects of the substrate and effects of other parameters of viscoelastic layer on propagation of SH waves, may find possible applications in seismology, exploration geophysics, non destructive testing techniques and in designing chemical and biochemical sensors coated with surface bound receptive layers possessing viscoelastic properties which are used to detect compounds in liquid or gases.

Chapter 5 contains study of propagation of SH waves in viscoelastic layer over a couple stress substrate with imperfect bonding at the interface. This chapter is an extension of chapter 4, where we studied SH waves in a layered structure for a perfectly bonded interface between two media, but this condition is difficult to achieve. Due to many reasons like thermal mismatch or some faults in manufacturing process, cracks or defects may appear at the interface which leads to an imperfect interface between two media. Components of displacement field are not continuous at the common boundary of two media in case of imperfect interface. The difference in displacement fields is assumed to depend linearly upon traction vector. These imperfections at the common boundary may affect the propagation of SH waves. Dispersion equation of SH waves in a viscoelastic layer overlying a couple stress substrate with imperfect interface between them has been obtained. Dispersion equations for propagation of SH waves with perfectly bonded interface and slippage interface between two media are also obtained as particular cases. Effects of degree of imperfectness of the interface are studied on the phase velocity of SH waves. Dispersion curves are plotted and effects of material properties of both couple stress substrate and viscoelastic layer are studied. Effects of internal microstructures of couple stress substrate in terms of characteristic length of the material are presented. Effects of heterogeneity, friction parameter and thickness of viscoelastic layer are also studied on the propagation of SH waves. The numerical results are presented graphically. It is found that imperfectness factor at the interface between two media has a significant effect on the phase velocity of SH waves. It is observed that with the decreasing value of imperfectness at the interface, phase velocity of SH waves increases and phase velocity is highest when interface becomes perfectly bonded. In comparison to perfectly bonded interface model for SH waves, this model is more realistic and further the

consideration of microstructural effects on the propagation of SH waves, may provide possible applications in the fields of non-destructive testing, semiconductor industry, seismology or geomechanics engineering.

Chapter 6 contains study of leaky Rayleigh waves in a homogeneous isotropic elastic solid half space loaded with homogeneous inviscid liquid layer of finite thickness (H) or a liquid half-space. It is interesting to study the changes in the profiles of Rayleigh type waves when homogeneous elastic half space is loaded with liquid. This study becomes more application oriented when the material of half space exhibits internal microstructures. Equations of couple stress theory are solved and dispersion equations for the propagation of leaky Rayleigh waves in a homogeneous solid elastic half space loaded with liquid layer of finite thickness or liquid half space are obtained. As a special case, dispersion equation for propagation of Rayleigh waves in a stress free homogeneous solid elastic half space using consistent couple stress theory is also derived. Rayleigh type waves at the solid-liquid interface are found to be dispersive in this considered model. Phase velocity of leaky Rayleigh waves is studied for three different values of characteristic length (l) which are of the order of internal cell size of the material. It is found that with the increase in the characteristic length of the material, phase velocity of Rayleigh waves also increases. Effects of thickness of liquid layer are also studied. It is observed that phase velocity of Rayleigh waves decreases with the increase in thickness of liquid layer. The properties of leaky Rayleigh waves like velocity, dispersion are affected by both, loaded liquid and underlying solid half space. Material properties of underlying solid can be indirectly obtained by studying profiles of these leaky Rayleigh waves. The applications of these waves range from geophysics to non destructive testing of structures. Generally, most of the non destructive methods for the detection of defects are based on classical model, so this proposed model may provide modifications to these existing methods by considering the microstructural effects of the underlying half space.

Chapter 7 Seeing the importance of Rayleigh waves to the fields of geophysics and seismology, in this chapter we have extended our work to study the effects of gravity together with microstructures of substrate and liquid loadings on the propagation of leaky Rayleigh waves. We have solved the problem of propagation of leaky Rayleigh waves in a model consisting of couple stress half space loaded with inviscid liquid layer of finite thickness or a

liquid half space under the effects of gravity. Dispersion relations for leaky Rayleigh waves in couple stress half space loaded with inviscid liquid layer of finite thickness or a liquid half space under the effects of gravity are derived using consistent couple stress theory. The effects of gravity, thickness of liquid layer and characteristic length are studied on propagation of leaky Rayleigh waves.

LIST OF RESEARCH PAPERS PUBLISHED/COMMUNICATED

1. **Velocity dispersion in an elastic plate with microstructure: effects of characteristic length in a couple stress model.** *Meccanica* **49**:1083–1090, 2014. Impact factor-1.949

2. **Effects of liquid loadings on lamb waves in context of size dependent couple stress theory.** *Journal of Theoretical and Applied Mechanics* **53**(4):925-934, 2015. Impact factor-0.636

3. **Influence of microstructure, heterogeneity and internal friction on SH waves propagation in a viscoelastic layer overlying a couple stress substrate.** *Structural Engineering and Mechanics* **57**(4):703-716, 2016. Impact factor-0.927

4. **Dispersion of SH waves in a viscoelastic layer imperfectly bonded with a couple stress substrate.** *Communicated to SCI indexed journal.*

5. **Effects of microstructure and liquid loading on velocity dispersion of leaky Rayleigh waves at liquid solid interface.** *Communicated to SCI indexed journal.*

6. **Dispersion of Rayleigh waves in a microstructural couple stress substrate loaded with liquid layer under the effects of gravity.** *Communicated to SCI indexed journal.*

TABLE OF CONTENTS

LIST OF SYMBOLS

$\vec{u}$	Displacement vector
u_i	Displacement components
e_{ij}	Strain tensor
τ_{ij}	Stress tensor
λ, μ	Lamé constants
δ_{ij}	Kronecker's delta
μ_{ji}	Couple stress tensor
ε_{ijk}	Permutation tensor
η	Couple stress coefficient
l	Characteristic length
ρ	Density
C_1	Longitudinal wave velocity
C_2	Shear wave velocity
$\phi, \vec{\psi}$	Scalar and vector potential functions
ξ	Wave number
ω	Frequency
ξ_L, ξ_T	Wave numbers of longitudinal and shear waves
V_L, V_T	Phase velocity of longitudinal and shear waves
c	Phase velocity
$u'_j,\ w'_j$	x and z components of displacement in liquid layers
ϕ_j, ψ_j	Potential functions for liquid layers
σ'_{ji}	Stress tensor for liquid layers
C_L	Velocity of sound in the liquid
λ_L	Bulk modulus for liquid layer
ρ_L	Density of inviscid liquid
P_{xy}, P_{yz}	Components of stress tensor for viscoelastic layer
ρ_1, ρ_o	Density of viscoelastic layer
β_1	Phase velocity in viscoelastic material
H	Width of liquid or viscoelastic layer

G	Measure of degree of imperfectness at the interface of two media
g	Acceleration due to Gravity
NDT	Non destructive techniques

LIST OF FIGURES

LIST OF TABLES

CHAPTER-1

INTRODUCTION

1.1 PRELIMINARIES

All materials to some extent possess the property of elasticity, by the virtue of which materials regain their shape and size after the removal of applied external forces. Deformation in the materials disappears with the removal of external forces only when external forces producing deformation do not exceed a certain limit. Depending on this property of the materials, they can be classified as *rigid, elastic and plastic*. *Rigid* bodies are those which do not deform under the application of external force and *plastic* bodies are those which never regain their original shape and size after the removal of external forces. Elasticity is a branch which deals with the determination of stress, strain and finding displacement distribution in materials under the influence of applied external forces. Theory of elasticity develops a mathematical model involving partial differential equations for a problem of deformation of an elastic material, using various principles of classical continuum mechanics. These mathematical formulations of the problem are further solved using various techniques by imposing the given initial or boundary conditions. Various methods which are used to solve mathematical model of a deformation problem in theory of elasticity are Potential method, Integral transform method, Complex variable method, Variational method and Numerical methods etc. The solution of mathematical model of the problem of theory of elasticity finds various applications in many scientific and engineering fields. Civil engineering applications include contribution of stress in deflection analysis of structures like rods, shells and plates. Mechanical engineering uses elasticity in analysis and design of machine elements. Such applications include general stress analysis, contact stresses, thermal stress analysis, fracture analysis and fatigue. Material engineering uses elasticity to determine stress fields in crystalline solids, around dislocations and in materials with microstructure. Applications in aeronautical and aerospace engineering include finding stresses, fracture and fatigue in aerostructures. Wave propagation in elastic solids also finds immense applications in science and industry. In the area of structures, for example, the interest is mainly in the response to impact or blast loads. Under transient loads of moderate strength, complete elastic conditions may prevail throughout the structure and elastic wave theory may suffice to predict all aspects of the response. There are numerous applications of these waves in the area of mining, where blasting is used to produce stress waves in the rocks. These shock waves are

used to fracture and for the removal of heavy rocks. In seismology, earth is treated as an elastic solid, so it also uses wave propagation to predict and analyse earthquakes. Whatever information we have about the constitution of earth's interior is because of studies of seismic waves. The division of earth's interior into crust, mantle and core and now treating it as inhomogeneous is all due to studies carried out about seismic waves. Ultrasonic is another major area of application of wave propagation. Lamb waves are used to inspect many industrial products in aerospace and transportation. Fundamental properties and defects in the materials can be investigated by using the technique of ultrasonic. These waves are extremely useful for detection of cracks, corrosion and other defects in materials using non destructive testing techniques.

1.2 BASIC CONCEPTS OF CLASSICAL THEORY OF ELASTICITY

For investigating an elastic problem completely, we need relation between stress and strain components called constitutive relations, certain laws of balance and initial or boundary conditions. Here, we briefly represent the basic concepts for classical theory of elasticity. A material is said to be strained under the application of applied external forces if relative position of the particles in the medium are changed and when change in the position of the particles is accompanied by change in distance between them, it is called *deformation. Strain* actually is the measure of deformation in the material. Consider a continuum medium with volume V and surface S which undergoes deformation.

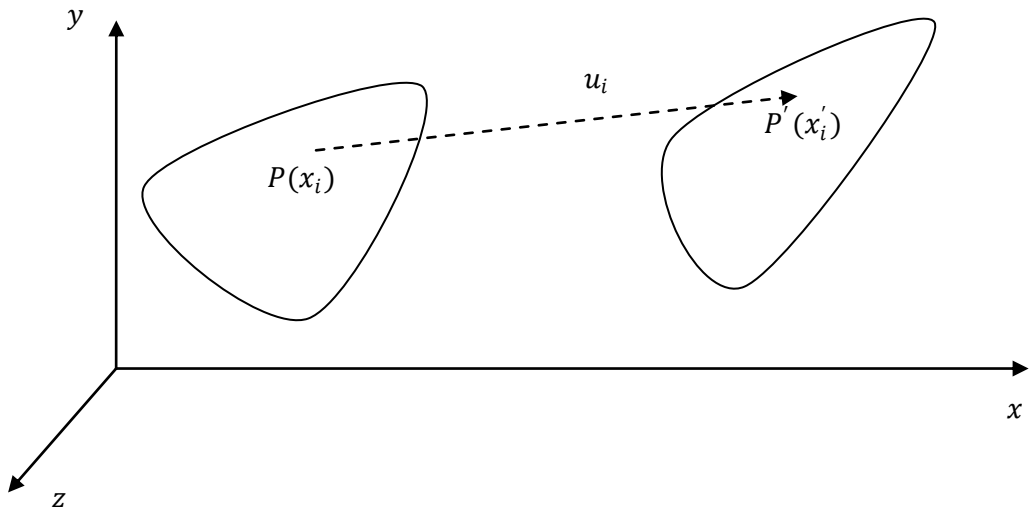

Figure 1.1 Deformation of an elastic body

Let a particle in the medium changes its position under deformation from $P(x_1, x_2, x_3)$ to $P'(x_1', x_2', x_3')$ and let the displacement of P to P' is measured by $u_i(x_1, x_2, x_3) = x_i' - x_i$ where $i = 1, 2, 3$, where u_1, u_2, u_3 represents displacement components. Infinitesimal deformation or strain in the medium is defined as $e_{ij} = \frac{1}{2}(u_{i,j} + u_{j,i}) = \frac{1}{2}\left(\frac{\partial u_i}{\partial x_j} + \frac{\partial u_j}{\partial x_i}\right)$, where $i, j = 1, 2, 3$ and here e_{ij} are called components of symmetric strain tensor.

Stress is the force on unit area within a material, which develops as a result of the externally applied forces. Consider an elementary surface area dS in the continuum with normal to the surface is v_i and $T_i^v dS$ be stress vector acting on the elementary area for defining transfer of interaction between two particles on the elementary area. Here T_i^v represents force traction vector which is defined in terms of symmetric stress tensor τ_{ij} as $T_i^v = \tau_{ij} v_j$ and τ_{ij} completely characterise the state of stress in the neighbourhood of point P. Here in τ_{ij} the first subscript (i), represents the direction of normal to the plane under consideration and second subscript (j) specifies the direction of components stress vector T_i^v. Figure 1.2, shows the components of stress tensor acting on a small rectangular parallelepiped.

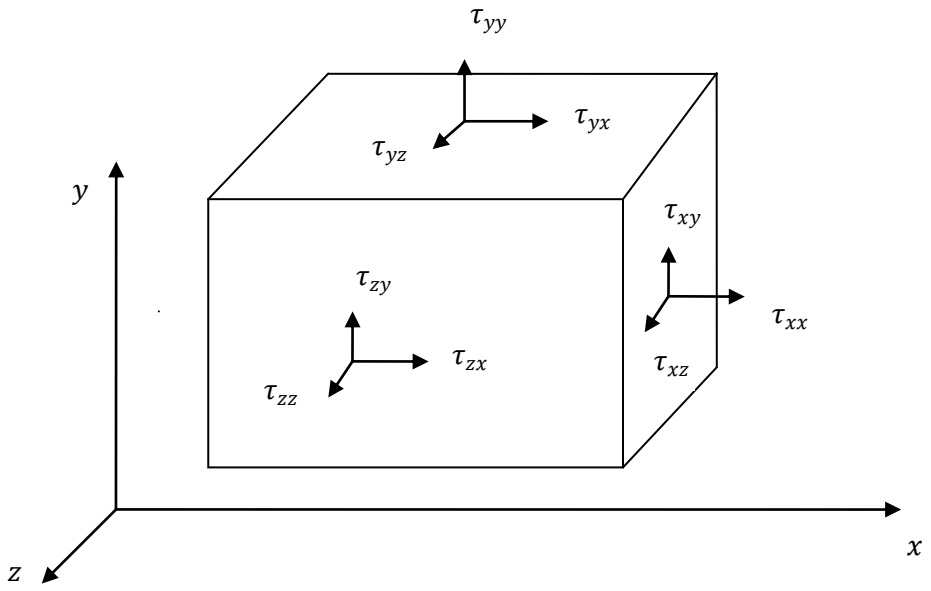

Figure 1.2 Components of force stress tensor in classical theory of elasticity

Robert Hooke in 1660 gave the famous law of proportionality between stress and strain acting at a point on the body due to the presence of external forces. It states that stress is directly proportional to the strain upto certain limits of the material called elastic limits.

Mathematically, it is written as $\tau_{ij} = C_{ijkl}\, e_{kl}$ where $i, j, k, l = 1, 2, 3$ and τ_{ij} is the stress tensor, e_{kl} is the strain tensor. Both stress and strain tensors have 9 components and C_{ijkl} is the fourth order coefficient tensor and these are called *elastic constants*. In the most general case, there are 81 elastic constants. Since, both stress and strain tensors are symmetric in classical elasticity, so by imposing these conditions elastic constants are reduced to 36. If we assume the system to be adiabatic or isothermal, we get $C_{ijkl} = C_{klij}$ and it further leads to the reduction of elastic constants from 36 to 21. In general, material possesses certain symmetries in their internal structure and if we assume the material to be symmetric with respect to one of the plane, elastic constants are reduced to 13 and they are further reduced to 9, by assuming the material to be symmetric with respect to two planes called *orthotropic* materials. If we further assume the material to be *transversely isotropic*, a material which possesses the axis of symmetry in the sense that all rays of light at right angle to this axis are equivalent, we are left with 5 elastic constants. Finally, for $isotropic$ materials properties are same in all directions. Elastic properties in *isotropic* materials are independent of the orientation of axes of coordinates. These materials possess a rotational symmetry with respect to two perpendicular axes. In this case, elastic constants are reduced to two and Hooke's law becomes

$$\tau_{ij} = \lambda \delta_{ij}\, e_{kk} + 2\mu e_{ij} \tag{1.2.1}$$

Eq. (1.2.1) is called constitutive relation which defines relation between state of stress and the state of strain, where i, j, k =1, 2, 3.

where $\delta_{ij} = \begin{cases} 1 & , \quad if \quad i = j \\ 0 & , \quad if \quad i \neq j \end{cases}$ is called Kronecker's delta.

λ, μ are two elastic constants called Lame constants. Here, μ is called shear modulus and is defined as ratio of the shearing stress to the change in angle produced by shearing stress also called *modulus of rigidity*. We can further define few standard material elastic constants which are combination of λ, μ as

$Poisson\, ratio -$ It is defined as the ratio of contraction of linear elements perpendicular to the axis of cylinder to the longitudinal extension of the rod and is denoted by $\nu = \frac{\lambda}{2(\lambda+\mu)}$

$Young's\, Modulus -$ It is the ratio of tensile stress to extension produced the by the tensile stress and is represented as $E = \frac{\mu(3\lambda+2\mu)}{(\lambda+\mu)}$.

$Bulk\ modulus -$ It is the ratio of compressive stress to the cubical compression and is denoted as $k = \frac{(3\lambda+2\mu)}{3}$

For a continuum medium occupying volume V and bounded by a closed surface S to be in equilibrium, the resultant forces acting on the material within V should vanish. In that case equation of equilibrium for classical theory of elasticity is given by $\tau_{ij\,,j} = -F_i$ where F_i are the components of body forces and $\tau_{ij\,,j} = \frac{\partial \tau_{ij}}{\partial x_j}$ represents first order partial derivatives. By using stress-strain relation $\tau_{ij} = \lambda\delta_{ij}\, e_{kk} + 2\mu e_{ij}$ in equation of equilibrium, we get

$$\mu u_{i,jj} + (\lambda + \mu) u_{j\,,ji} + F_i = 0 \tag{1.2.2}$$

where u_i are the displacement components and this equation in vector form can be written as

$$\mu\nabla^2\vec{u} + (\lambda + \mu)\nabla(\nabla.\vec{u}) + \vec{F} = 0 \tag{1.2.3}$$

where

$$\nabla = \hat{\imath}\frac{\partial}{\partial x} + \hat{\jmath}\frac{\partial}{\partial y} + \hat{k}\frac{\partial}{\partial z}$$

$$\nabla^2 = \frac{\partial^2}{\partial x^2} + \frac{\partial^2}{\partial y^2} + \frac{\partial^2}{\partial z^2}$$

If ρ is the density of the continuum medium, then the components of force of inertia acting on mass contained in elementary volume dV are $-\rho\frac{\partial^2 u_i}{\partial t^2}dV, 1 \le i \le 3$ and hence to get total forces acting on the continuum medium, we add components of body force F_i and components of force of inertia per unit volume. Hence, from equation of equilibrium defined in Eq. (1.2.2), we get equation of motion for an isotropic elastic solid as

$$\mu u_{i,jj} + (\lambda + \mu) u_{j\,,ji} + F_i = \rho\ddot{u}_i \tag{1.2.4}$$

where $\ddot{u}_i = \frac{\partial^2 u_i}{\partial t^2}$, Eq.(1.2.4) in vector form becomes

$$\mu\nabla^2\vec{u} + (\lambda + \mu)\nabla(\nabla.\vec{u}) + \vec{F} = \rho\frac{\partial^2\vec{u}}{\partial t^2} \tag{1.2.5}$$

1.3 COUPLE STRESS THEORY

The results given by classical model of elasticity (Cauchy [15]) is in agreement with the experimental outcomes, performed on materials like steel, aluminium etc., when internal stresses do not exceed the elastic limits of material. In classical theory of elasticity atomic structure of the material is not considered. It is based on the assumptions that all materials are homogeneous and are continuously distributed over its volume without any kind of defects, so that even the smallest particle of the material possess same physical properties as the whole material. It is also assumed that a point particle is represented by a geometrical point which is infinitesimal in size without any internal structure. There are many materials like particulate composites, polymers and cellular solids which do not satisfy above said assumptions. Classical theory of elasticity does not consist any length scale parameters which account for internal microstructures of the material. It is now, a well known fact that materials do behave differently at microscale as compared to their behaviour at macroscale. Even steel which is assumed to be homogeneous when studied at the microscopic level is observed to have crystals of various sizes arranged in different orientation and hence is far from being a homogeneous material. Although, classical elasticity can very well explain the behaviour of steel within the elastic limits and reason for this is that there are millions of crystals even in a very small piece of steel. If geometrical dimensions of the material are larger in comparison to dimensions of crystals defining internal structure of the material, assumptions of homogeneity can be applied. Classical theory of elasticity is unable to explain the stress concentrations at holes and cracks in the material. It cannot explain the dispersive nature of the certain type of waves in elastic media. There are many materials like polymers, fibrous and composites where experimental results deviate from the findings predicted by classical theory of elasticity. Many materials have heterogeneous microstructures which play a dominant role in determining physical properties of the material at macroscale and also how material behaves to the applied external forces. This has generated considerable interest in micro mechanical modelling of the materials. Materials which exhibit this type of behaviour include granular materials, particulate composites, soil, rocks etc. These materials have internal microstructures which ranges from nanometres to micrometres and those cases are of interest where these internal microstructures are comparable with the other characteristic lengths involved in the problem. Classical theory of elasticity has limited scope to predict the behaviour of such materials, so these short comings of classical theory has led to the

development of new micromechanical theories of solids which accounts for microstructure of the material and are called microcontinuum theories.

Voigt [143] was the first who gave an idea that interaction between two parts of the continuum not only depends upon force stress vector but also on the couple stress vector. However, Cosserat and Cosserat [22] gave the mathematical formulation to analyse materials with couple stresses, by considering that the deformation of the medium is described by displacement vector and an independent rotation vector. Displacements and rotations are associated with non symmetric stresses and couple stresses through constitutive relations. This was contrary to the classical theory which described stress as symmetric tensor. In classical theory of elasticity material particles have only three displacement degrees of freedom, whereas Cosserat model describe three additional degrees of freedom related to the rotation of particle. This idea of Cosserat brothers did not receive much attention at that time and after almost fifty years Cosserat theory was reworked by many researchers (Toupin [133], Mindlin and Tiersten [87], Koiter [58], Eringen [30], Nowacki [92]), but instead of taking rotation as independent of displacement field, it was considered to be compatible with the displacement. In literature, Toupin's [134] theory was called 'Cosserat theory with constrained rotation', Koiter's [58] theory was called 'Couple stress theory', Mindlin theory [83], Mindlin and Eshel [86] was called strain gradient theory, Eringen's [31] theory was called 'Indeterminate couple stress theory', Nowacki's [92] theory was called 'Cosserat pseudo-continuum theory'.

These theories do have certain drawbacks like indeterminacy of the spherical part of the couple-stress tensor and inclusion of the body couple in the constitutive relation for the force stress tensor was also disturbing. These theories have been referred to as inconsistent or indeterminate couple stress theories. Classical theory of elasticity was extended by adding additional degrees of freedom which accounts for deformation of the microstructure of the material and these additional degrees of freedom are independent of existing degrees of freedom of displacement field. In micromorphic theory (Eringen and Suhubi [33], Eringen [32]), a material point possesses three deformable directors that give nine additional degrees of freedom and these are dimensionless quantities. This corresponds to rotation and deformation of a 'micro-element' embedded in the continuum which is independent of the local deformation of the 'macro-element'. In case of the micropolar continuum theory (Eringen [30]), there are three degrees of freedom in addition to the three degrees of freedom for displacement field and directors are assumed to be rigid. If macromotion of the particle

and the micromotion of its inner structure are not distinguished, micropolar theory reduces to couple stress theory.

The couple stress theory of elasticity was developed to describe the size dependent effects of material and many researchers used couple stress theory to study various types of problems. Mindlin [83] studied influence of couple stresses on stress concentration. Yang and Lakes [150] did experimental study of micropolar and couple stress elasticity on compact bone in bending. Lubarda and Markenscoff [80] derived general conservation laws for couple stress theory. They have also discussed the relationship of derived path integrals with other similar quantities of couple stress theory. Bardet and Vardoulakis [5] discussed the importance of couple stresses in granular medium. Yang *et al*. [149] have developed a modified couple stress theory in which, strain energy has been shown to be a quadratic function of the strains (which are symmetric), the symmetric curvatures and only a single material length scale parameter is involved. Yang *et al*. [149] tried to simplify couple stress theory, but it also carries few problems like spherical part of couple stress tensor is indeterminate and they assumed couple stress tensor to be symmetric based on an artificial law of equilibrium of moment of couples and even the boundary conditions assumed were inconsistent. Lubarda [79] used the couple stress theory to study an anti plane strain problem of circular inclusions. Akgoz and Civalek [3] has analysed micro sized plates resting on elastic medium using modified couple stress theory. They derived equations for bending, buckling and vibration using Hamilton's principles and also discussed the effect of length scale parameter on these properties.

Hadjesfandiari and Dargush [46] have proposed consistent couple stress theory by considering true continuum kinematical displacement and rotation. In this theory, it is shown that the couple stress tensor is skew symmetric and the skew symmetric part of the gradient of the rotation tensor is the consistent curvature tensor. They also showed that displacement field and its corresponding rotation field are the only degrees of freedom at each point. This means that the rigid body motion of each infinitesimal element of material at any point of the continuum is described by six degrees of freedom, out of which three are translational and other three are rotational. With these mentioned assumptions they have tried to remove the difficulties which are there in the existing continuum theories. It is also shown that for isotropic material the two Lame parameters λ, μ and one length scale parameter η can completely characterise the behaviour of material. η is a length scale parameter which accounts for couple stress effects for isotropic solids and evaluation of η requires the

knowledge of characteristic material length parameter l, which was absent in Cauchy elasticity. Hadjesfandiari and Dargush ([47], [48]) further gave boundary element formulation for plane problems in couple stress elasticity and they also derived fundamental solutions for two and three dimensional isotropic size-dependent couple stress elasticity, using decomposition of displacement field into dilatational and solenoidal components. One of the major problem in these size dependent elastic theories (Cosseret [22]), micropolar (Eringen [30], [31]) and couple stress (Toupin [133]; Mindlin and Tiersten [87]; Koiter [58]) is determination of these length scale parameters. It was observed (Lakes [67]) that characteristic length would be undetectable in any macroscopic mechanical experiment, but have relevance in studies involving composite and cellular solids. In fibrous composites, the characteristic length may be of the order of spacing between fibres. In cellular solids it may be comparable to the average cell size of the material.

1.3.1 *Basic stresses and equilibrium equations of consistent couple stress theory* **(**Hadjesfandiari and Dargush [46]**)**

Consider a continuum material with volume V which is bounded by surface S. Consider an elementary surface area dS in the continuum with unit normal to the surface as v_i and $T_i^v dS$ be stress vector and $M_i^v dS$ be the moment vector acting on the elementary area for defining transfer of interaction between two particles on the elementary area. Here T_i^v represents force traction vector and M_i^v represents moment traction vector which are defined in terms of non-symmetric stresses σ_{ji} and couple stresses μ_{ji} as

$$T_i^v = \sigma_{ji} v_j \tag{1.3.1.1}$$

$$M_i^v = \mu_{ji} v_j \tag{1.3.1.2}$$

Stress tensor σ_{ji} and couple stress tensor μ_{ji} can be written as a sum of symmetric and skew symmetric parts as

$$\sigma_{ji} = \sigma^S{}_{ji} + \sigma^A{}_{ji} \tag{1.3.1.3}$$

$$\mu_{ji} = \mu^S{}_{ji} + \mu^A{}_{ji} \tag{1.3.1.4}$$

Here $\sigma^S{}_{ji}$ and $\mu^S{}_{ji}$ represent symmetric part of stresses and couple stresses and $\sigma^A{}_{ji}$ and $\mu^A{}_{ji}$ represent skew symmetric part of stresses and couple stresses.

Now using linear and angular balance equations, we get

$$\int T_i^v dS + \int F_i dV = 0 \tag{1.3.1.5}$$

$$\int \left[\varepsilon_{ijk}\, x_j T_k^v + M_i^v\right] dS + \int \left[\varepsilon_{ijk}\, x_j F_k + H_i\right] dV = 0 \tag{1.3.1.6}$$

Here F_i are the body forces and H_i are the body couple per unit volume. ε_{ijk} is the permutation tensor and its value is zero, when any two subscripts of i, j, k are equal and the value is 1 if i, j, k are in cyclic permutation of 1, 2, 3 and otherwise it is -1.

By using the values of T_i^v, M_i^v in above equations, we get

$$\int \sigma_{ji}\, v_j\, dS + \int F_i dV = 0 \tag{1.3.1.7}$$

$$\int \left[\varepsilon_{ijk}\, x_j \sigma_{lk}\, v_l + \mu_{li}\, v_l\right] dS + \int \left[\varepsilon_{ijk}\, x_j F_k + H_i\right] dV = 0 \tag{1.3.1.8}$$

Now, by using divergence theorem we get

$$\int \sigma_{ji,j}\, dV + \int F_i dV = \int \left(\sigma_{ji,j} + F_i\right) dV = 0 \tag{1.3.1.9}$$

$$\int \left[\varepsilon_{ijk} \left(x_j \sigma_{lk}\right)_{,l} + \mu_{li,l}\right] dV + \int \left[\varepsilon_{ijk}\, x_j F_k + H_i\right] dV = 0 \tag{1.3.1.10}$$

Here commas represent derivatives with respect to spatial coordinates. Solving these equations further we get equilibrium equations of couple stress theory as

$$\sigma_{ji,j} + F_i = 0 \tag{1.3.1.11}$$

$$\mu_{ji,j} + \varepsilon_{ijk}\, \sigma_{jk} + H_i = 0 \tag{1.3.1.12}$$

Let us consider two neighbouring points in a continuum as Q and Q' with position vectors as x_i and $x_i + dx_i$. The relative displacement vector of Q' with Q is given by

$$du_i = u_{i,j}\, dx_j \tag{1.3.1.14}$$

Here u_i are the displacement components and $u_{i,j} = \frac{\partial u_i}{\partial x_j}$ is the gradient of displacement field and it can further decomposed as

$$u_{i,j} = \frac{1}{2}\left(u_{i,j} + u_{j,i}\right) + \frac{1}{2}\left(u_{i,j} - u_{j,i}\right) = e_{ij} + w_{ij} \tag{1.3.1.15}$$

Where

$$e_{ij} = \frac{1}{2}\left(u_{i,j} + u_{j,i}\right)$$

is the symmetric tensor that represents infinitesimal deformation strain.

$$w_{ij} = \frac{1}{2}\left(u_{i,j} - u_{j,i}\right)$$

is a skew symmetric tensor which represents rotational part.

The vector w_i which is dual to rotation tensor is

$$w_i = \frac{1}{2}\varepsilon_{ijk}\, w_{kj} = \frac{1}{2}\varepsilon_{ijk}\, u_{k,j} \tag{1.3.1.16}$$

For finding curvature of an arbitrary element dx_i in continuum, we consider relative rotation of the same neighbouring points Q and Q' as

$$dw_i = w_{i,j}\, dx_j \tag{1.3.1.17}$$

Here $w_{i,j}$ represents gradient of rotation vector and can be further written as

$$w_{i,j} = \frac{1}{2}\left(w_{i,j} + w_{j,i}\right) + \frac{1}{2}\left(w_{i,j} - w_{j,i}\right) = \psi_{ij} + \Upsilon_{ij} \tag{1.3.1.18}$$

Where

$$\psi_{ij} = \frac{1}{2}\left(w_{i,j} + w_{j,i}\right)$$

is symmetric tensor showing strain of the rotation vector.

$$\Upsilon_{ij} = \frac{1}{2}\left(w_{i,j} - w_{j,i}\right)$$

is skew symmetric tensor representing rotation of rotation vector.

ψ_{ij} is referred as torsion tensor and it is assumed that it will not act as a fundamental measure of deformation in a continuum. Υ_{ij} is the curvature tensor and curvature vector Υ_i dual to this tensor is defined as

$$\Upsilon_i = \frac{1}{2}\varepsilon_{ijk}\, \Upsilon_{kj} = \frac{1}{2}\varepsilon_{ijk}\, w_{k,j} \tag{1.3.1.19}$$

Now for the small deformation

$$\left|e_{ij}\right| \ll 1$$

$$|\Upsilon_i| \ll \frac{1}{L}$$

where L is the smallest characteristic length in the continuum.

Further using principal of virtual work, it is shown that for consistent couple stress theory, the body couple stress is not distinguishable from body force and hence, in couple stress theory only body forces should be considered. It is also established that normal surface moment traction must vanish and it leads to the skew symmetric character of couple stress tensor μ_{ji} that is

$$\mu_{ji} = -\mu_{ij}$$

and it was not recognised in the earlier microcontinuum theories.

It is also shown that body couple should not be distinguished from body forces F_i and hence equilibrium equations of couple stress theory reduce to

$$\sigma_{ji,j} + F_i = 0 \tag{1.3.1.20}$$

$$\mu_{ji,j} + \varepsilon_{ijk}\,\sigma_{jk} = 0 \tag{1.3.1.21}$$

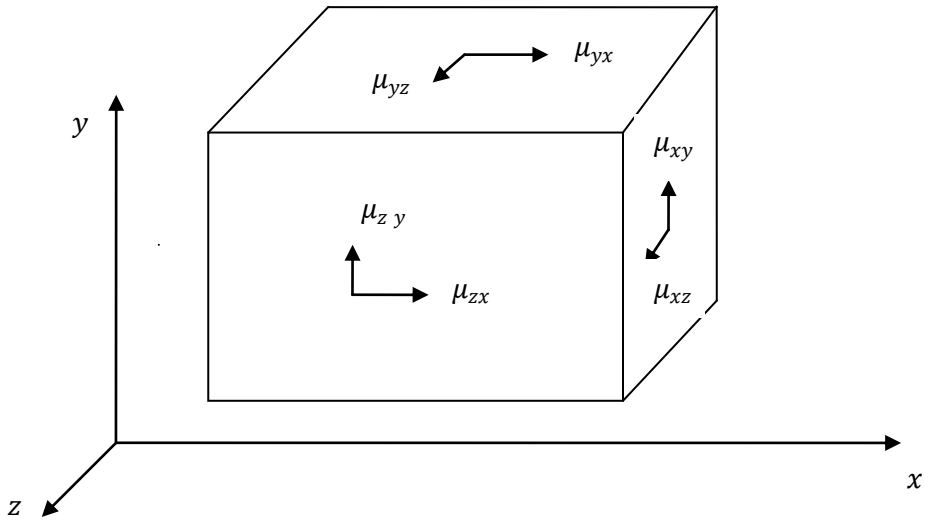

Figure 1.3 Components of couple stress tensor in consistent couple stress theory

Now for an elastic material energy density function is defined as $U = U(e_{ij}\,, \Upsilon_{ij})$ and for bi-anisotropic material it is written as

$$U = \frac{1}{2} a'_{ijkl}\, e_{ij}\, e_{kl} + \frac{1}{2} b'_{ijkl}\, \Upsilon_{ij}\, \Upsilon_{kl} + c'_{ijkl}\, e_{ij}\, \Upsilon_{kl} \qquad (1.3.1.22)$$

where a'_{ijkl} , b'_{ijkl} , c'_{ijkl} are elastic constitutive coefficients and should be such that elastic energy density function becomes positive definite. For an isotropic elastic material

$$a'_{ijkl} = \lambda\delta_{ij}\,\delta_{kl} + \mu\delta_{ik}\,\delta_{jl} + \mu\delta_{il}\,\delta_{jk}$$

$$b'_{ijkl} = 4\eta\delta_{ik}\,\delta_{jl} - 4\eta\delta_{il}\,\delta_{jk}$$

$$c'_{ijkl} = 0$$

and hence energy density function becomes

$$U = \frac{1}{2}\lambda e_{jj}\, e_{kk} + \mu e_{ij}\, e_{ij} + 4\eta\Upsilon_{ij}\,\Upsilon_{ij} \qquad (1.3.1.23)$$

For energy density function U to be positive definite, we are required to satisfy following conditions

$3\lambda + 2\mu > 0$, $\mu > 0$, $\eta > 0$ and also the ratio $\frac{\eta}{\mu} = l^2$ defines a characteristic length parameter which actually accounts for size dependency at microscale in consistent couple stress theory of elasticity.

Hence, for an isotropic elastic material stress tensor is defined as

$$\sigma_{ji} = \lambda u_{k,k}\,\delta_{ij} + \mu\left(u_{i,j} + u_{j,i}\right) - \eta\nabla^2\left(u_{i,j} - u_{j,i}\right) \qquad (1.3.1.24)$$

and couple stress tensor is defined as

$$\mu_{ji} = 4\eta\left(w_{i,j} - w_{j,i}\right) \qquad (1.3.1.25)$$

where $w_i = \frac{1}{2}\epsilon_{ijk}\, u_{k,j}$

These equations are called constitutive relations for consistent couple stress theory.

The basic governing equations of motion or equilibrium equation for consistent couple stress elasticity for isotropic material in the absence of body forces are given by

$$(\lambda + \mu + \eta\nabla^2)u_{k,ki} + (\mu - \eta\nabla^2)\nabla^2 u_i = \rho\ddot{u}_i \qquad (1.3.1.26)$$

1.4 WAVES IN ELASTIC MEDIUM

A wave is a periodic disturbance in a medium that carries energy from one point to another. The disturbance in the medium at point is not instantaneously felt at the points which are at a distance from the source of disturbance in the medium. It takes some time for the disturbance to reach to the other points in the medium and this phenomenon is known as *wave propagation*. There are many simple examples where this simple phenomenon can be felt in real life like transmission of seismic wave in earth, spreading of ripples on the surface of water, vibrations felt at railway platform when train runs on railway track etc. Waves in an elastic medium originate due to forced motion of a portion of the medium. As the particles of the elastic medium are deformed, the disturbance is transmitted from one point to another in the medium and thus wave propagates in the medium. As disturbance is carried from one point to another in the medium it carries amount of energy with it in the form of both kinetic and potential energies. Disturbances can transmit this energy over considerable distances in the medium. Resistance is offered to the process of propagation of disturbance or deformation by the consistency of the material as well as by the inertia of the particles in the medium. Due to these resistances a wave propagating in the medium gradually dies down. In an elastic solid, two different types of actions are possible for a wave. In first case, solid can transmit tensile and compressive stress and the motion of the particles will be in the direction of wave propagation and in second case, solid can transmit shear stresses also and here the motion of particles will be transverse to the direction of wave propagation. Waves in an elastic medium can be classified as *body waves* and *surface waves*. *Body waves* can propagate into the interior of the medium and *surface waves* propagate along the free surface of the medium. Electromagnetic waves in vacuum, acoustic waves in air are examples of body waves. Body waves are further divided into two categories longitudinal or compressional or dilatational or irrotational waves and transverse or shear or equivoluminal or rotational waves. These waves travel in an infinite media. In longitudinal waves particles of the medium vibrate about its equilibrium position in the direction of propagation of wave and sound wave is an example of these waves. These waves involve compression and rarefaction of the material as wave propagates, but there is no rotation. In transverse waves, the motion of particles is perpendicular to the propagation of wave. These waves involve shearing and rotation of the material as wave propagates through it. Light, X-ray and spreading of ripples in the water are few examples of these waves.

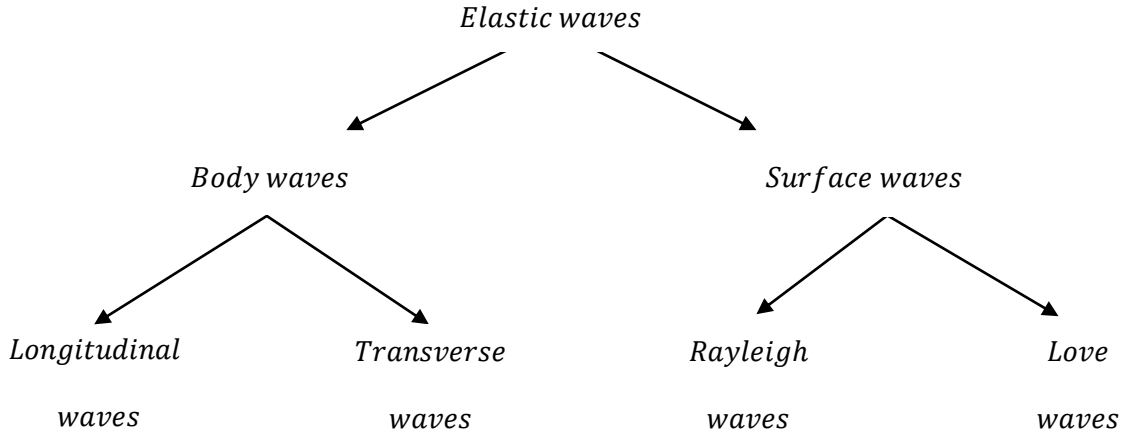

In equation of motion for an isotropic elastic solid by neglecting the effects of body forces, from Eq. (1.2.5) we get,

$$\mu\nabla^2\vec{u} + (\lambda+\mu)\nabla(\nabla.\vec{u}) = \rho\frac{\partial^2\vec{u}}{\partial t^2} \tag{1.4.1}$$

Where $\vec{u} = (u, v, w)$ are displacement components, λ, μ are Lame constants, ρ is the density of material.

By using standard formula $\nabla \times (\nabla \times \vec{u}) = \nabla(\nabla.\vec{u}) - \nabla^2\vec{u}$ of vector calculus, Eq. (1.4.1) can be written as

$$(\lambda+2\mu)\nabla(\nabla.\vec{u}) - \mu\nabla \times (\nabla \times \vec{u}) = \rho\frac{\partial^2\vec{u}}{\partial t^2} \tag{1.4.2}$$

$$C_1^2\nabla(\nabla.\vec{u}) - C_2^2\nabla \times (\nabla \times \vec{u}) = \frac{\partial^2\vec{u}}{\partial t^2} \tag{1.4.3}$$

where $C_1^2 = \frac{\lambda+2\mu}{\rho}$ and $C_2^2 = \frac{\mu}{\rho}$

Now, using Helmholtz decomposition theorem, we write displacement vector as

$$\vec{u} = \nabla\phi + \nabla \times \vec{\psi} \text{ and } \nabla.\vec{\psi} = 0 \tag{1.4.4}$$

$$\vec{u} = \hat{\imath}\frac{\partial\phi}{\partial x} + \hat{\jmath}\frac{\partial\phi}{\partial y} + \hat{k}\frac{\partial\phi}{\partial z} + \hat{\imath}\left(\frac{\partial\psi_z}{\partial y} - \frac{\partial\psi_y}{\partial z}\right) - \hat{\jmath}\left(\frac{\partial\psi_z}{\partial x} - \frac{\partial\psi_x}{\partial z}\right) + \hat{\imath}\left(\frac{\partial\psi_y}{\partial x} - \frac{\partial\psi_x}{\partial y}\right) \tag{1.4.5}$$

We get

$$u = \frac{\partial\phi}{\partial x} + \frac{\partial\psi_z}{\partial y} - \frac{\partial\psi_y}{\partial z}$$

$$v = \frac{\partial \phi}{\partial y} - \frac{\partial \psi_z}{\partial x} + \frac{\partial \psi_x}{\partial z}$$

$$w = \frac{\partial \phi}{\partial z} + \frac{\partial \psi_y}{\partial x} - \frac{\partial \psi_x}{\partial y}$$

Here, $\vec{u} = (u, v, w)$ is displacement vector and ϕ is a scalar potential and $\vec{\psi} = (\psi_x, \psi_y, \psi_z)$ is a vector potential function. $\nabla\phi$ is the irroational part as $curl(grad\phi) = 0$ and $\nabla \times \vec{\psi}$ is solenoidal part because $div(curl\vec{\psi}) = 0$. Eq. (1.4.3) reduces to

$$grad\left(C_1^2 \nabla^2 \phi - \frac{\partial^2 \phi}{\partial t^2}\right) + curl\left(C_2^2 \nabla^2 \vec{\psi} - \frac{\partial^2 \vec{\psi}}{\partial t^2}\right) = 0 \tag{1.4.6}$$

Eq. (1.4.6) will be satisfied, only if

$$\nabla^2 \phi = \frac{1}{C_1^2} \frac{\partial^2 \phi}{\partial t^2} \tag{1.4.7}$$

$$\nabla^2 \vec{\psi} = \frac{1}{C_2^2} \frac{\partial^2 \vec{\psi}}{\partial t^2} \tag{1.4.8}$$

Eqs. (1.4.7) and (1.4.8) both represent standard wave equations. Hence equation of motion for an isotropic elastic solid by neglecting the effects of body forces and with the assumption of small motion reduces to wave equation. It can also be concluded that two types of wave can be propagated through elastic solid with velocities C_1 and C_2 respectively. Since, $curl(grad\phi) = 0$ so the ϕ movement is purely irrotational or dilatational or longitudinal and $div(curl\vec{\psi}) = 0$, hence $\vec{\psi}$ motion is purely distortional or transverse or equivoluminal. Since $C_1 > C_2$, in seismology, longitudinal are called *primary waves* (*P*) because they represent first wave appearing on the seismograms. Transverse waves travelling with velocity C_2 are also called *secondary waves* (*S*). Secondary waves are polarized waves and the part polarized in vertical plane is denoted as S_V and that in horizontal plane is S_H. Longitudinal waves can propagate into all media may be solid, liquid and gases, but transverse waves can propagate into solids only. Liquid and gases do not support shear motion, so $\mu = 0$ and consequently $C_2 = 0$.

Surface waves appear when there is a boundary in the medium, as in semi-infinite media or in plates of finite width. These waves are Rayleigh waves, Love waves and Lamb waves. During earthquakes, seismic event starts with recording of longitudinal waves, followed by

transverse waves and finally by surface waves. Surface wave are higher in amplitudes and of longer periods.

1.4.1 Rayleigh Waves

In 1887, Lord Rayleigh [76] discovered that a specific wave can be formed near the free surface of a homogeneous and semi infinite medium, which cannot penetrate far beneath the surface because its amplitude decreases exponentially with distance from the surface. These waves propagate along the surface at a velocity which is less than velocity of both longitudinal and shear waves. These waves are polarised with elliptical motion of the particle in a plane, determined by normal to the surface and by the direction of propagation. The major axis of elliptical motion of the particle is along the normal to the surface and motion of the particles is in counter clock wise direction. These waves are called *Rayleigh Waves*. Rayleigh waves in an elastic medium under classical elasticity were found to be non dispersive, that is they were independent of frequency. These waves propagate with a velocity slightly less than transverse wave velocity. Rayleigh wave velocity is 0.9 times (approximately) of velocity of transverse waves. Rayleigh surface waves are widely used for material characterisation, to discover the mechanical and structural properties of objects. Rayleigh waves in ultrasonic frequency range are used in non-destructive testing applications (Viktorov [138]) to find cracks and other imperfections in the material. Rayleigh waves are also useful to detect surface flaws (Reinhardt and Dally [104]).

It is always interesting to study the changes in the profiles of Rayleigh waves when homogeneous elastic half space is loaded with liquid. This model has practical applications in the field of seismology, geophysics and NDT techniques. Love [77] gave the first comprehensive treatment to dispersion of Rayleigh and Love waves in case of an elastic solid half space covered by a single solid layer. Nayfeh and Nasser [89] studied the propagation of plane harmonic and Rayleigh waves in thermoelastic solids using generalized thermoelasticity. They studied Rayleigh waves propagating in a linear elastic half space which can conduct heat, using Maxwell's modified heat conduction equation. Sengupta and Ghosh ([110], [111]) studied the effects of couple stresses on surface waves in elastic media, they deduced the equations of surface waves in elastic media under the influence of couple stresses and observed that couple stresses affects the velocity of Rayleigh and Love wave propagation. Plona *et al.* [100] studied Rayleigh and Lamb waves at liquid-solid boundaries. They examined governing equations of Lamb and Rayleigh waves propagating in free and

liquid loaded solids. Bhattacharya and De [9] studied surface waves in a viscoelastic media under the effect of gravity. They briefly investigated various surface waves and showed that results are in agreement with classical theory, when effects of gravity and viscosity are neglected. Sharma *et al.* [125] gave a uniformly valid analytical solution to the problem of a decaying shock wave. Das *et al*. [25] studied thermo viscoelastic Rayleigh waves under the influence of couple stress and gravity. They derived more general equation of phase velocity of Rayleigh waves and also proved that it reduces to classical Rayleigh wave equation in the absence of viscosity, gravity and couple stress. Qi [101] studied the influence of viscous fluid loading on the propagation of leaky Rayleigh wave in the presence of heat conduction effects. He showed that attenuation of the leaky Rayleigh waves gets affected by both viscosity and heat conduction in the layer. He also observed that leaky Rayleigh wave speed is smaller at interface of a viscous boundary layer over a solid half space as compared to Rayleigh wave speed at the interface of a vacuum and a solid half space. Hassan and Nagy [49] investigated leaky Rayleigh waves in a fluid filled cylindrical cavity and found that the dispersive Rayleigh wave propagating around a concave cylindrical surface is substantially less attenuated by fluid loading than the corresponding wave on a flat surface. Ottosen *et al*. [96] studied Rayleigh waves by applying the indeterminate couple stress theory. They proved that Rayleigh waves are dispersive and velocity of Rayleigh waves is higher than conventional Rayleigh wave speed. Destrade [27] studied Rayleigh waves in crystals with at least one plane of symmetry and also derived the secular wave equation for Rayleigh waves propagating in any direction in the plane of symmetry. Georgiadis and Velgaki [42] studied the dispersive nature of Rayleigh waves propagating along the surface of a half space at high frequencies using couple stress theory. They tried to explore the applicability of couple stress theory in checking the dispersion of Rayleigh waves and they showed that Rayleigh waves propagating along the surface of a half space are dispersive at high frequencies. Vinh and Ogden [142] studied formulas for Rayleigh waves speed in orthotropic compressible elastic materials using theory of cubic equations and expressed these formulae as a continuous function of certain dimensionless material parameters. Georgiadis *et al.* [41] applied theory of dipolar gradient elasticity to analyse Rayleigh type waves propagating along the surface of a half space. Classical theory of elasticity predicts that Rayleigh waves are not dispersive at any frequency, which contradicts the experimental data and by applying theory of dipolar gradient elasticity they showed that these waves are indeed dispersive at high frequencies. They have also given certain relations which are helpful for estimating the values of various microstructural parameters involved in the theory. Zhu *et al.* [152] studied the propagation of

leaky Rayleigh and Scholte waves at the fluid-solid interface generated by transient normal point load at the interface by using Laplace and Hankel integral transform technique. Liu and Liu [75] discussed propagation characteristic of Rayleigh waves in orthotropic fluid saturated porous media. They derived governing equations of Rayleigh waves for orthotropic fluid saturated porous media and also showed that Rayleigh waves exhibit different characteristics in orthotropic fluid saturated porous media as compared to isotropic or transversely isotropic fluid-saturated porous media. Sharma and Pathania [118] discussed the propagation of leaky surface waves in an isotropic, homogeneous and thermally conducting elastic material bordered with inviscid liquid layer or half space using generalized theory of thermoelasticity. Destrade [28] studied Seismic Rayleigh waves on an exponentially graded, orthotropic half space. He found that Rayleigh wave is dispersive in the considered model and also showed that for the considered model wave travels at a slower speed and penetrates deeper than in homogeneous case. Lamkanfi *et al.* [70] did analysis of transmission of leaky Rayleigh waves at the extremity of a fluid loaded thick plate using finite element techniques. Sharma *et al.* [116] studied the propagation of Rayleigh surface waves in microstretch thermoelastic continua under inviscid fluid loadings in context of classical and non classical theories of thermoelasticity. They derived secular equation for generalized Rayleigh wave in close form and under isolated mathematical conditions. Kumar and Kansal [61] investigated effect of rotation on the phase velocity and attenuation coefficient of Rayleigh waves propagating in homogeneous, isotropic, thermoelastic diffusive half-space using different theories of thermoelastic diffusion. Kumar and Kansal [62] studied propagation of Rayleigh waves on free surface of transversely isotropic generalized thermoelastic diffusion using Green-Lindsay (GL) theory. They derived secular equation for the propagation of Rayleigh wave in considered media and presented the effects of anisotropy and diffusion on phase velocity and attenuation coefficient. Sharma and Sharma [120] did modelling of thermoelastic Rayleigh waves in a solid underlying a fluid layer with varying temperature by studying the propagation of surface waves in a homogeneous isotropic, thermally conducting and elastic solid underlying a layer of viscous liquid with finite thickness in the context of generalized theories of thermoelasticity. Sharma *et al.* [121] studied Rayleigh waves in a thermo viscoelastic solid loaded with viscous fluid of varying temperature. They found that mechanical relaxation times have significant effects on the profiles of phase velocity, attenuation coefficient and specific loss factor of energy dissipation of these waves. They also observed the effects of viscosity of both media on phase velocity, attenuation coefficient and specific loss factor of energy. Vinh and Linh [140] gave an approximate secular equation of

Rayleigh waves propagating in an orthotropic elastic half space coated by a thin orthotropic elastic layer. Ahmed and Dahab [2] studied influence of initial stress and gravity field on propagation of Rayleigh and Stoneley waves in a thermoelastic orthotropic granular medium and showed that frequency equations of both Rayleigh and Stoneley waves are affected by the influence of initial stress, density and gravity parameter. Sharma and Kumar [126] studied the effect of high-frequency vertical vibration in a suspension of gyrotactic micro-organisms. They derived secular equation involving bioconvection Rayleigh number and vibrational Rayleigh number. Kocaturk and Akbas [57] studied wave propagation in a microbeam based on a modified couple stress theory. They studied the influence of material length scale parameter on wave propagation. Kumar *et al.* [59] studied Rayleigh waves in isotropic microstretch thermoelastic diffusion solid half space. They observed the effects of relaxation times on various parameters involved in the problem. They also examined the path of surface particle during the propagation of Rayleigh waves. Vinh *et al.* [139] studied Rayleigh waves in an isotropic elastic half space coated by a thin isotropic elastic layer with smooth contact. By using the effective boundary condition method they derived secular equation of fourth-order in terms of the dimensionless thickness of the layer. Vinh *et al.* [141] studied the propagation of Rayleigh waves in an incompressible orthotropic half space coated by a thin elastic layer. They have given an approximate secular equation of third-order and based on this secular equation, an approximate formula of third-order for the Rayleigh wave velocity was also derived. Kakar and Kakar [54] studied propagation of surface waves in electro-magneto thermoelastic orthotropic granular non-homogeneous medium subjected to gravity and initial compression. They concluded that phase velocity of Stoneley and Rayleigh waves not only depend upon gravity field but also on the non-homogeneity, magnetic field, electric field, temperature, initial stress and granular notations of the material medium. Vavva *et al.* [136] studied dispersion of Rayleigh waves in bone using gradient elasticity. They studied dispersion of Rayleigh waves in an isotropic elastic half space and to consider micro structure of bone they incorporated four intrinsic parameters in the stress analysis. They presented their results by doing comparison of dispersion curves of group and phase velocity with already established results. They concluded that Mindlin's form II gradient elasticity can very well describe the dispersive nature of Rayleigh waves. Tanuma *et al.* [132] studied dispersion of Rayleigh waves in weakly anisotropic media with vertically-inhomogeneous initial stress. They derived high-frequency asymptotic formula for dispersion relations of Rayleigh waves that propagate in various directions along the free surface of a vertically-inhomogeneous, prestressed and anisotropic half-space. He *et al.* [50] did comparison of properties of

Rayleigh waves in elastic and viscoelastic media using a technique of finite difference method in time space domain. Kaur *et al*. [55], studied propagation of Rayleigh-type surface wave in a self-reinforced semi-infinite medium loaded by an inviscid liquid layer under the effect of gravity. They derived Secular equation for the propagation of Rayleigh-type wave in closed form and studied the effect of reinforcement, gravity and liquid loading on phase velocity of Rayleigh type waves. They made the comparison between results obtained using reinforced semi infinite medium and reinforced free semi infinite medium.

1.4.2 Lamb waves

Lamb waves travel in a thin stress free elastic plate and these waves were originally studied by Horace Lamb [69] and these waves are also called plate waves. Lamb waves are formed by interference of multiple reflections at the free surfaces of the plate and mode conversion of longitudinal waves (P-waves) and shear waves (S-waves). In Lamb waves particle displacement occur both in the direction of wave propagation and perpendicularly to the plane of the plate. Lamb waves are further categorised as symmetric and skew symmetric. In symmetric modes or longitudinal modes the average displacement over the thickness of the plate is in the longitudinal direction. In skew symmetric modes or flexural modes average displacement is in the transverse direction. These modes exist infinite in number for a specific plate thickness and acoustic frequency and are identified through their phase velocities. Lamb waves are dispersive in nature, so both phase and group velocities are function of frequency.

Osborne and Hart [94] examined Lamb waves activated in steel plate structures in underwater explosions. They briefly compared theoretical and experimental results. They suggested that methods given by them are also applicable to evaluate the phase velocity of electromagnetic wave guides. Schoch [106] investigated the effect of an inviscid liquid loading on the propagation of Lamb waves and derived the dispersion relation for leaky Lamb waves for an isotropic plate. Firestone and Ling ([35], [36]) used Lamb waves for damage detection using non destructive techniques in metal sheets. Gazis [39] gave considerable details about Lamb waves. Viktorov [138] proved dispersive nature of the Lamb waves and explained that they are formed by interference of multiple reflections and mode conversion of longitudinal and shear waves at the free surfaces of the plate. For the better understanding Worlton [145], Frederick and Worlton [37] made intensive experimental investigations on Lamb waves. They tried to correlate theory with experimental results and also derived dispersion equations

involving phase velocity, frequency and thickness of the plates. Sengupta and Benerji [109] investigated the effects of couple stresses on propagation of waves in elastic layer immersed in an infinite liquid. They showed that real part of wave velocity increases and imaginary part of wave velocity decreases due to the presence of couple stresses. Das *et al*. [24] studied effects of couple stress on propagation of waves in a thermo-visco-elastic layer of finite thickness. They solved equation of motion using potential functions and derived wave velocity equation using various boundary conditions. Wu and Zhu [146] studied the propagation of Lamb waves in a plate bordered with inviscid liquid layers on both sides. They derived dispersion equations and showed that phase velocity varies with thickness of the liquid layers. They have given the applications of Lamb waves in biosensing. Nayfeh and Nagy [88] studied excess attenuation of leaky Lamb waves due to viscous fluid loading. They have presented an analytical technique to estimate the effect of viscous fluid loading on the propagation of Lamb waves in submerged and fluid coated plates. They observed that the effect of viscosity on the phase velocity of the Lamb modes is negligible as compared to the effect on attenuation. In case plates are coated with a finite-thickness fluid layer the Lamb modes are not leaky and viscosity is the only source of attenuation. If plates are immersed in an infinite fluid then Lamb modes become leaky and the attenuation caused by fluid loading is the combined effects of radiation losses due to energy leakage into the fluid and dissipative losses due to viscous friction at the interfaces. Sengupta *et al.* [112] did a review of some problems in elasto-dynamics under the influence of gravity. They discussed influence of gravity on Lamb, Rayleigh, Love and Stoneley waves using Biot's theory of initial stresses. Pagneux and Maurel [97] discussed Lamb wave modes using eigenvalues method. They showed that in this method initial guess for the wave number is not needed which is contrary to the traditional method of root finding of frequency equation in complex plane. Ahmad *et al*. [1] studied guided waves in a fluid loaded transversely isotropic plate. They derived dispersion relations for both symmetric and anti symmetric modes of propagation in a free transversely isotropic plate. They have plotted dispersion curves for first four symmetric modes by considering a magnesium plate immersed in water. Sharma and Pathania [117] studied the propagation Lamb waves in a homogeneous isotropic, thermally conducted plate bordered with layers of inviscid liquid or inviscid half space using generalized theory of thermoelasticity. They studied secular equations both for symmetric and anti symmetric wave modes and also deduced secular equation for thermoelastic leaky Lamb waves. Sharma *et al.* [119] did the analysis of thermoelastic Lamb waves in a transversely isotropic plate bordered with layers of inviscid liquid or liquid half space. They derived secular equation for

homogeneous transversely isotropic plate and also deduced secular equation for leaky Lamb waves. Kumar and Partap [63] studied propagation of Rayleigh Lamb waves in micropolar isotropic elastic plate. They derived secular equations both for symmetric and skew symmetric wave modes. Wang and Yuan [144] studied propagation of Lamb waves in composites. They calculated group velocity and characteristic wave curves both numerically and experimentally. Their experimental study was focused on the existence of higher Lamb wave modes. They have also developed a new semi exact method for the calculation of group velocity. Shao *et al*. [113] studied dispersion curve of guided wave in a layered media with overlying liquid surface. They have studied the effects of thickness of overlying liquid layer on the dispersion curves and through their study they have tried to provide theoretical basis for the use of guided waves exploration in liquid covered areas. Singh and Tomar [128] studied propagation of Rayleigh–Lamb waves in an infinite microstretch elastic plate of finite thickness with top and bottom of the plate are cladded with layers of a homogeneous and an inviscid liquid of finite thickness. They derived frequency equations for symmetric and anti symmetric modes of these waves and found that waves are dispersive in both the cases and also concluded that microstretch has negligible effect on dispersion curves. They found that attenuation coefficient is influenced by the presence of microstretch and also observed that liquid layers have significant effect on the dispersion curves. Vavva *et al*. [137] discussed velocity dispersion of guided waves propagating in an elastic plate using gradient theory by showing its application to cortical bone. They included two additional microstructural parameters in constitutive relations for representing characteristic lengths in bone. Sharma and Kumar [115] studied the propagation of Lamb waves in micropolar thermoelastic solid plates immersed in liquid layer of finite thickness or liquid half space from both sides with varying temperature. They observed that fluid loadings have significant effect on phase velocity, attenuation coefficient and specific loss for both symmetric and anti symmetric modes. They showed that characteristic length and coupling factor also have notable effect on the phase velocity. Wu *et al*. [148] investigated the vibration characteristics in a microscale fluid loaded rectangular isotropic plate attached to a uniformly distributed mass. They studied plate vibrations under the simultaneous effect of fluid loadings and attached mass loadings. They obtained numerical results using different boundary conditions and compared these with experimental results and with already established results in the literature. Pathania *et al.* [98] studied generalized thermoelastic waves in anisotropic plates bordered both sides by viscous liquid layers of finite thickness. They derived secular equations for symmetric and anti symmetric wave motion in a plate. They made comparisons of their findings with already

published results in the literature. Liao ([72], [73]) studied computational method to estimate the unknown coefficient in a wave equation using boundary measurements. Kumar *et al.* [65] studied generalized thermoelastic waves in microstretch plates loaded with fluid of varying temperature. They applied theory of generalized thermo-microstretch elasticity to study the propagation of both straight and circular crested waves in microstretch thermoelastic plates bordered with inviscid liquid layers or half-spaces on both sides, with varying temperature. They derived secular equations for wave propagation in rectangular and cylindrical plates and also discussed special cases for thin and thick plates and did the comparison of their findings with already established results in the literature. Sharma *et al.* [114] studied reflection and transmission of acoustic waves at an interface of semiconductor half space underlying an inviscid liquid. Sharma *et al.* [123] studied Lamb waves in a homogeneous isotropic thermoelastic micropolar solid with two temperatures, bordered with layers or half-spaces of inviscid liquid subjected to stress free boundary conditions. They derived secular equations for symmetric and anti symmetric Lamb wave modes using coupled thermoelasticity theory. They have presented various results for phase velocity and attenuation coefficient of these waves. Chen and Li [19] proposed a new modified couple stress theory for anisotropic elasticity containing three length scale parameters and developed composite laminated Kirchhoff plate models under this theory. Hussain and Ahmad [51] studied zero group velocity for Lamb waves in an incompressible orthotropic plate. They showed that existence of these modes depend upon anisotropy parameter of the material.

1.4.3 Shear horizontal (SH) waves

There is one more type of waves which can propagate in semi infinite space in contact with an isotropic elastic layer of finite thickness called Love waves (L-waves) and they cause the circular shearing of the ground. These waves are named after A.E.H. Love [77], who was first to give a mathematical model for the existence of these waves. These waves travel slightly faster than Rayleigh waves and about 90% of the Shear wave velocity, and have the largest amplitude. SH waves are horizontally polarised shear waves, where a single displacement component is involved. The particle motions are polarised in a single direction. The particle motion in these waves is transverse and parallel to the surface. These waves are observed only when a low velocity layer is overlying a high velocity layer or a half space. Love waves cannot propagate in a homogeneous half space.

The study of guided SH waves has received much attention in the areas of non destructive testing for studying the surface mechanical properties of underlying solids (Simonetti and Cawley [127], Lee *et al.* [71], Petcher *et al.* [99], Qingzeng *et al.* [102]), exploration geophysics and in the field of seismology for estimating damage capabilities of seismic waves. SH waves are studied by many researchers under different conditions. Bhattacharya [8] pointed out some possible exact solutions of SH wave equation for inhomogeneous media. Schoenberg [107] studied transmission and reflection of plane waves at an elastic-viscoelastic interface. He concluded that some properties of these waves depend on the frequency of incident wave and the angle of incidence of impinging wave. Kaushik and Chopra [56] studied transmission and reflection of inhomogeneous plane SH waves at an interface between two horizontally and vertically heterogeneous viscoelastic solids. They calculated mathematical expression for reflected and transmitted waves in viscoelastic material. Chakraborty [16] studied reflection and transmission of SH waves at an interface between homogeneous and inhomogeneous media. He showed effects of inhomogeneity on the reflection and transmission coefficients graphically and concluded that inhomogeneity plays a vital role in phase change, total reflection and transmission of the wave. Debnath and Roy [26] studied propagation of edge waves in a thinly layered laminated medium with stress couples under initial stresses. They showed that for a specific compression, the presence of couple stresses increases the velocity of wave propagation with the increase of wave number, whereas the case is exactly reverse when there is no couple stress. The problems of multiply connected materials with holes and multi phase simply connected materials have been addressed in a review article by Jasiuk and Strazewski [52]. Among various studies of SH waves, one of the prominent study is to examine SH waves in the context of size dependent microcontinuum theories. One such attempt was made by Vardoulakis and Georgiadis [135], they studied SH surface waves in a homogeneous gradient elastic half space with surface energy. They showed the existence of SH waves in a homogeneous gradient elastic half space. They concluded that SH surface waves may exist in a homogeneous half space if the problem is analysed by a continuum theory with appropriate microstructure. Singh *et al.* [130] studied displacement and strain fields due to axially symmetric sources in an elastic half space welded with another elastic half space. Du *et al.* [29] studied Love wave propagation in layered magneto-electro-elastic structures by considering a piezomagnetic material thin layer bonded with semi infinite piezoelectric substrate. They calculated phase velocity of Love waves under different conditions and also studied the effects of initial stresses and magneto-electromechanical coupling factor on phase velocity. Yang *et al.* [151]

investigated transient scattering of SH waves due to sub surface and interface cracks which are parallel to the free surface in a layered elastic solid. Borcherdt [11] has studied the propagation of SH waves in viscoelastic media. Chattopadhyay *et al.* [17] studied the propagation of SH waves in an irregular non homogeneous monoclinic crustal layer over a semi infinite monoclinic medium with an irregularity. They studied the influence of depth of irregularity and non-homogeneity parameters on phase velocity of SH waves. Chaudhary *et al.* [18] studied transmission of plane SH waves through a monoclinic layer embedded between two different self-reinforced elastic solid half spaces and derived closed form expressions of reflection and transmission coefficients. They showed that reinforcement parameters of the half space strongly affect the reflection and transmission coefficients. Gupta *et al.* [45] investigated propagation of Love waves in non homogeneous substratum over initially stressed heterogeneous half space. They derived dispersion equation of phase velocity of Love waves in the considered problem. They observed that with the increase in compressive initial stresses phase velocity of Love waves decreases for the same frequency and presence of tensile initial stress of small magnitude in the half space increase the velocity of Love waves. Kundu *et al.* [66] studied propagation of Love waves in porous rigid layer lying over an initially stressed half space. They derived dispersion equation for phase velocity in the considered model. They concluded that phase velocity of Love waves is considerably affected by porosity, rigidity, anisotropy of the layer and inhomogeneity of the half space. They have plotted dispersion curves of Love waves by considering different values of inhomogeneity factor and initial stress parameter. Sahu *et al.* [105] studied SH waves in viscoelastic heterogeneous layer over half space with self-weight. They studied the effect of gravity, heterogeneity and internal friction on both phase velocity and damping velocity of propagation of SH waves in viscoelastic layer over a half space. They observed that heterogeneity of the medium significantly affects the velocity profile of SH wave. Kakar [53] studied propagation of SH waves in heterogeneous layer laying over an inhomogeneous isotropic elastic half space. He derived dispersion relation for SH waves using Green's function method and Fourier transforms. He observed that SH wave velocity increases with increases of inhomogeneity parameter.

SH waves in a layered structure for a perfectly bonded interface between two media are studied by many researchers, but this condition is difficult to achieve, in reality. Due to certain reasons like thermal mismatch or some faults during manufacturing process, cracks or defects can appear at the interface which leads to an imperfect interface between two media.

Components of displacement field are not continuous at the common boundary of two media in case of imperfect interface. The difference in displacement fields is assumed to depend linearly upon traction vector. These imperfections at the common boundary may affect the propagation of SH waves.

Schoenberg [108] studied elastic wave behaviour across linear slip interface between two media by assuming that displacement discontinuity is linearly related to stress traction. He calculated reflection and transmission coefficient for harmonic plane waves incident at arbitrary angles upon a plane linear slip interface. Wu and Dzenis [147] derived dispersion relation for antiplane surface acoustic waves propagating in elastic half space coated with an anisotropic laminate. Madan *et al.* [82] studied displacements and stresses in an anisotropic medium due to non-uniform slip along a very long strike-slip fault. Liu *et al.* [74] studied Love waves in layered graded composite structures with imperfectly bonded interface. By using shear spring model they derived dispersion equation for Love waves and also calculated an approximate analytical solution for these waves. They observed that for imperfectly bonded interface, the phase velocity of Love waves lies in the range of velocities for the rigid and slip interface conditions. Bokhari *et al*. [10] studied exact solutions of some general nonlinear wave equations in elasticity. They also presented some cases wherein the velocities of the longitudinal and transversal plane waves are variable. Kumar and Chawla [60] studied surface wave propagation at the imperfect boundary between transversely isotropic thermodiffusive elastic layer and half space in the context of the Green–Lindsay theory. They developed mathematical model and derived secular equation for surface waves in compact form. They have plotted dispersion curves to measure the effect of various parameters involved in the problem on the propagation of surface waves. Nie *et al*. [90] studied shear horizontal guided waves in a coupled plate consisting of a piezoelectric layer and a piezomagnetic layer, by assuming that both layers are transversely isotropic and are perfectly bonded at the interface. They concluded that phase velocity of SH waves approaches the smaller bulk shear wave velocity of the two materials in the system with the increase in the wave number. Otero *et al.* [95] studied dispersion relations for SH waves on a magnetoelectroelastic heterostructure with imperfect interfaces, they showed with the decreasing value of imperfect bonding parameter, propagation velocity also decreases. Singh *et al*. [129] studied propagation of waves at an imperfectly bonded interface between two monoclinic thermoelastic half spaces. They studied reflection and transmission of plane waves in the context of generalized thermoelasticity. Chugh *et al.* [21] studied static

deformation of an orthotropic elastic layered medium due to a nonuniform discontinuity along a very long strike-slip fault. Cui *et al.* [23] studied propagation of SH waves in piezoelectric structure with an imperfectly bonded viscoelastic layer, they used shear lag model to describe the imperfectness factor at the interface and have studied the effects of interfacial imperfection and viscosity of the layer on the dispersive relationship and wave attenuation. Gaur and Rana [38] studied shear wave propagation in piezoelectric-piezoelectric composite layered structure. They showed that thickness and elastic constants have significant effect on the propagation of shear waves.

1.5 VISCOELASTIC MATERIALS

While studying response of elastic materials, the concept of time does not comes into discussion. Elastic material shows time independent material behaviour. Elastic materials deform with the application of external load and regain their original shape after the removal of applied external loads. We have one different category of materials like biological materials, metals at high temperature, coaltar etc. where material response is dependent upon how quickly the load is applied or removed that is the extent of deformation being dependent upon the rate at which the deformation causing loads are applied. Hence the stress response of these materials depends on both the strain applied and the strain rate at which it was applied. These type of materials are called viscoelastic materials. In these materials the relationship between stress and strain depends on time or on frequency. The stress strain diagram for elastic solids is very much unique, but for viscoelastic materials stress strain diagram is not unique as it depends upon the rate at which strain is developed in the material. Hence the slope of plot between stress and strain depends on strain rate. Viscoelastic materials are excellent impact absorbers. Viscoelastic materials are used in automobile bumpers, in helmets (the foam padding inside), shoe insoles etc. Viscoelasticity is made up of two words, viscosity and elasticity. Viscosity is a property of fluid and measures resistance to the flow. Elasticity, on the other hand, is a property of solid material. Hence, a viscoelastic material possesses the properties of both fluid and solid.

Viscoelastic materials have numerous applications in industrial and engineering fields. Many researchers have studied propagation of waves in viscoelastic materials under different conditions. Ma *et al*. [81] discussed propagation of harmonic wave in an infinite viscoelastic medium with a periodic array of cylindrical elastic fiber. They used finite element method technique which leads to a non linear eigen value problem. Using iteration technique they

obtained two modes of dispersion for both real and imaginary wave numbers. Carcione *et al.* [14] studied wave propagation simulation in linear viscoelastic materials. They used theory of linear viscoelasticity for describing attenuation and dispersion of seismic waves. Carcione [13] studied wave propagation in anisotropic linear viscoelastic media: theory and simulated wave fields. He has calculated phase, group and energy velocities of plane waves in anisotropic viscoelastic medium and had shown they all are different from each other. He used some new integration techniques to solve the numerical problem of wave propagation in linear viscoelastic wave. Kumar and Singh [64] discussed reflection of plane waves at a planar interface between viscoelastic solid half space and micropolar elastic half space. They calculated amplitude ratios for different reflected and refracted waves and concluded that it depends upon angle of emergence and angle between propagation vector and attenuation vector. Benatar *et al.* [6] did theoretical and experimental analysis of longitudinal wave propagation in cylindrical viscoelastic rods. They said for viscoleastic materials during the propagation of stress or strain pulses, both geometric and material dispersion are possible when wavelength and diameter of rod are of same order. Banks *et al*. [4] has written a review article on elastic and viscoelastic solids for the better understanding of these solids. Chirita *et al*. [20] studied Rayleigh surface waves in exponentially graded half space made of Kelvin-Voigt viscoelastic material. They studied effect of the viscoelastic dissipation energy upon the corresponding wave solutions. They derived explicit form of secular wave equation in the considered model. Sharma *et al.* [124] studied effect of viscosity on wave propagation in anisotropic thermoelastic medium. They derived phase velocity, attenuation coefficients and presented graphical effects of viscosity. Sharma and Bhargava [122] studied reflection and transmission of thermoelastic plane waves at an imperfect interface between a thermal conducting viscous liquid and generalized thermoelastic solid half space. They concluded that stiffness and thermal properties of the media affects amplitude ratio of reflected and transmitted waves. Bernstein *et al.* [7] studied dispersive optical solitons with Schrödinger-Hirota equation by travelling wave hypothesis.

CHAPTER-2

VELOCITY DISPERSION IN AN ELASTIC PLATE WITH MICROSTRUCTURE: EFFECTS OF CHARACTERISTIC LENGTH IN A COUPLE STRESS MODEL[1]

2.1 INTRODUCTION

Lamb waves are used for characterisation of the material, as they propagate throughout the thickness of material in different modes with different velocities, which depend on the frequency of wave. Thus profiles of Lamb wave propagation can provide information of various useful non destructive testing parameters. Lamb waves as mentioned in section-1.4.2, of chapter-1, have been studied by many researchers under different conditions and using various theories, but Lamb waves have not been studied by applying couple stress theory of elasticity describing effects of microstructures in terms of internal characteristic length of the material. Microstructural effects become important, when dimensions of a heterogeneous material are comparable to the length scale of microstructure and the state of stress needs to be defined in a non-local manner. Linear theory of elasticity, which is associated with the concept of homogeneity of material and local stresses, cannot describe the behaviour of the materials with microstructures. In this chapter, Couple stress theory of elasticity (Hadjesfandiari and Dargush [46]) has been employed to capture the size effects on the propagation of Lamb waves in an elastic plate with microstructure. Effects on the dispersion curves of Lamb waves are studied, when the characteristic length of the material is comparable to cell size. The governing equations of couple stress theory, involving stresses and couple stresses are solved to study the impact of different values of characteristic lengths, comparable with cell size. Since bone is a material with microstructure (Vavva *et al*. [137]), so for numerical calculations and graphical representation of the results, the plate is considered to have mechanical properties typically used for bones.

[1]Contents of this chapter are published in SCI indexed journal, *Meccanica* (2014) 49:1083–1090 with impact factor-1.949

2.2 COUPLE STRESS THEORY AND WAVE DISPERSION

Hadjesfandiari and Dargush [46] in 2011, formulated a couple stress theory for isotropic material involving three parameters λ, μ and η. The constants λ, μ have the same meaning as Lamé constants in Cauchy elasticity and η is a length scale parameter which accounts for couple stress effects for isotropic solids. Evaluation of η requires characteristic material length l, which is absent in Cauchy elasticity. One of the major problem in these size dependent elastic theories (Cosserat [22], Eringen [31], Toupin [133], Mindlin and Tiersten [87], Koiter [58] and Hadjesfandiari and Dargush [46]) is determination of these length scale parameters. It was observed (Lakes [67]) that characteristic length would be undetectable in any macroscopic mechanical experiment, but have relevance in studies involving composite and cellular solids. In fibrous composites, the characteristic length may be of the order of spacing between fibres. In cellular solids it may be comparable to the average cell size of the material.

The basic governing equations of couple stress elasticity for isotropic material in the absence of body forces (Hadjesfandiari and Dargush [46]) are given by

$$(\lambda + \mu + \eta\nabla^2)u_{k\,,ki} + (\mu - \eta\nabla^2)\nabla^2 u_i = \rho\ddot{u}_i \tag{2.2.1}$$

where λ and μ are Lam$\acute{e}$ constants, $\eta = \mu l^2$ is couple-stress coefficient, l is characteristic length, ρ is the density of the plate, u_i are the displacement components, commas are used for partial differentiation and (.) dot notation is used for partial differentiation with time and $\nabla^2 \equiv \frac{\partial^2}{\partial x^2} + \frac{\partial^2}{\partial y^2} + \frac{\partial^2}{\partial z^2}$

Eq. (2.2.1) in vector form can be written as

$$(\lambda + \mu + \eta\nabla^2)\nabla(\nabla.\vec{u}) + (\mu - \eta\nabla^2)\nabla^2\vec{u} = \rho\frac{\partial^2\vec{u}}{\partial t^2} \tag{2.2.2}$$

where $\vec{u} = (u, v, w)$ are displacement components

By using $\nabla \times (\nabla \times \vec{u}) = \nabla(\nabla.\vec{u}) - \nabla^2\vec{u}$ above equation can also be written as

$$\frac{(\lambda+2\mu)}{\rho}\nabla(\nabla.\vec{u}) - \frac{\mu}{\rho}(1 - l^2\nabla^2)\nabla \times (\nabla \times \vec{u}) = \frac{\partial^2\vec{u}}{\partial t^2} \tag{2.2.3}$$

In component form above equation can be written as

$$\frac{(\lambda+2\mu)}{\rho}\left(\frac{\partial^2 u}{\partial x^2}+\frac{\partial^2 v}{\partial x\partial y}+\frac{\partial^2 w}{\partial x\partial z}\right)-\frac{\mu}{\rho}(1-l^2\nabla^2)\left(\frac{\partial^2 v}{\partial x\partial y}-\frac{\partial^2 u}{\partial y^2}-\frac{\partial^2 u}{\partial z^2}+\frac{\partial^2 w}{\partial z\partial x}\right)=\frac{\partial^2 u}{\partial t^2}$$

$$\frac{(\lambda+2\mu)}{\rho}\left(\frac{\partial^2 u}{\partial x\partial y}+\frac{\partial^2 v}{\partial y^2}+\frac{\partial^2 w}{\partial y\partial z}\right)-\frac{\mu}{\rho}(1-l^2\nabla^2)\left(\frac{\partial^2 u}{\partial x\partial y}-\frac{\partial^2 v}{\partial x^2}-\frac{\partial^2 v}{\partial z^2}+\frac{\partial^2 w}{\partial z\partial y}\right)=\frac{\partial^2 v}{\partial t^2}$$

$$\frac{(\lambda+2\mu)}{\rho}\left(\frac{\partial^2 u}{\partial x\partial z}+\frac{\partial^2 v}{\partial y\partial z}+\frac{\partial^2 w}{\partial z^2}\right)-\frac{\mu}{\rho}(1-l^2\nabla^2)\left(\frac{\partial^2 u}{\partial x\partial z}-\frac{\partial^2 w}{\partial x^2}-\frac{\partial^2 w}{\partial y^2}+\frac{\partial^2 v}{\partial y\partial z}\right)=\frac{\partial^2 w}{\partial t^2}$$

The constitutive relations are given by

$$\sigma_{ji}=\lambda u_{k,k}\delta_{ij}+\mu\left(u_{i,j}+u_{j,i}\right)-\eta\nabla^2\left(u_{i,j}-u_{j,i}\right) \tag{2.2.4}$$

$$\mu_{ji}=4\eta\left(\omega_{i,j}-\omega_{j,i}\right) \tag{2.2.5}$$

where

$$\omega_i=\frac{1}{2}\epsilon_{ijk}\,u_{k,j}$$

Hence

$$\omega_1=\frac{1}{2}\left(\frac{\partial w}{\partial y}-\frac{\partial v}{\partial z}\right)$$

$$\omega_2=\frac{1}{2}\left(\frac{\partial u}{\partial z}-\frac{\partial w}{\partial x}\right)$$

$$\omega_3=\frac{1}{2}\left(\frac{\partial v}{\partial x}-\frac{\partial u}{\partial y}\right)$$

Here, σ_{ji} is the non-symmetric force-stress tensor, μ_{ji} is skew symmetric couple-stress tensor, $\delta_{ij}=\begin{cases}1, & i=j\\ 0, & i\neq j\end{cases}$ is Kronecker's delta, ω_i is rotation vector and

$$\epsilon_{ijk}=\begin{cases}1, & i,j,k\ are\ in\ cyclic\ order\\ -1, & i,j,k\ are\ not\ in\ cyclic\ order\\ 0, & any\ two\ of\ i,j,k\ are\ equal\end{cases}$$

is permutation tensor

By taking divergence and curl of Eq. (2.2.1), and using a standard formula $\nabla\times(\nabla\varsigma)=Curl(grad\varsigma)=0$ where ς is any scalar valued function. The equations governing propagation of dilatations and rotations are given by

$$(\lambda+2\mu)\nabla^2(\nabla.\vec{u})=\rho\frac{\partial^2}{\partial t^2}(\nabla.\vec{u}) \tag{2.2.6}$$

$$(\mu - \eta\nabla^2)\nabla^2(\nabla \times \vec{u}) = \rho \frac{\partial^2}{\partial t^2}(\nabla \times \vec{u}) \tag{2.2.7}$$

Considering plane waves of the form

$$(\nabla . \vec{u}) = Ae^{i(\xi x - \omega t)} \tag{2.2.8}$$

$$(\nabla \times \vec{u}) = \vec{B}e^{i(\xi x - \omega t)} \tag{2.2.9}$$

where A and $\vec{B}$ represent amplitudes, ξ is the wave number, ω is the frequency of the propagating waves and $i = \sqrt{-1}$.

Inserting Eqs. (2.2.8) and (2.2.9) into Eqs. (2.2.6) and (2.2.7) respectively and representing the classical phase velocities of longitudinal and shear waves by C_1 and C_2, we obtain the following dispersion relations

$$\left.\begin{aligned} \omega^2 &= C_1^2\xi_L^2, && \text{for longitudinal waves} \\ \omega^2 &= C_2^2(1 + l^2\xi_T^2)\xi_T^2, && \text{for shear waves} \end{aligned}\right\} \tag{2.2.10}$$

where

$C_1^2 = \frac{(\lambda+2\mu)}{\rho}$, $C_2^2 = \frac{\mu}{\rho}$ are the longitudinal and shear waves speed respectively in classical theory of elasticity and ξ_L and ξ_T are the wave numbers of longitudinal and shear waves.

Using these two equations, we obtain the following expressions for phase velocities V_L and V_T of the longitudinal and shear waves, respectively

$$V_L = \frac{\omega}{\xi_L} = C_1 \tag{2.2.11}$$

$$V_T = \frac{\omega}{\xi_T} = C_2\sqrt{(1 + l^2\xi_T^2)} \tag{2.2.12}$$

From these two expressions, it is clear that characteristic length has no impact on the phase velocity of longitudinal waves. It can also be observed that phase velocity does not depend upon wave number, hence these waves are non dispersive in nature. Shear waves in case of couple stress theory are function of wave number, which indicates dispersion. This dispersion is because of the presence of l, internal characteristic length of the material. If we take $l = 0$, it is obvious that $V_L = C_1$ and $V_T = C_2$, it is the case of classical theory of elasticity with constant speed of both longitudinal and shear waves and hence no dispersion in wave propagation.

Fig. 2.1, provides the dispersion curves of shear waves for different combinations of characteristic lengths (l), when (i) $l = h$ (Cell size of microstructure of bone) (ii) $l > h$ (iii) $l < h$. It can been seen that with the increasing value of characteristic length parameter, which is of the order of internal cell size of bone's microstructure, shear wave velocity is also increasing.

Solving Eqs. (2.2.11) and (2.2.12) for the wave number ξ_L and ξ_T respectively, we get

$$\xi_L = \frac{\omega}{C_1}$$

$$\xi_T = \sqrt{\frac{-{C_2}^2 \pm \sqrt{{C_2}^4 + 4{C_2}^2 l^2 \omega^2}}{2{C_2}^2 l^2}} \tag{2.2.13}$$

By solving Eqs. (2.2.11) and (2.2.12), we get group velocity of longitudinal and shear waves as

$$V_L^g = \frac{d\omega}{d\xi_L} = C_1 \tag{2.2.14}$$

$$V_T^g = \frac{d\omega}{d\xi_T} = C_2 \frac{1 + 2l^2 {\xi_T}^2}{\sqrt{1 + l^2 {\xi_T}^2}} \tag{2.2.15}$$

where V_L^g, V_T^g are the group velocity of longitudinal and shear waves respectively.

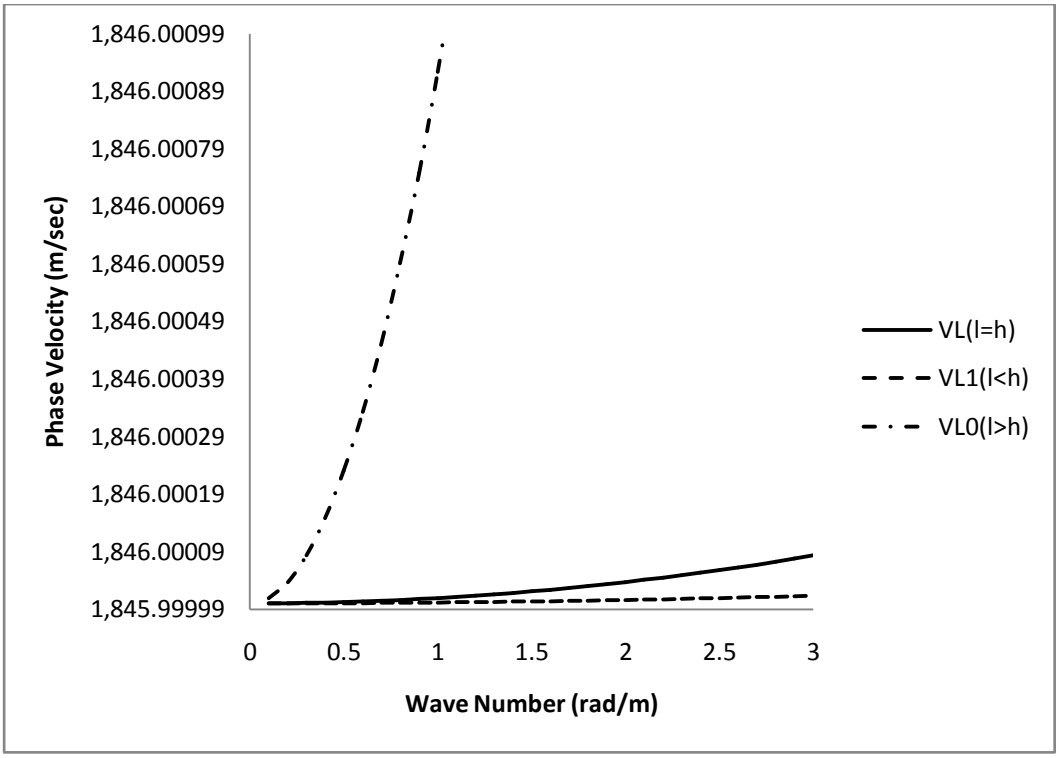

Figure 2.1 Phase velocity profile of Shear waves with wave number under varying characteristic lengths (VL is the phase velocity, when $l = h = 0.0001\, m$; VL1 is the phase velocity, when $l = 0.00004\, m < h$ and VL0 is the phase velocity, when $l = 0.001\, m > h$)

2.3 WAVE PROPAGATION IN A STRESS AND COUPLE STRESS FREE ELASTIC PLATE

We consider an infinite homogeneous isotropic plate of thickness $2d$.We take origin of the cartesian coordinate system (x, y, z) in the middle of the plate. The XY-plane is chosen to coincide with the middle surface of the plate and z-axis is normal to the plate and is pointing vertically downwards, along the thickness of the plate. The surfaces of the plate are assumed to be stress/couple stress free.

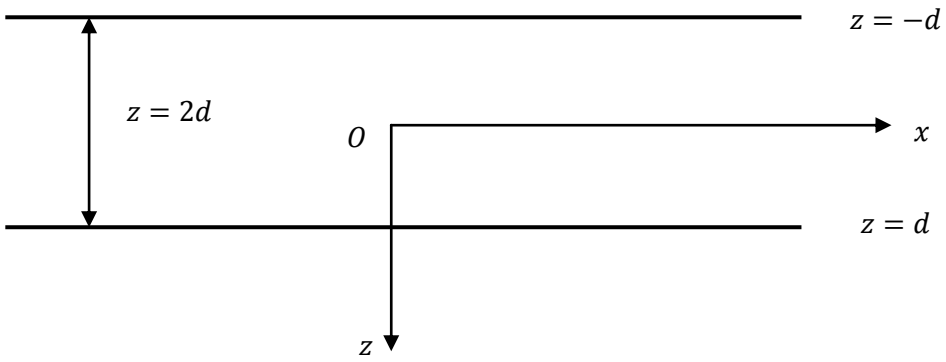

Figure 2.2 Geometry of the problem

2.4 BOUNDARY CONDITIONS

Boundary conditions to be satisfied at two surfaces of the plate are given by

(i) Shear stress should vanish at two free surfaces of the plate that is

$\sigma_{zx} = 0$ at $z = \pm d$.

(ii) Normal stress should also vanish, both at top and bottom surfaces of the plate that is $\sigma_{zz} = 0$ at $z = \pm d$.

(iii) Couple stress should be zero at the top and bottom surfaces of the plate that is

$\mu_{zy} = 0$ at $z = \pm d$

2.5 FORMAL SOLUTION OF THE PROBLEM

Solving Eq. (2.2.1) by taking $\vec{u} = (u, 0, w)$ and $\frac{\partial}{\partial y} \equiv 0$, we get following two equations

$$C_1^2 \left(\frac{\partial^2 u}{\partial x^2} + \frac{\partial^2 w}{\partial x \partial z}\right) - C_2^2 (1 - l^2 \nabla^2) \left(\frac{\partial^2 w}{\partial x \partial z} - \frac{\partial^2 u}{\partial z^2}\right) = \frac{\partial^2 u}{\partial t^2} \tag{2.5.1}$$

$$C_1^2 \left(\frac{\partial^2 u}{\partial z \partial x} + \frac{\partial^2 w}{\partial z^2}\right) - C_2^2 (1 - l^2 \nabla^2) \left(\frac{\partial^2 u}{\partial x \partial z} - \frac{\partial^2 w}{\partial x^2}\right) = \frac{\partial^2 w}{\partial t^2} \tag{2.5.2}$$

Solution of Eqs. (2.5.1) and (2.5.2) can be obtained by Helmholtz decomposition of displacement field $\vec{u} = \nabla\phi + \nabla \times \vec{\psi}$, which gives us

$$u = \frac{\partial \phi}{\partial x} - \frac{\partial \psi}{\partial z} \text{ and } w = \frac{\partial \phi}{\partial z} + \frac{\partial \psi}{\partial x} \tag{2.5.3}$$

Where ϕ and $\vec{\psi} = (0, \psi, 0)$ are velocity potential functions of longitudinal and shear waves in solids. From Eqs. (2.5.1) and (2.5.2) we get,

$$\frac{\partial}{\partial x}\left[C_1^2 \left(\frac{\partial^2 \phi}{\partial x^2} + \frac{\partial^2 \phi}{\partial z^2}\right) - \frac{\partial^2 \phi}{\partial t^2}\right] - \frac{\partial}{\partial z}\left[C_2^2 (1 - l^2 \nabla^2) \left(\frac{\partial^2 \psi}{\partial x^2} + \frac{\partial^2 \psi}{\partial z^2}\right) - \frac{\partial^2 \psi}{\partial t^2}\right] = 0 \tag{2.5.4}$$

$$\frac{\partial}{\partial z}\left[C_1^2 \left(\frac{\partial^2 \phi}{\partial x^2} + \frac{\partial^2 \phi}{\partial z^2}\right) - \frac{\partial^2 \phi}{\partial t^2}\right] + \frac{\partial}{\partial x}\left[C_2^2 (1 - l^2 \nabla^2) \left(\frac{\partial^2 \psi}{\partial x^2} + \frac{\partial^2 \psi}{\partial z^2}\right) - \frac{\partial^2 \psi}{\partial t^2}\right] = 0 \tag{2.5.5}$$

Eqs. (2.5.4) and (2.5.5), leads to two uncoupled equations as

$$\nabla^2 \phi = \frac{1}{C_1^2} \frac{\partial^2 \phi}{\partial t^2} \tag{2.5.6}$$

$$\nabla^2\psi - l^2\nabla^4\psi = \frac{1}{C_2^2}\frac{\partial^2\psi}{\partial t^2} \tag{2.5.7}$$

As characteristic length (l) is already absent in Eq. (2.5.6) and if we take $l = 0$ in Eq. (2.5.7), we get the case of classical theory of elasticity.

From constitutive relations (2.2.4) and (2.2.5), we get

$$\sigma_{zx} = \mu\left(\frac{\partial u}{\partial z} + \frac{\partial w}{\partial x}\right) - \mu l^2\left(\frac{\partial^3 u}{\partial x^2\partial z} - \frac{\partial^3 w}{\partial x^3} + \frac{\partial^3 u}{\partial z^3} - \frac{\partial^3 w}{\partial z^2\partial x}\right) \tag{2.5.8}$$

$$\sigma_{zz} = \lambda\left(\frac{\partial u}{\partial x} + \frac{\partial w}{\partial z}\right) + 2\mu\frac{\partial w}{\partial z} \tag{2.5.9}$$

$$\mu_{zy} = 2\eta\left(\frac{\partial^2 u}{\partial z^2} - \frac{\partial^2 w}{\partial z\partial x}\right) \tag{2.5.10}$$

Now by using Eq. (2.5.3), in Eqs (2.5.8), (2.5.9) and (2.5.10), we get

$$\sigma_{zx} = \mu\left(\frac{\partial^2\psi}{\partial x^2} - \frac{\partial^2\psi}{\partial z^2} + 2\frac{\partial^2\phi}{\partial x\partial z}\right) + \mu l^2\left(\frac{\partial^4\psi}{\partial x^4} + \frac{\partial^4\psi}{\partial z^4} + 2\frac{\partial^4\psi}{\partial x^2\partial z^2}\right) \tag{2.5.11}$$

$$\sigma_{zz} = \mu\left[\frac{C_1^2}{C_2^2}\left(\frac{\partial^2\phi}{\partial x^2} + \frac{\partial^2\phi}{\partial z^2}\right) - 2\frac{\partial^2\phi}{\partial x^2} + 2\frac{\partial^2\psi}{\partial x\partial z}\right] \tag{2.5.12}$$

$$\mu_{zy} = -2\mu l^2\left(\frac{\partial^3\psi}{\partial z^3} + \frac{\partial^3\psi}{\partial z\partial x^2}\right) \tag{2.5.13}$$

Assuming a solution of the form

$$\phi = f(z)\mathrm{e}^{i\xi(x-ct)} \tag{2.5.16}$$

$$\psi = g(z)\mathrm{e}^{i\xi(x-ct)} \tag{2.5.17}$$

where c is the phase velocity and ξ is the wave number.

Putting the solution (2.5.16) in Eq. (2.5.6) and by solving it, gives us following differential equation

$$\frac{d^2f(z)}{dz^2} + \alpha^2 f(z) = 0 \tag{2.5.18}$$

where $\alpha^2 = \frac{\xi^2c^2}{C_1^2} - \xi^2$

Solution to this differential equation is

$$f(z) = [A_1 Cos(\alpha z) + A_2 Sin(\alpha z)]$$

Putting it in Eq. (2.5.16), we get

$$\phi = (A_1 Cos\alpha z + A_2 Sin\alpha z)\mathrm{e}^{i\xi(x-ct)} \tag{2.5.19}$$

where A_1 and A_2 are unknown constants

Again using solution (2.5.17) in Eq. (2.5.7), we get following differential equation

$$\frac{d^4 g(z)}{dz^4} + (\beta^2 + \gamma^2)\frac{d^2 g(z)}{dz^2} + \beta^2\gamma^2 g(z) = 0 \tag{2.5.20}$$

where

$$(\beta^2 + \gamma^2) = -\left(2\xi^2 + \frac{1}{l^2}\right)$$

$$\beta^2\gamma^2 = \frac{\xi^2}{l^2}\left(1 + \xi^2 l^2 - \frac{c^2}{C_2^2}\right)$$

Differential Eq. (2.5.20) can be written as

$$(D^2 + \beta^2)(D^2 + \gamma^2)g(z) = 0 \tag{2.5.21}$$

where $D \equiv \frac{d}{dz}$ and $D^2 \equiv \frac{d^2}{dz^2}$

Hence solution to differential Eq. in (2.5.21) is

$$g(z) = [A_3 Cos(\beta z) + A_4 Sin(\beta z) + A_5 Cos(\gamma z) + A_6 Sin(\gamma z)]$$

where A_3, A_4, $A_5$and A_6 are unknown constants and putting it in Eq. (2.5.17), we get

$$\psi = (A_3 Cos\beta z + A_4 Sin\beta z + A_5 Cos\gamma z + A_6 Sin\gamma z)\mathrm{e}^{i\xi(x-ct)} \tag{2.5.22}$$

Now substituting the values of ϕ and ψ from (2.5.19) and (2.5.22) in Eq. (2.5.3), we get the displacement components as

$$u = \begin{bmatrix} (A_1 Cos\alpha z + A_2 Sin\alpha z)i\xi - \\ (-A_3\beta Sin\beta z + A_4\beta Cos\beta z - A_5\gamma Sin\gamma z + A_6\gamma Cos\gamma z) \end{bmatrix}\mathrm{e}^{i\xi(x-ct)} \tag{2.5.23}$$

$$w = \begin{bmatrix} (-A_1\alpha Sin\alpha z + A_2\alpha Cos\alpha z) + \\ (A_3 Cos\beta z + A_4 Sin\beta z + A_5 Cos\gamma z + A_6 Sin\gamma z)i\xi \end{bmatrix}\mathrm{e}^{i\xi(x-ct)} \tag{2.5.24}$$

Now putting the values of potential functions ϕ and ψ from Eqs. (2.5.19) and (2.5.22) in Eqs. (2.5.11), (2.5.12) and (2.5.13), we get stresses and couple stress as

$$\sigma_{zx} = \mu \begin{Bmatrix} -2i\xi\alpha Sin(\alpha z)A_1 + 2i\xi\alpha Cos(\alpha z)A_2 + \\ (-\xi^2 + \beta^2 + l^2\xi^4 + l^2\beta^4 + 2l^2\xi^2\beta^2)Cos(\beta z)A_3 + \\ (-\xi^2 + \beta^2 + l^2\xi^4 + l^2\beta^4 + 2l^2\xi^2\beta^2)Sin(\beta z)A_4 + \\ (-\xi^2 + \gamma^2 + l^2\xi^4 + l^2\gamma^4 + 2l^2\xi^2\gamma^2)Cos(\gamma z)A_5 + \\ (-\xi^2 + \gamma^2 + l^2\xi^4 + l^2\gamma^4 + 2l^2\xi^2\gamma^2)Sin(\gamma z)A_6 \end{Bmatrix} e^{i\xi(x-ct)} \quad (2.5.25)$$

$$\sigma_{zz} = \mu \begin{Bmatrix} \left(-\frac{C_1^2}{C_2^2}(\xi^2 + \alpha^2) + 2\xi^2\right) Cos(\alpha z)A_1 \\ + \left(-\frac{C_1^2}{C_2^2}(\xi^2 + \alpha^2) + 2\xi^2\right) Sin(\alpha z)A_2 \\ -(2i\xi\beta)Sin(\beta z)A_3 + (2i\xi\beta)Cos(\beta z)A_4 \\ -(2i\xi\gamma)Sin(\gamma z)A_5 + (2i\xi\gamma)Cos(\gamma z)A_6 \end{Bmatrix} e^{i\xi(x-ct)} \quad (2.5.26)$$

$$\mu_{zy} = -2\eta \begin{Bmatrix} (\beta^3 + \xi^2\beta)Sin(\beta z)A_3 - (\beta^3 + \xi^2\beta)Cos(\beta z)A_4 + \\ (\gamma^3 + \xi^2\gamma)Sin(\gamma z)A_5 - (\gamma^3 + \xi^2\gamma)Cos(\gamma z)A_6 \end{Bmatrix} e^{i\xi(x-ct)} \quad (2.5.27)$$

2.6 DERIVATION OF SECULAR EQUATION

Invoking boundary conditions $\sigma_{zx} = 0$, $\sigma_{zz} = 0$ and $\mu_{zy} = 0$, at the surfaces $z = \pm d$, of the plate and using Eqs. (2.5.25), (2.5.26) and (2.5.27), we obtain the following system of equations

$$\mu \begin{Bmatrix} -2i\xi\alpha S_1 A_1 + 2i\xi\alpha C_{11} A_2 + (-\xi^2 + \beta^2 + l^2\xi^4 + l^2\beta^4 + 2l^2\xi^2\beta^2)C_{22} A_3 \\ +(-\xi^2 + \beta^2 + l^2\xi^4 + l^2\beta^4 + 2l^2\xi^2\beta^2)S_2 A_4 + \\ (-\xi^2 + \gamma^2 + l^2\xi^4 + l^2\gamma^4 + 2l^2\xi^2\gamma^2)C_3 A_5 + \\ (-\xi^2 + \gamma^2 + l^2\xi^4 + l^2\gamma^4 + 2l^2\xi^2\gamma^2)S_3 A_6 \end{Bmatrix} = 0 \quad (2.6.1)$$

$$\mu \begin{Bmatrix} \left(-\frac{C_1^2}{C_2^2}(\xi^2 + \alpha^2) + 2\xi^2\right) C_{11} A_1 + \left(-\frac{C_1^2}{C_2^2}(\xi^2 + \alpha^2) + 2\xi^2\right) S_1 A_2 \\ -(2i\xi\beta)S_2 A_3 + (2i\xi\beta)C_{22} A_4 - (2i\xi\gamma)S_3 A_5 + (2i\xi\gamma)C_3 A_6 \end{Bmatrix} = 0 \quad (2.6.2)$$

$$2\eta \begin{Bmatrix} (\beta^3 + \xi^2\beta)S_2 A_3 - (\beta^3 + \xi^2\beta)C_{22} A_4 + \\ (\gamma^3 + \xi^2\gamma)S_3 A_5 - (\gamma^3 + \xi^2\gamma)C_3 A_6 \end{Bmatrix} = 0 \quad (2.6.3)$$

where

$S_1 = Sin(\alpha d)$, $S_2 = Sin(\beta d)$, $S_3 = Sin(\gamma d)$

$C_{11} = Cos(\alpha d)$, $C_{22} = Cos(\beta d), C_3 = Cos(\gamma d)$.

For symmetric modes of Lamb waves $w = 0$ at $z = 0$, by imposing this condition on Eq. (2.5.24), we get $A_2 = A_3 = A_5 = 0$, using this condition in Eqs. (2.6.1), (2.6.2) and (2.6.3) we obtain

$$\mu\begin{Bmatrix}(-2i\xi\alpha)S_1A_1+(-\xi^2+\beta^2+l^2\xi^4+l^2\beta^4+2l^2\xi^2\beta^2)S_2A_4\\ +(-\xi^2+\gamma^2+l^2\xi^4+l^2\gamma^4+2l^2\xi^2\gamma^2)S_3A_6\end{Bmatrix}=0 \quad (2.6.4)$$

$$\mu\left\{\left(-\frac{C_1^2}{C_2^2}(\xi^2+\alpha^2)+2\xi^2\right)C_{11}A_1+(2i\xi\beta)C_{22}A_4+(2i\xi\gamma)C_3A_6\right\}=0 \quad (2.6.5)$$

$$2\eta\{-(\beta^3+\xi^2\beta)C_{22}A_4-(\gamma^3+\xi^2\gamma)C_3A_6\}=0 \quad (2.6.6)$$

Above three equations will have a non-trivial solution if determinant of coefficients of unknowns A_1, A_4 and A_6 vanishes.

$$\begin{vmatrix}-2i\xi\alpha S_1 & (-\xi^2+\beta^2+l^2(\beta^2+\xi^2)^2)S_2 & (-\xi^2+\gamma^2+l^2(\gamma^2+\xi^2)^2)S_3\\ PC_{11} & (2i\xi\beta)C_{22} & (2i\xi\gamma)C_3\\ 0 & (\beta^3+\xi^2\beta)C_{22} & (\gamma^3+\xi^2\gamma)C_3\end{vmatrix}=0 \quad (2.6.7)$$

By solving the determinant we get secular equation for symmetric modes of Lamb wave as

$$\beta K_\beta\left[(\gamma^2-\xi^2)+l^2K_\gamma^2\right]\left(\frac{t_3}{t_1}\right)-\gamma K_\gamma\left[(\beta^2-\xi^2)+l^2K_\beta^2\right]\left(\frac{t_2}{t_1}\right)=\frac{4\alpha\beta\gamma\,\xi^2(K_\beta-K_\gamma)}{P} \quad (2.6.8)$$

For skew symmetric modes of Lamb waves $u=0$ at $z=0$, by imposing this condition on Eq. (2.5.23), we get $A_1=A_4=A_6=0$, using this condition Eqs. (2.6.1), (2.6.2) and (2.6.3) we obtain

$$\mu\begin{Bmatrix}(2i\xi\alpha)C_{11}A_2+(-\xi^2+\beta^2+l^2\xi^4+l^2\beta^4+2l^2\xi^2\beta^2)C_{22}A_3\\ +(-\xi^2+\gamma^2+l^2\xi^4+l^2\gamma^4+2l^2\xi^2\gamma^2)C_3A_5\end{Bmatrix}=0 \quad (2.6.9)$$

$$\mu\left\{\left(-\frac{C_1^2}{C_2^2}(\xi^2+\alpha^2)+2\xi^2\right)S_1A_2-(2i\xi\beta)S_2A_3-(2i\xi\gamma)S_3A_5\right\}=0 \quad (2.6.10)$$

$$2\eta\{(\beta^3+\xi^2\beta)S_2A_3+(\gamma^3+\xi^2\gamma)S_3A_5\}=0 \quad (2.6.11)$$

Above three equations will have a non-trivial solution if determinant of coefficients of unknowns A_2, A_3 and A_5 vanishes.

$$\begin{vmatrix}2i\xi\alpha C_{11} & (-\xi^2+\beta^2+l^2(\beta^2+\xi^2)^2)C_{22} & (-\xi^2+\gamma^2+l^2(\gamma^2+\xi^2)^2)C_3\\ PS_1 & -(2i\xi\beta)S_2 & -(2i\xi\gamma)S_3\\ 0 & (\beta^3+\xi^2\beta)S_2 & (\gamma^3+\xi^2\gamma)S_3\end{vmatrix}=0 \quad (2.6.12)$$

By solving the determinant, we get secular equation for skew symmetric modes of Lamb wave as

$$\beta K_\beta\left[(\gamma^2-\xi^2)+l^2K_\gamma^2\right]\left(\frac{t_1}{t_3}\right)-\gamma K_\gamma\left[(\beta^2-\xi^2)+l^2K_\beta^2\right]\left(\frac{t_1}{t_2}\right)=\frac{4\alpha\beta\gamma\,\xi^2(K_\beta-K_\gamma)}{P} \quad (2.6.13)$$

Hence, by joining both (2.6.12) and (2.6.13) together, we obtain the following secular equations for the Lamb waves in a stress and couple stress free elastic plate

$$\beta K_\beta\left[(\gamma^2-\xi^2)+l^2K_\gamma^2\right]\left(\frac{t_3}{t_1}\right)^{\pm1}-\gamma K_\gamma\left[(\beta^2-\xi^2)+l^2K_\beta^2\right]\left(\frac{t_2}{t_1}\right)^{\pm1}=\frac{4\alpha\beta\gamma\,\xi^2(K_\beta-K_\gamma)}{P} \qquad (2.6.14)$$

where

$K_\beta=(\beta^2+\xi^2)$

$K_\gamma=(\gamma^2+\xi^2)$

$P=\left(-\frac{C_1^2}{C_2^2}(\xi^2+\alpha^2)+2\xi^2\right)$

$t_1=\frac{S_1}{C_{11}}$, $t_2=\frac{S_2}{C_{22}}$ and $t_3=\frac{S_3}{C_3}$

Here the superscript +1 corresponds to symmetric and -1 refers to skew symmetric modes of Lamb wave propagation. Eq. (2.6.14) represents the dispersion relation involving wave number, phase velocity of Lamb waves and characteristic length (l) of the material for different modes of propagation of lamb waves in a plate under the effect of couple stresses.

2.7 NUMERICAL RESULTS AND DISCUSSION

Following Vavva *et al*. [137], physical constants for bone like material are

E= Young's Modulus	$\frac{\mu(3\lambda+2\mu)}{(\lambda+\mu)}$	$14\ GPa$
ν =Poisson Ratio	$\frac{\lambda}{2(\lambda+\mu)}$	0.37
ρ =Density		1500 kg/m^3

Table 2.1 Physical data for cortical bone

The values of bulk longitudinal and shear velocities comes out to be C_1 = 4063 m/s, C_2 = 1846 m/s respectively. Here, $h=10^{-4}m=0.0001m$ comparable with the size of bone's microstructure.

In Fig. 2.3, it is observed that the dispersion of the lowest skew symmetrical mode (m=0) of Lamb waves is significantly modified from that of classical theory of elasticity. These effects

are more pronounced for the higher wave numbers. For better graphical representation of the results, this figure is drawn by considering phase velocity on the logarithmic scale.

The variation of phase velocity of Lamb waves for m=1 skew symmetrical mode are plotted in Fig. 2.4. Here, profiles seem to be quite in agreement, therefore to study the difference in two profiles, ratios of the phase velocities are plotted in Fig. 2.5. It is observed that for higher wave numbers phase velocity increases under the effect of couple stresses.

Fig. 2.6, shows the ratio of phase velocity under the effect of couple stresses and in classical theory of elasticity, for m=2 skew symmetrical mode. It can again be seen, even in this case, that for the higher wave numbers phase velocity of Lamb waves, under the effect of couple stresses has increased as compared to their velocity in classical theory of elasticity and for the lower wave numbers profiles are same.

Thus from Figs. 2.3-2.6, it can be concluded that though meagre, but impact of characteristic length is observed on the phase velocity profiles in the higher wave number region.

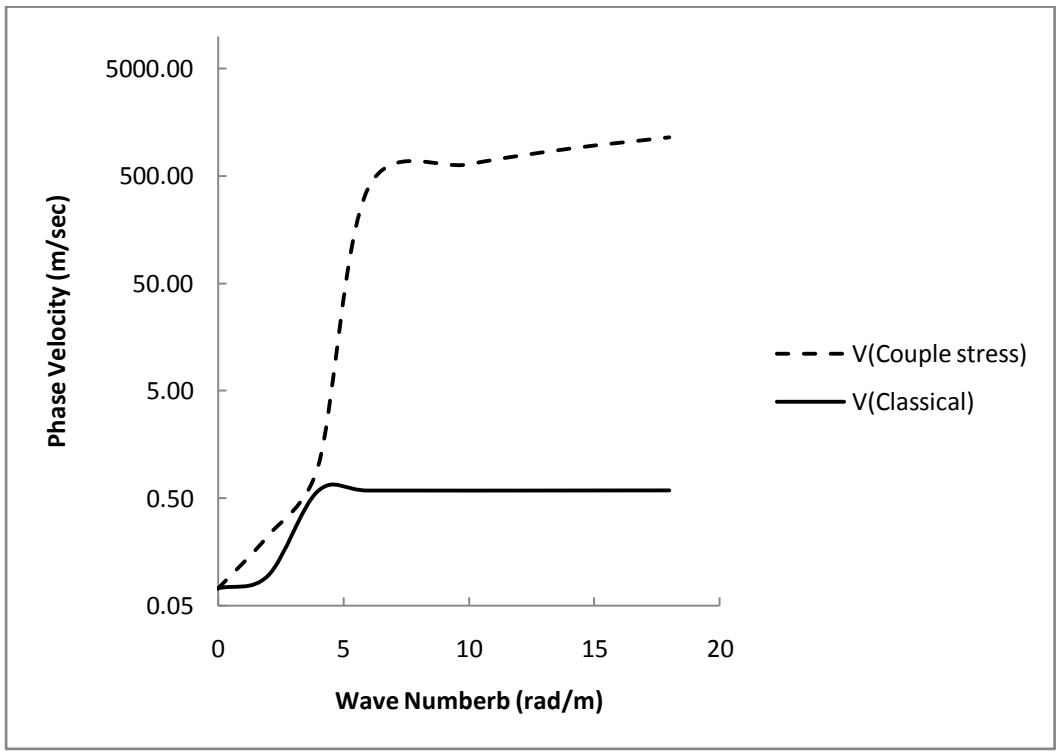

Figure 2.3 Phase velocity profile of lamb waves with wave number in lowest ($m = 0$) skew symmetrical mode in logarithmic scale

Fig. 2.7, shows the phase velocity of skew symmetrical Lamb waves in different modes, under the effect of couple stresses. It is observed, that for a fixed wave number phase velocity

of higher skew symmetrical modes is greater as compared to the lower modes and this same pattern can also be seen in the case of classical theory of elasticity. In Figs. 2.3-2.7, characteristic length l is assumed to be of the order of cell size ($h = 0.0001$m) of the material.

Variation of phase velocity profiles are plotted in Fig. 2.8, for different combinations of characteristic length with respect to the cell size of the material for m=0, skew symmetrical mode. By keeping the cell size $h = 0.0001$ m, we have shown the phase velocity of Lamb waves for different values of internal characteristic length of the material (i) VL1, represents the phase velocity of Lamb waves when $l = 0.00004m < h$ (ii) VL represents the phase velocity of Lamb waves when $l = 0.0001m = h$ (iii) VL0, represents the phase velocity of Lamb waves when $l = 0.001m > h$. It can be seen that profiles are modified with change in characteristic length. Fig. 2.9 describes the variations in the phase velocity profiles for m=1 skew symmetrical mode, since the variations are very small, so again ratios have been plotted. The departure of $l < h$ and $l > h$ profiles can be easily seen from $l = h$ profile.

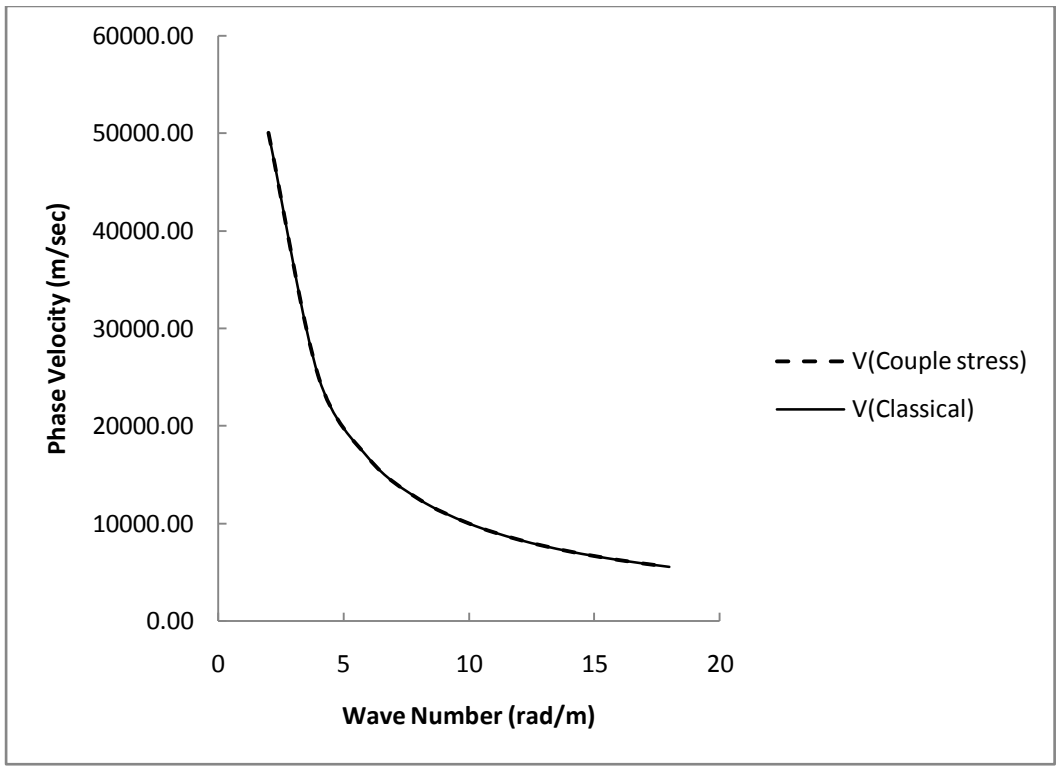

Figure 2.4 Phase velocity profile of lamb waves with wave number in $m = 1$ skew symmetrical mode

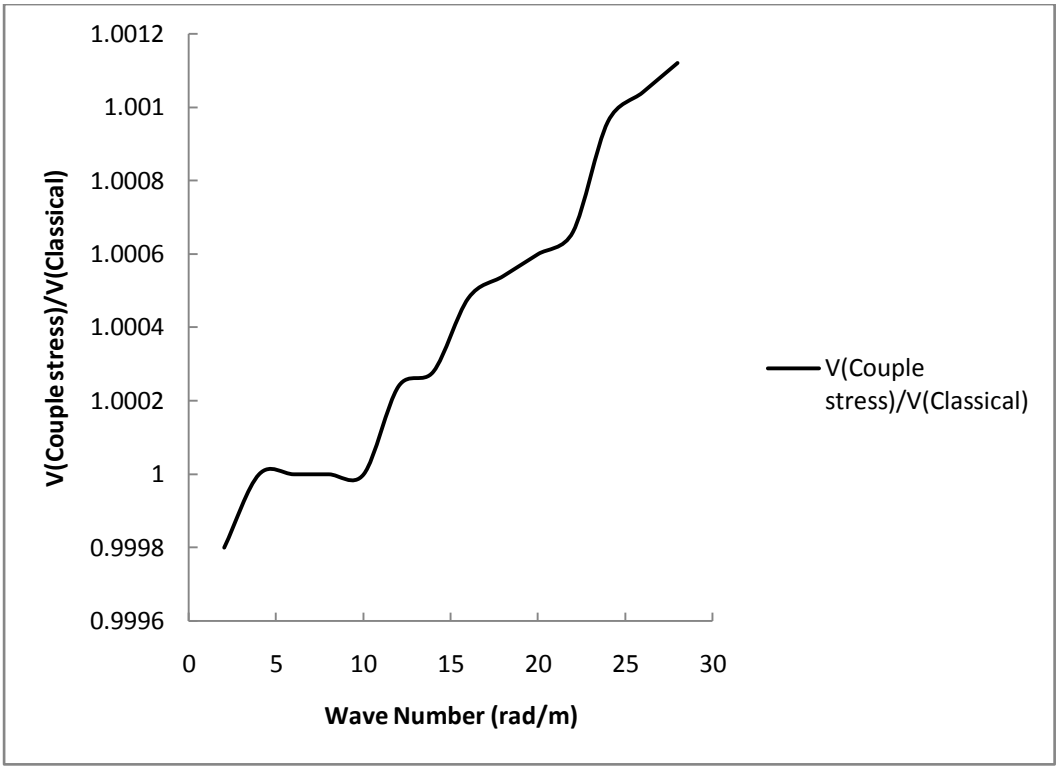

Figure 2.5 Ratio of phase velocity of skew symmetrical Lamb waves in couple stress and classical model for $m = 1$ mode

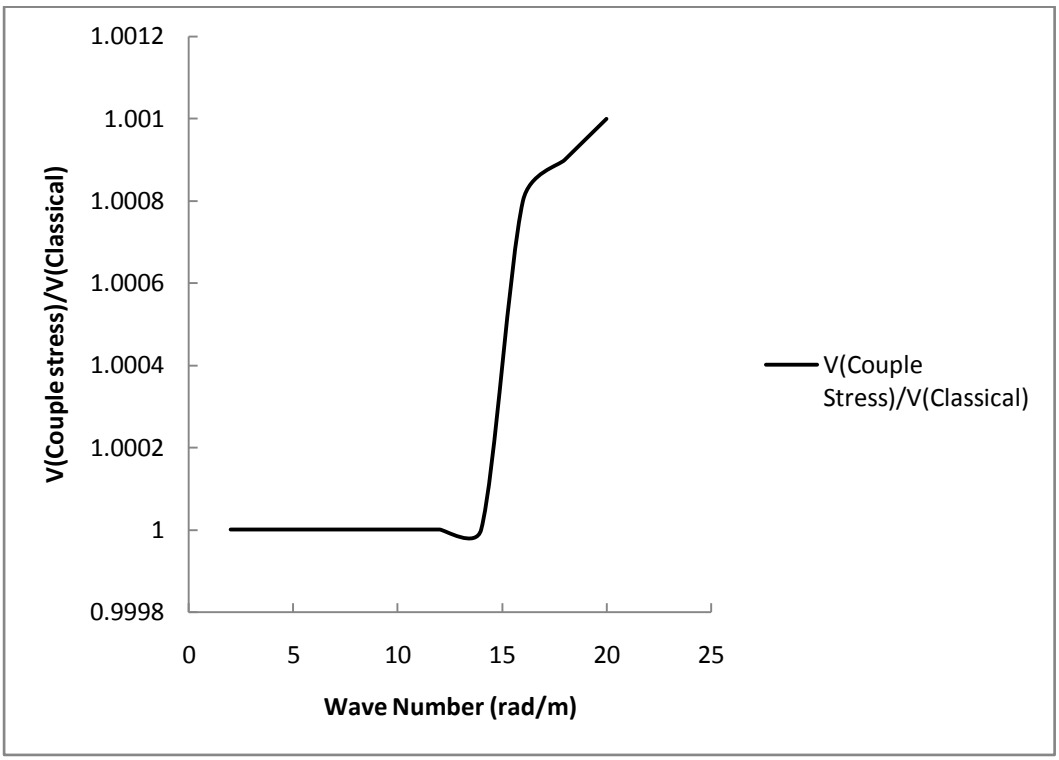

Figure 2.6 Ratio of phase velocity of skew symmetrical Lamb waves in couple stress and classical model for $m = 2$ mode

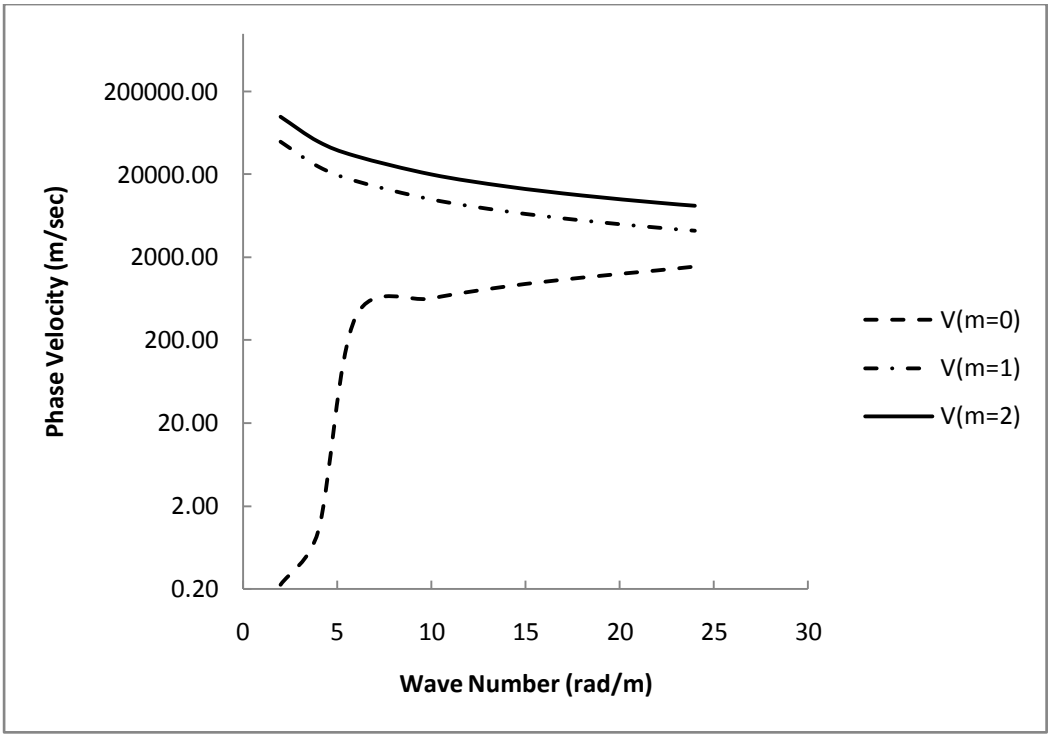

Figure 2.7 Phase velocity profile of lamb waves with wave number in different skew symmetrical modes under the effect of couple stress in logarithmic scale

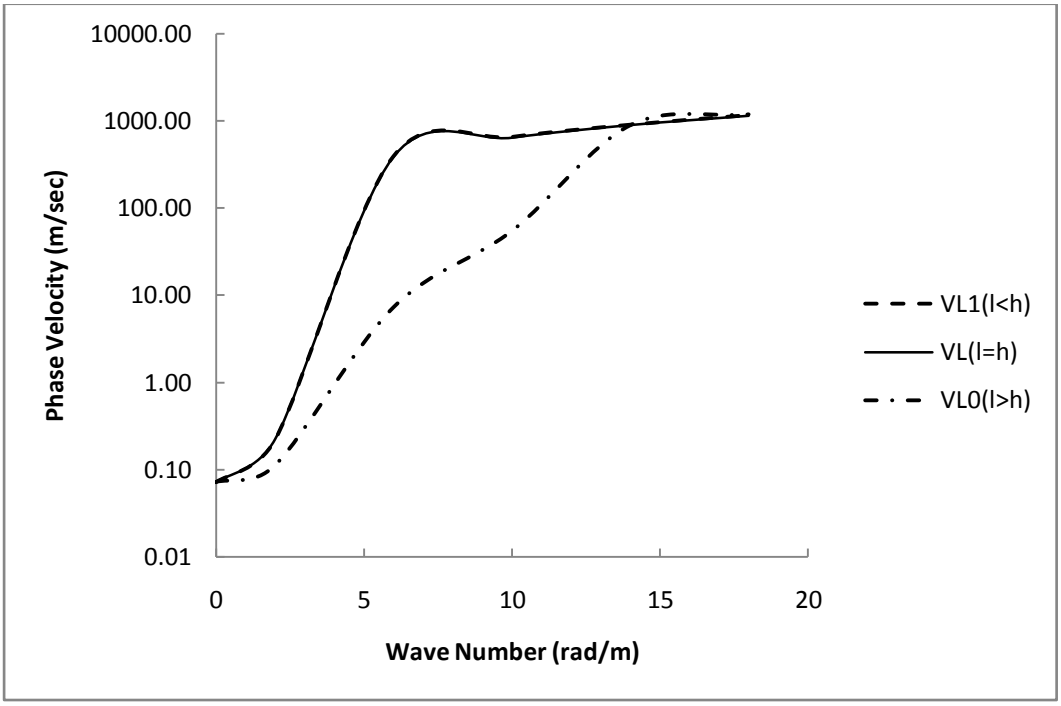

Figure 2.8 Phase velocity profile of Lamb waves in $m = 0$ skew symmetric mode under varying characteristic length (VL is the phase velocity, when $l = h = 0.0001\ m$; VL1 is the phase velocity, when $l = 0.00004\ m < h$ and VL0 is the phase velocity, when $l = 0.001\ m > h$)

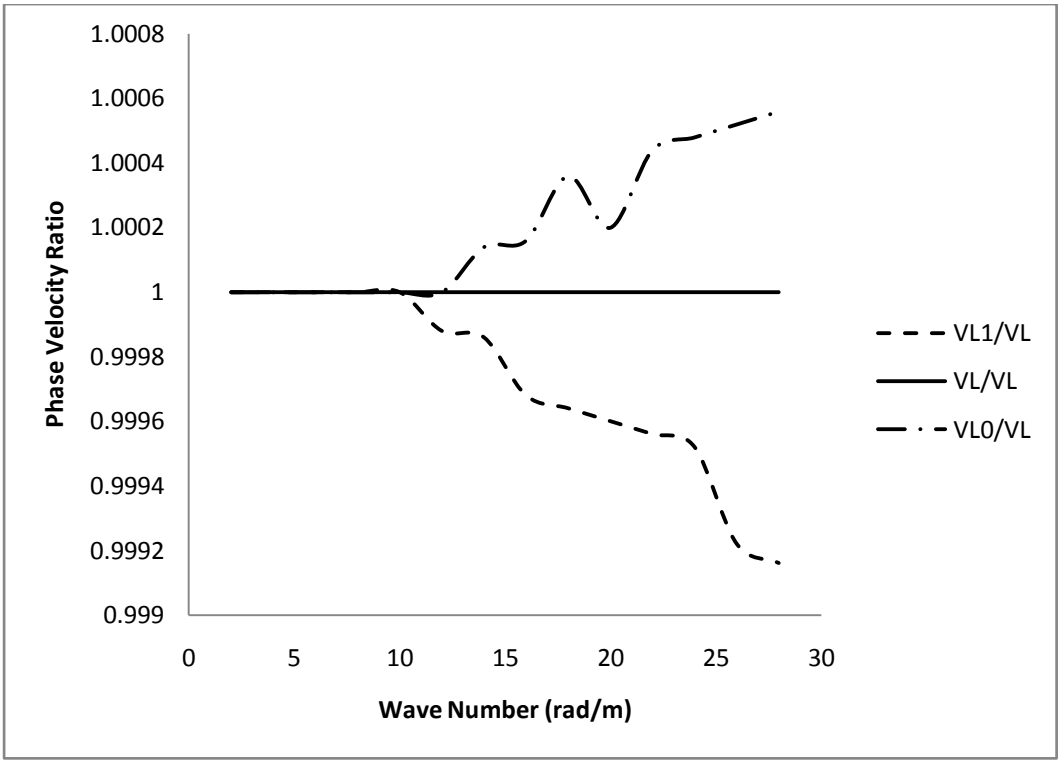

Figure 2.9 Ratio of phase velocity profile of Lamb waves in $m = 1$ skew symmetric mode with varying characteristic length (VL is the phase velocity, when $l = h = 0.0001\, m$, VL1 is the phase velocity, when $l = 0.00004\, m < h$ and VL0 is phase velocity, when $l = 0.001\, m > h$)

2.8 CONCLUSION

In this chapter, microstructural effects on the propagation of skew symmetric modes of Lamb waves have been presented. Comparisons of the results obtained under couple stress theory have been made with the results of classical theory of elasticity. Effects of varying characteristic length as compared to cell size have been observed. Couple stress theory is proposed to incorporate the microstructural effects into stress analysis. It is observed that characteristic length plays a major role in the propagation of shear waves and phase velocity increases with the increase in characteristic length. Phase velocity profiles for different Lamb wave modes are modified under the effect of couple stress theory. In case of Lamb wave modes, distinctions in the profiles for various combinations of characteristic lengths are observed. Since bones have a microstructure (Fatemi *et al*. [34] and Vavva *et al*. [137]), so the study has been carried out for a cortical bone type material and this work will be quite useful for evaluation of characteristics of bones and the material exhibiting microstructures.

CHAPTER-3

EFFECTS OF LIQUID LOADINGS ON LAMB WAVES IN CONTEXT OF SIZE DEPENDENT COUPLE STRESS THEORY[2]

3.1 INTRODUCTION

The dynamical characteristics of a structure get affected when it is surrounded by a fluid. This study becomes more important when the material under consideration exhibits internal microstructure. Lamb waves are guided waves, propagating in a traction free plate surface, however if the surface of the plate is in contact with the fluid a part of energy will leak into the liquid and this phenomena may find possible applications not only in non destructive evaluation of materials, but also in biomedical field. Keeping this in mind, the fluid-solid model adopted by Sharma and Kumar [115] is applied, to extend the study of Lamb waves carried in chapter-2 using a thin elastic plate with microstructure. The problem of propagation of Lamb waves in a plate with internal microstructure and loaded with inviscid liquid on both sides is studied using couple stress theory. Dispersion equation of Lamb waves with liquid loadings is derived. The impact of liquid loadings is studied on the propagation of Lamb waves. Effect of characteristic length (l) is also studied on the phase velocity of Lamb waves in plate for various modes in the presence of liquid loadings

3.2 FORMULATION AND SOLUTION OF THE PROBLEM

Consider an infinite homogeneous isotropic, elastic plate of thickness $2d$. The plate is bordered both on the top and bottom with infinitely large homogeneous inviscid liquid layers of thickness H. Consider the origin of the coordinate system (x, y, z) in the middle of the plate. The XY- plane is chosen to coincide with the middle surface of the plate and z-axis is normal to the plate, along the thickness of the plate pointing vertically downwards. We consider the XZ- plane as the plane of incidence and assume that solutions are explicitly independent of y that is $\frac{\partial}{\partial y} \equiv 0$.

[2] Contents of this chapter are published in SCI indexed journal, *Journal of Theoretical and Applied Mechanics* (2015), **53**(4):925-934 with impact factor-0.636

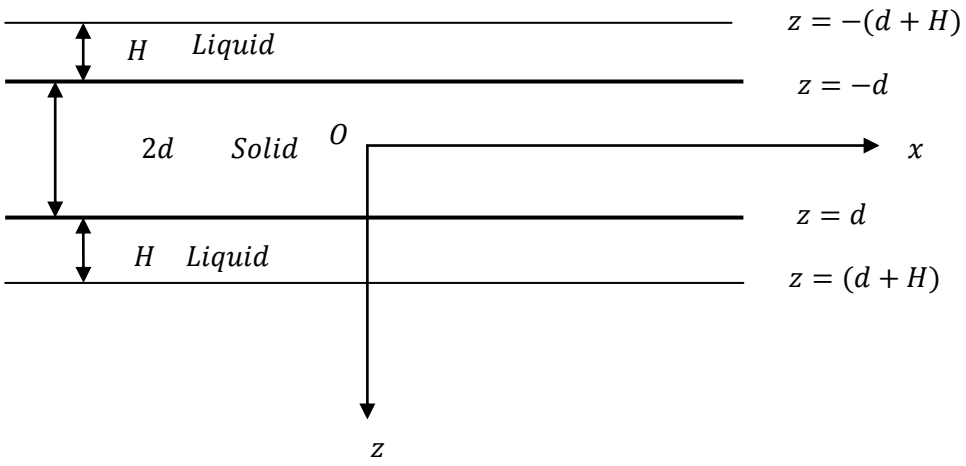

Figure 3.1 Geometry of the problem

The basic governing equation of motion and constitutive relations of couple stress elasticity for isotropic material in the absence of body forces (Hadjesfandiari and Dargush, [46]) are given in chapter-2 in Eqs. (2.2.1), (2.2.4) and (2.2.5)

In the liquid boundary layers, we have

$$\left.\begin{aligned} u'_1 &= \frac{\partial \phi_1}{\partial x} - \frac{\partial \psi_1}{\partial z} \\ w'_1 &= \frac{\partial \phi_1}{\partial z} + \frac{\partial \psi_1}{\partial x} \end{aligned}\right\} \tag{3.2.1}$$

$$\left.\begin{aligned} u'_2 &= \frac{\partial \phi_2}{\partial x} - \frac{\partial \psi_2}{\partial z} \\ w'_2 &= \frac{\partial \phi_2}{\partial z} + \frac{\partial \psi_2}{\partial x} \end{aligned}\right\} \tag{3.2.2}$$

where ϕ_j and ψ_j, $j = 1, 2$ are the scalar and vector potential functions for the bottom liquid layer $(j = 1)$ and for the top liquid layer $(j = 2)$, u'_j and w'_j are respectively, x and z components of the particle displacement in the layers of liquid. Because inviscid liquid does not support the shear motion, so shear modulus of the liquid vanishes that is $\mu = 0$ and hence $\psi_j = 0, j = 1, 2$. Hence Eqs. (3.2.1) and (3.2.2) reduce to

$$\left.\begin{aligned} u'_1 &= \frac{\partial \phi_1}{\partial x} \\ w'_1 &= \frac{\partial \phi_1}{\partial z} \end{aligned}\right\} \tag{3.2.3}$$

$$\left.\begin{aligned} u'_2 &= \frac{\partial \phi_2}{\partial x} \\ w'_2 &= \frac{\partial \phi_2}{\partial z} \end{aligned}\right\} \tag{3.2.4}$$

The potential function ϕ_j satisfy the basic governing equation

$$\nabla^2\phi_j = \frac{1}{C_L^2}\frac{\partial^2\phi_j}{\partial t^2} \tag{3.2.5}$$

where $C_L^2 = \frac{\lambda_L}{\rho_L}$, C_L is the velocity of sound in the liquid and λ_L is the bulk modulus of inviscid liquid.

For the liquid stresses are given by

$$\sigma'_{ji} = \lambda_L u'_{k,k}\delta_{ij}$$

and couple stresses in case of liquid are all zero. Prime denotes same quantities for the liquid layer as defined in couple stress theory.

$$\sigma'_{zz} = \lambda_L\left(\frac{\partial u_j^{'}}{\partial x} + \frac{\partial w_j^{'}}{\partial z}\right) \tag{3.2.6}$$

The value of stresses in liquid in terms of potential function becomes

$$\sigma'_{zz} = \lambda_L\left(\frac{\partial^2\phi_j}{\partial x^2} + \frac{\partial^2\phi_j}{\partial z^2}\right) \tag{3.2.7}$$

We assume solutions of the form

$$\phi = f(z)\, e^{i\xi(x-ct)} \tag{3.2.8}$$

$$\psi = g(z)e^{i\xi(x-ct)} \tag{3.2.9}$$

$$\phi_j = \bar{\phi}_j(z)\, e^{i\xi(x-ct)} \tag{3.2.10}$$

Using solutions (3.2.8), (3.2.9) and (3.2.10) in Eqs. (2.5.6), (2.5.7) and (3.2.5) and solving the resulting differential equations, we get the expressions for ϕ, ψ and ϕ_j as

$$\phi = (A_1 Cos\alpha z + A_2 Sin\alpha z)e^{i\xi(x-ct)} \tag{3.2.11}$$

$$\psi = (A_3 Cos\beta z + A_4 Sin\beta z + A_5 Cos\gamma z + A_6 Sin\gamma z)e^{i\xi(x-ct)} \tag{3.2.12}$$

$$\phi_1 = A_7 Sin\delta[z-(d+H)]e^{i\xi(x-ct)},\ d < z < d+H \tag{3.2.13}$$

$$\phi_2 = A_8 Sin\delta[z+d+H]e^{i\xi(x-ct)},\ -(d+H) < z < -d \tag{3.2.14}$$

Where

$$\delta^2 = \xi^2\left(\frac{c^2}{C_L^2} - 1\right)$$

Here ϕ_1 and ϕ_2 are solutions of standing waves and are chosen in such a way that acoustical pressure is zero at $z = \pm(d + H)$.

Using Eqs. (3.2.13) and (3.2.14) in (3.2.3), (3.2.4) and (3.2.7), we get

$$u_1^{'} = A_7 i\xi Sin\delta[z - (d + H)]e^{i\xi(x-ct)} \tag{3.2.15}$$

$$u_2^{'} = A_8 i\xi Sin\delta[z + (d + H)]e^{i\xi(x-ct)} \tag{3.2.16}$$

$$w_1^{'} = A_7 \delta Cos\delta[z - (d + H)]e^{i\xi(x-ct)} \tag{3.2.17}$$

$$w_2^{'} = A_8 \delta Cos\delta[z + (d + H)]e^{i\xi(x-ct)} \tag{3.2.18}$$

$$\sigma_{zz}^{'} = \lambda_L(-\xi^2 - \delta^2)\phi_j \tag{3.2.19}$$

3.3 BOUNDARY CONDITIONS

The boundary conditions to be satisfied at the solid – liquid interfaces $z = \pm d$ are

(i) The magnitude of the normal component of the stress tensor of the plate should be equal to the pressure of the liquid that is $\sigma_{zz} = \sigma'_{zz}$ that is

$$\lambda\left(\frac{\partial u}{\partial x} + \frac{\partial w}{\partial z}\right) + 2\mu\frac{\partial w}{\partial z} = \lambda_L\left(\frac{\partial u_j^{'}}{\partial x} + \frac{\partial w_j^{'}}{\partial z}\right)$$

(ii) Since liquid does not support the shear motion so, the tangential component of the stress in plate should be equal to zero, which implies $\sigma_{zx} = 0$ that is

$$\mu\left(\frac{\partial u}{\partial z} + \frac{\partial w}{\partial x}\right) - \mu l^2\left(\frac{\partial^3 u}{\partial x^2 \partial z} - \frac{\partial^3 w}{\partial x^3} + \frac{\partial^3 u}{\partial z^3} - \frac{\partial^3 w}{\partial z^2 \partial x}\right) = 0$$

(iii) Couple stress tensor, μ_{zy} should vanish at the interface that is $\mu_{zy} = 0$ that is

$$2\eta\left(\frac{\partial^2 u}{\partial z^2} - \frac{\partial^2 w}{\partial z \partial x}\right) = 0$$

(iv) Normal component of the displacement field of the solid plate should be equal to that of the liquid that is $w = w'_j$ where $j = 1, 2$

3.4 DERIVATION OF SECULAR EQUATION

Imposing these above mentioned boundary conditions and using the Eqs. (2.5.25), (2.5.26), (2.5.27) and (3.2.17), (3.2.18), (3.2.19), we get the following four equations

$$\mu\begin{Bmatrix}\left(-\frac{C_1^2}{C_2^2}(\xi^2+\alpha^2)+2\xi^2\right)C_{11}A_1+\\ \left(-\frac{C_1^2}{C_2^2}(\xi^2+\alpha^2)+2\xi^2\right)S_1A_2\\ -2i\xi\beta S_2A_3+2i\xi\beta C_{22}A_4-2i\xi\gamma S_3A_5+2i\xi\gamma C_3A_6\end{Bmatrix}-\lambda_L(\xi^2+\delta^2)A_7S_4=0 \qquad (3.4.1)$$

$$\mu\begin{Bmatrix}-2i\xi\alpha S_1A_1+2i\xi\alpha C_{11}A_2+\\ (-\xi^2+\beta^2+l^2\xi^4+l^2\beta^4+2l^2\xi^2\beta^2)C_{22}A_3+\\ (-\xi^2+\beta^2+l^2\xi^4+l^2\beta^4+2l^2\xi^2\beta^2)S_2A_4+\\ (-\xi^2+\gamma^2+l^2\xi^4+l^2\gamma^4+2l^2\xi^2\gamma^2)C_3A_5\\ +(-\xi^2+\gamma^2+l^2\xi^4+l^2\gamma^4+2l^2\xi^2\gamma^2)S_3A_6\end{Bmatrix}=0 \qquad (3.4.2)$$

$$2\eta\begin{Bmatrix}(\beta^3+\xi^2\beta)S_2A_3-(\beta^3+\xi^2\beta)C_{22}A_4+\\ (\gamma^3+\xi^2\gamma)S_3A_5-(\gamma^3+\xi^2\gamma)C_3A_6\end{Bmatrix}=0 \qquad (3.4.3)$$

$$-A_1\alpha S_1+A_2\alpha C_{11}+A_3i\xi C_{22}+A_4i\xi S_2+A_5i\xi C_3+A_6i\xi S_3-A_7\delta C_4=0 \qquad (3.4.4)$$

where

$S_1=Sin(\alpha d),\ S_2=Sin(\beta d),\ S_3=Sin(\gamma d)$

$C_{11}=Cos(\alpha d),\ C_{22}=Cos(\beta d), C_3=Cos(\gamma d)$

$S_4=Sin(\delta H)$ and $C_4=Cos(\delta H)$

For symmetric modes of Lamb waves $w=0$ at $z=0$, we get $A_2=A_3=A_5=0$, using these conditions in Eqs. (3.4.1) to (3.4.4), we obtain following four equations

$$\mu\left\{\left(-\frac{C_1^2}{C_2^2}(\xi^2+\alpha^2)+2\xi^2\right)C_{11}A_1+2i\xi\beta C_{22}A_4+2i\xi\gamma C_3A_6\right\}-\lambda_L(\xi^2+\delta^2)A_7S_4=0 \qquad (3.4.5)$$

$$\begin{Bmatrix}(-2i\xi\alpha)S_1A_1+(-\xi^2+\beta^2+l^2\xi^4+l^2\beta^4+2l^2\xi^2\beta^2)S_2A_4\\ +(-\xi^2+\gamma^2+l^2\xi^4+l^2\gamma^4+2l^2\xi^2\gamma^2)S_3A_6\end{Bmatrix}=0 \qquad (3.4.6)$$

$$-(\beta^3+\xi^2\beta)C_{22}A_4-(\gamma^3+\xi^2\gamma)C_3A_6=0 \qquad (3.4.7)$$

$$-A_1\alpha S_1+A_4i\xi S_2+A_6i\xi S_3-A_7\delta C_4=0 \qquad (3.4.8)$$

Above three equations will have a non-trivial solution if determinant of coefficients of unknowns A_1, A_4, A_6 and A_7 vanishes, so by imposing this condition we get

$$\begin{vmatrix} \mu P C_{11} & 2i\xi\beta\mu C_{22} & 2i\xi\gamma\mu C_3 & -\lambda_L(\xi^2+\delta^2)S_4 \\ -2i\xi\alpha S_1 & (\beta^2-\xi^2+l^2(\beta^2+\xi^2)^2)S_2 & (\gamma^2-\xi^2+l^2(\gamma^2+\xi^2)^2)S_3 & 0 \\ 0 & (\beta^3+\xi^2\beta)C_{22} & (\gamma^3+\xi^2\gamma)C_3 & 0 \\ -\alpha S_1 & i\xi S_2 & i\xi S_3 & -\delta C_4 \end{vmatrix} = 0$$

(3.4.9)

By solving above determinant, we get secular equation for symmetric modes of Lamb wave in a plate loaded with inviscid liquid layer on both sides as

$$\alpha\lambda_L K_\beta K_\gamma K_\delta\left[\beta\left(1+l^2K_\gamma\right)t_3t_4-\gamma\left(1+l^2K_\beta\right)t_2t_4\right]+\beta K_\beta\left[(\gamma^2-\xi^2)+l^2K_\gamma^2\right]\mu\delta P\left(\frac{t_3}{t_1}\right)-$$

$$\gamma K_\gamma\left[(\beta^2-\xi^2)+l^2K_\beta^2\right]\mu\delta P\left(\frac{t_2}{t_1}\right)=4\alpha\beta\gamma\delta\mu\xi^2\left(K_\beta-K_\gamma\right) \quad (3.4.10)$$

For skew symmetric modes of Lamb waves $u=0$ at $z=0$, we get $A_1=A_4=A_6=0$, using this condition in Eqs. (3.4.1) to (3.4.4), we obtain following four equations

$$\mu\left\{\left(-\frac{C_1^2}{C_2^2}(\xi^2+\alpha^2)+2\xi^2\right)S_1A_2-2i\xi\beta S_2A_3-2i\xi\gamma S_3A_5\right\}-\lambda_L(\xi^2+\delta^2)A_7S_4=0 \quad (3.4.11)$$

$$\left\{\begin{matrix}(2i\xi\alpha)C_{11}A_2+(-\xi^2+\beta^2+l^2\xi^4+l^2\beta^4+2l^2\xi^2\beta^2)C_{22}A_3\\ +(-\xi^2+\gamma^2+l^2\xi^4+l^2\gamma^4+2l^2\xi^2\gamma^2)C_3A_5\end{matrix}\right\}=0 \quad (3.4.12)$$

$$(\beta^3+\xi^2\beta)S_2A_3+(\gamma^3+\xi^2\gamma)S_3A_5=0 \quad (3.4.13)$$

$$A_2\alpha C_{11}+i\xi C_{22}A_3+i\xi C_3A_5-A_7\delta C_4=0 \quad (3.4.14)$$

Above four equations will have a non-trivial solution if determinant of coefficients of unknowns A_2, A_3, A_5 and A_7 vanishes.

$$\begin{vmatrix} \mu P S_1 & -2i\xi\beta\mu S_2 & -2i\xi\gamma\mu S_3 & -\lambda_L(\xi^2+\delta^2)S_4 \\ 2i\xi\alpha C_{11} & (\beta^2-\xi^2+l^2(\beta^2+\xi^2)^2)C_{22} & (\gamma^2-\xi^2+l^2(\gamma^2+\xi^2)^2)C_3 & 0 \\ 0 & (\beta^3+\xi^2\beta)S_2 & (\gamma^3+\xi^2\gamma)S_3 & 0 \\ \alpha C_{11} & i\xi C_{22} & i\xi C_3 & -\delta C_4 \end{vmatrix} = 0$$

(3.4.15)

By solving the determinant, we get secular equation for skew symmetric modes of Lamb wave in a plate loaded with inviscid liquid layer on both sides as

$$\alpha\lambda_L K_\beta K_\gamma K_\delta\left[-\beta\left(1+l^2K_\gamma\right)\frac{t_4}{t_3}+\gamma\left(1+l^2K_\beta\right)\frac{t_4}{t_2}\right]+\beta K_\beta\left[(\gamma^2-\xi^2)+l^2K_\gamma^2\right]\mu\delta P\left(\frac{t_1}{t_3}\right)-$$

$$\gamma K_\gamma\left[(\beta^2-\xi^2)+l^2K_\beta^2\right]\mu\delta P\left(\frac{t_1}{t_2}\right)=4\alpha\beta\gamma\delta\mu\xi^2\left(K_\beta-K_\gamma\right) \qquad (3.4.16)$$

Hence, we obtain the following secular equations for the Lamb waves in a plate loaded with inviscid liquid layer on both sides.

$$\left\{\begin{array}{c}\pm\alpha\lambda_L K_\beta K_\gamma K_\delta\left[-\beta\left(1+l^2K_\gamma\right)\dfrac{t_4}{(t_3)^{\pm1}}+\gamma\left(1+l^2K_\beta\right)\dfrac{t_4}{(t_2)^{\pm1}}\right]\\ +\beta K_\beta\left[(\gamma^2-\xi^2)+l^2K_\gamma^2\right]\mu\delta P\left(\dfrac{t_1}{t_3}\right)^{\pm1}\\ -\gamma K_\gamma\left[(\beta^2-\xi^2)+l^2K_\beta^2\right]\mu\delta P\left(\dfrac{t_1}{t_2}\right)^{\pm1}\end{array}\right\}=4\alpha\beta\gamma\delta\mu\xi^2\left(K_\beta-K_\gamma\right)$$

(3.4.17)

where

$K_\beta=(\beta^2+\xi^2)$

$K_\gamma=(\gamma^2+\xi^2)$

$K_\delta=(\delta^2+\xi^2)$

$P=\left(-\frac{C_1^2}{C_2^2}(\xi^2+\alpha^2)+2\xi^2\right)$

$t_1=\frac{S_1}{C_{11}}$, $t_2=\frac{S_2}{C_{22}}$, $t_3=\frac{S_3}{C_3}$ and $t_4=\frac{S_4}{C_4}$

Here + sign corresponds to skew symmetric modes and − sign refers to symmetric modes of Lamb waves. In the absence of liquid layer, ($\lambda_L\to0$), Eq. (3.4.17) reduces to

$$\beta K_\beta\left[(\gamma^2-\xi^2)+l^2K_\gamma^2\right]\left(\frac{t_1}{t_3}\right)^{\pm1}-\gamma K_\gamma\left[(\beta^2-\xi^2)+l^2K_\beta^2\right]\left(\frac{t_1}{t_2}\right)^{\pm1}=\frac{4\alpha\beta\gamma\,\xi^2\left(K_\beta-K_\gamma\right)}{P} \qquad (3.4.18)$$

This equation is same as (2.6.14) obtained and studied in chapter-2, for Lamb waves in a stress/couple stress free isotropic elastic plate using consistent couple stress theory.

3.5 NUMERICAL RESULTS AND DISCUSSION

(i) To investigate the effects of characteristic length and inner microstructure on the propagation of Lamb waves, the material of the plate is assumed to have properties similar to

cortical bone, so following Vavva *et al*. [137], the material properties are E = Young's Modulus = $\frac{\mu(3\lambda+2\mu)}{(\lambda+\mu)} = 14\,GPa$, ν = Poisson Ratio = $\frac{\lambda}{2(\lambda+\mu)} = 0.37$ and Density = $\rho = 1500\,kg/m^3$. The values of bulk longitudinal and shear velocities comes out to be $C_1 = 4063\,m/s$, $C_2 = 1846\,m/s$ respectively. Since the bone's internal microstructure ranges from 10 to 500 μm. Here, to study the impact of characteristic length, three different cases of characteristic length (l), $l = 0.0003\,m$, $l = 0.0001\,m$, $l = 0.00003\,m$ are considered, which all lie in the range of bone's internal microstructure.

(ii) The fluid medium used is inviscid liquid with $C_L = 1.5 \times 10^3\,m/s$ and density $\rho_L = 1000\,kg/m^3$.

Figs. 3.2 and 3.3, show the phase velocity profile of Lamb waves in an elastic plate under the effect of inviscid liquid layer on both sides for a fixed characteristic length ($l = 0.0001m$) and fixed thickness of liquid layer ($H = 0.02\,m$). Fig. 3.2, shows the phase velocity profiles of fundamental modes of symmetric (S0) and skew symmetric (A0) Lamb waves. Phase velocity profiles of skew symmetric Lamb waves for different modes (M=1, M=2 and M=3) are shown in Fig. 3.3. It is observed that in the wave number range from 0-2, there exist only fundamental modes i.e. S0 and A0. As the wave number increases, new modes start appearing for both symmetric and skew symmetric cases. It is observed that magnitude of phase velocity of these profiles is quite high for the lower wave number, which decreases at a steady rate and becomes asymptotic for the higher wave numbers.

Lamb waves propagating in a plate bordered by liquid on both sides leak some of its energy into the liquid and this situation has practical importance in the field of NDT. To study the impact of loadings on Lamb waves, Figs. 3.4 and 3.5, are drawn showing phase velocity profiles of skew symmetrical Lamb waves for two different values of thickness of liquid layer ($H1 = 0.01\,m$ and $H2 = 0.02\,m$) and profiles are compared with the case of no liquid loadings $H0$. Fig. 3.4, is for M=1 skew symmetrical mode and Fig. 3.5, is for M=2 mode. In both the cases, characteristic length ($l = 0.0001\,m$) is kept fixed. It can be seen that with the increase in the thickness of the liquid loadings phase velocity of the skew symmetrical Lamb waves decreases for the same wave number. As the variation in the phase velocity is very small with the increasing value of thickness of liquid layer and it is not possible to show these variations graphically for a wide range of wave numbers, so figures are drawn with very small variations in wave numbers to depict the effects more precisely.

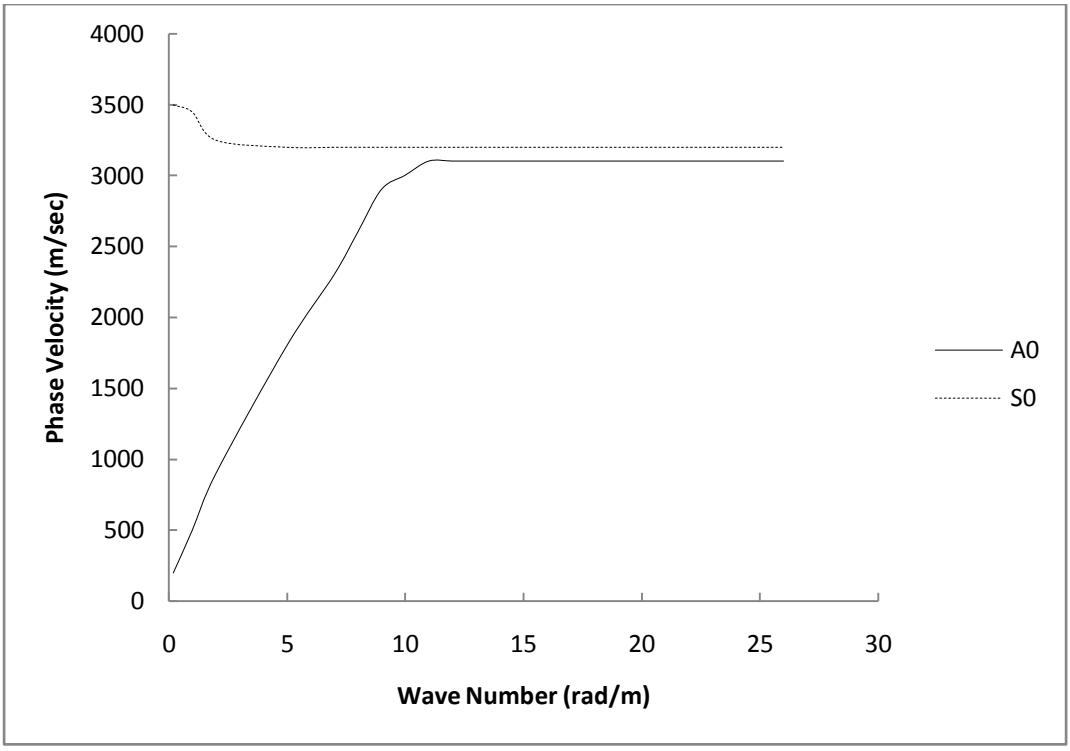

Figure 3.2 Phase velocity profile of fundamental modes of Lamb wave (Symmetrical ($S0$) and Skew symmetrical ($A0$)) with wave number in an elastic plate bordered with liquid layer

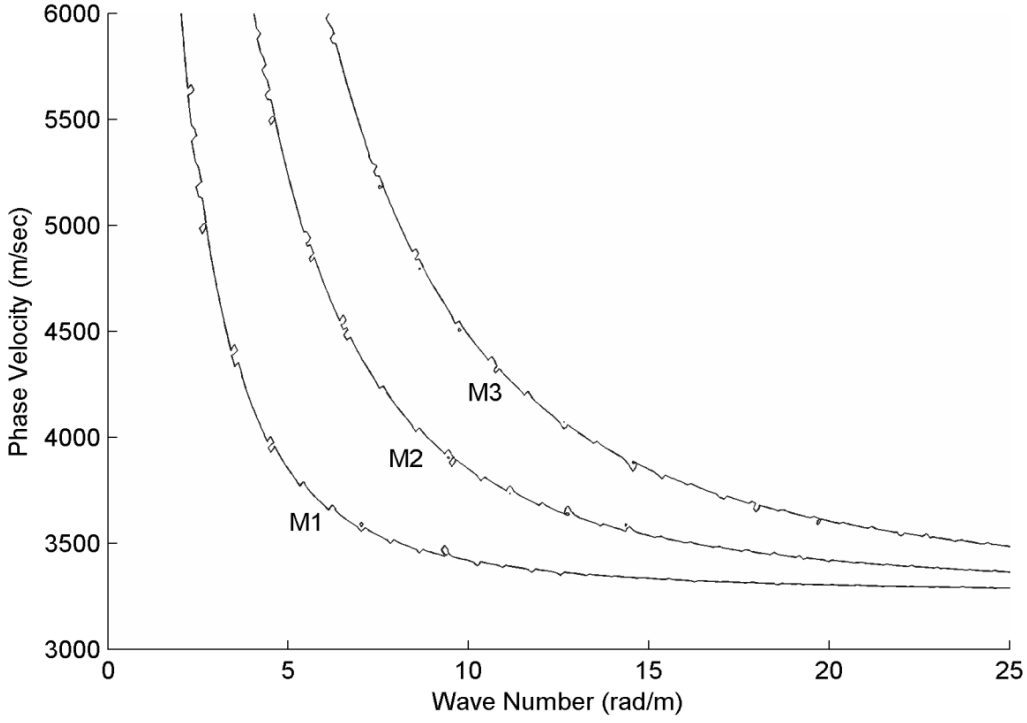

Figure 3.3 Phase velocity profiles of skew symmetrical modes ($M1, M2$ and $M3$ for $M = 1, 2, 3$ respectively) of Lamb wave with wave number in an elastic plate bordered with liquid layer

The effect of characteristic length parameter (l), on the phase velocity profiles of skew symmetric Lamb waves, are shown in Figs. 3.6 and 3.7. Characteristic length parameter (l) is a microstructural parameter involved in couple stress theory and is assumed to be of the order of internal cell size of the considered material. As discussed earlier, here we are taking three different values of characteristic lengths, for profile L1, characteristic length is $l = 0.00003\, m$, for L2 profile, characteristic length is $l = 0.0001\, m$ and for L3, characteristic length is $l = 0.0003\, m$. As the problem deals with the study of microstructural effects and to observe these effects, graphs are again drawn with a very small variation in wave number and phase velocity of Lamb waves. Fig. 3.6, shows the phase velocity profiles of skew symmetric Lamb waves for M=1 mode, with three different considered values of characteristic length and fixed thickness of liquid layer ($H = 0.02\, m$). Fig. 3.7 shows the phase velocity profiles of skew symmetric Lamb waves for M=2 mode, again with the same considered values of characteristic length and fixed thickness of liquid layer ($H = 0.02\, m$). From both the figures it is observed that with the increase in characteristic length parameter (l), the phase velocity of skew symmetric Lamb waves is also increasing, for the same value of wave number.

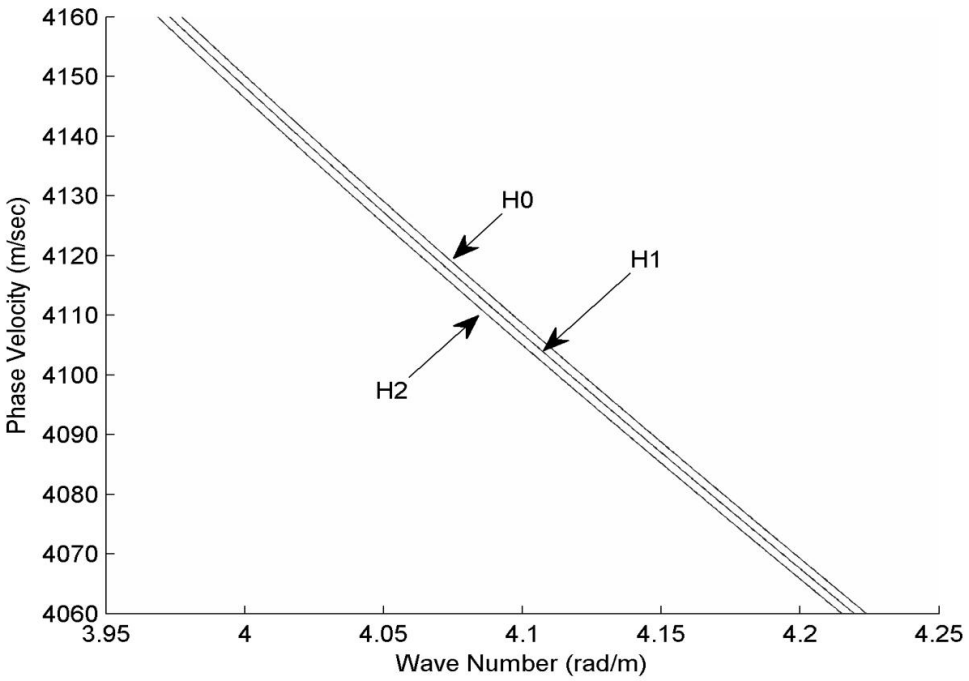

Figure 3.4 Phase velocity profile of Lamb wave for skew symmetrical mode ($M = 1$) with wave number in an elastic plate bordered with liquid layer of different thicknesses ($H0 = 0.00\, m, H1 = 0.01\, m$ and $H2 = 0.02\, m$)

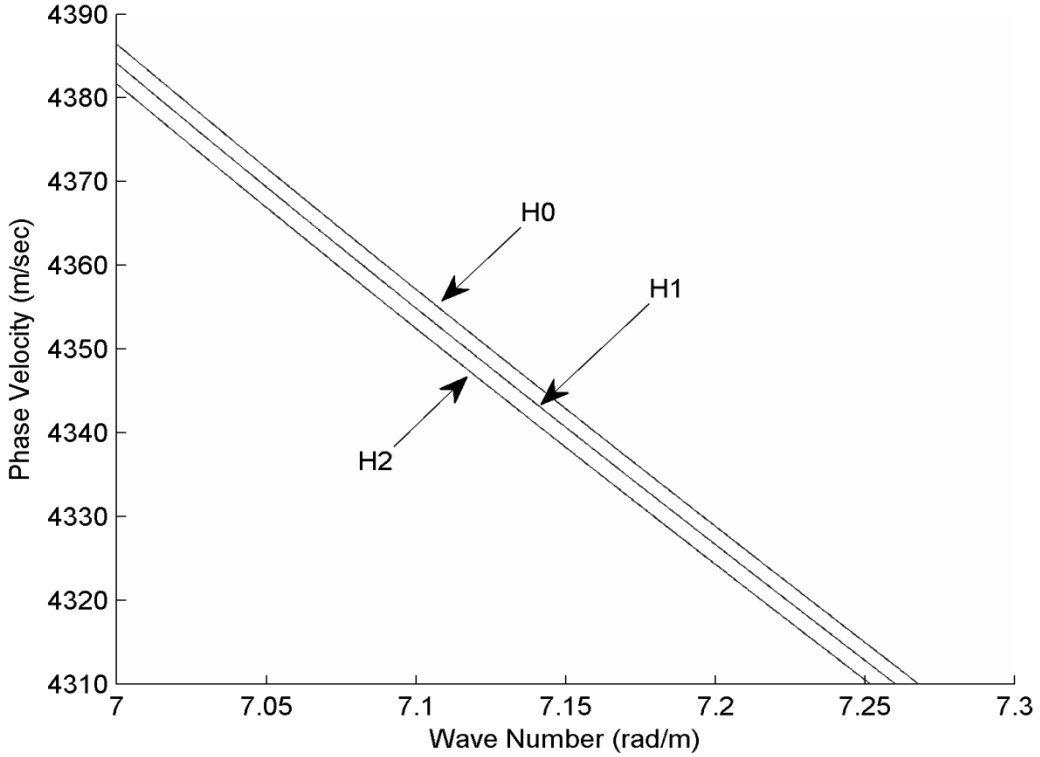

Figure 3.5 Phase velocity profile of Lamb wave for skew symmetrical mode ($M = 2$) with wave number in an elastic plate bordered with liquid layer of different thicknesses ($H0 = 0.00\ m, H1 = 0.01\ m$ and $H2 = 0.02\ m$)

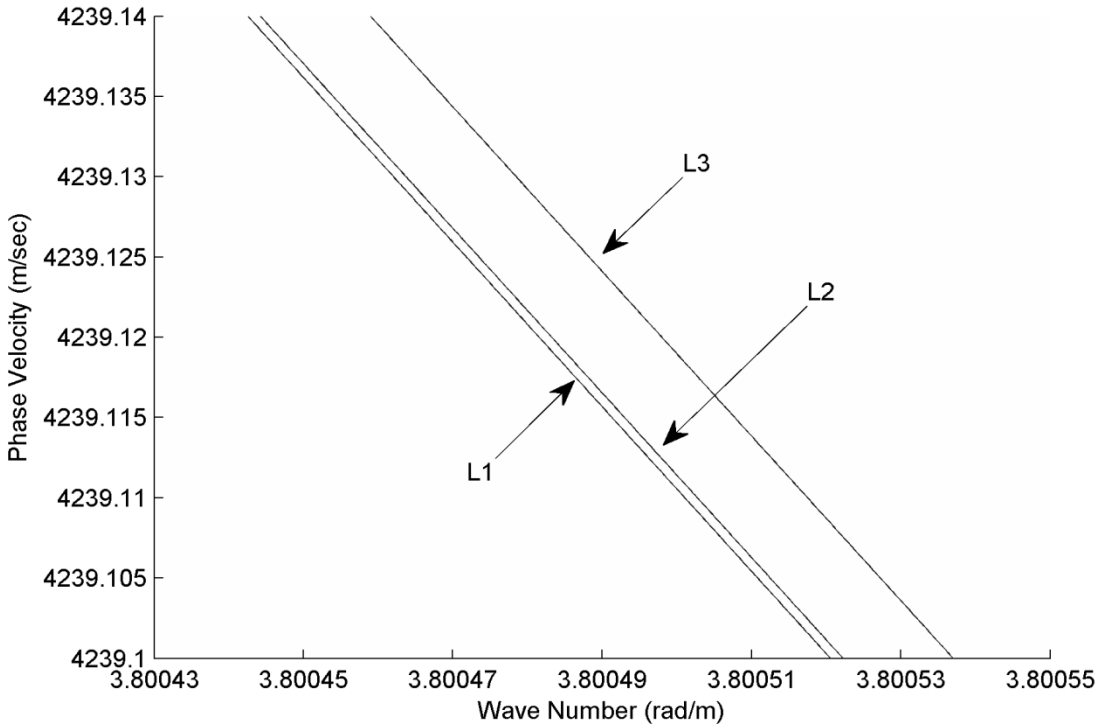

Figure 3.6 Phase velocity profile of Lamb wave for skew symmetrical mode ($M = 1$) with wave number in an elastic plate bordered with liquid layer of fixed thickness and different characteristic lengths $L1 = 0.00003\ m, L2 = 0.0001\ m$ and $L3 = 0.0003\ m$

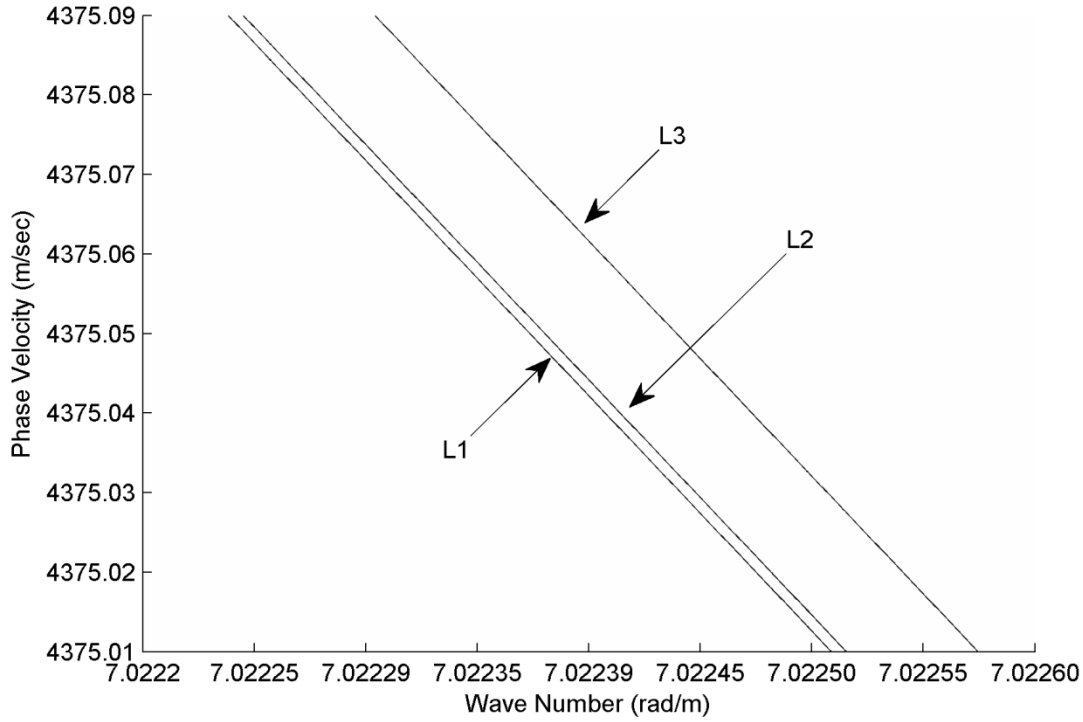

Figure 3.7 Phase velocity profile of Lamb wave for skew symmetrical mode ($M = 2$) with wave number in an elastic plate bordered with liquid layer of fixed thickness and different characteristic lengths $L1 = 0.00003\ m, L2 = 0.0001\ m$ and $L3 = 0.0003\ m$

3.6 CONCLUSION

As the physical model of the problem consists of thin plate loaded with inviscid liquid on both sides, it is of practical use in ultrasonic immersion testing of plates. The impact of liquid loadings is studied on the propagation of phase velocity of Lamb waves. Three different cases for the thickness of liquid loaded on both side of the plate are considered. It is observed that with the increase in the thickness of the loadings the phase velocity tends to decrease. The material of the plate considered, is assumed to have properties similar to cortical bone (Vavva *et al*. [137]), so it also enhances the applicability of this model in the characterisation of the properties of bones loaded with different type of fluids.

To find the impact of microstructural parameter, the problem is solved by applying consistent couple stress theory (Hadjesfandiari and Dargush [46]). Here, three different values of characteristic length are considered, comparable with the internal cell size of the material and their effect is studied on the phase velocity of the Lamb waves. It is observed that with the increase in the value of this parameter the phase velocity of skew symmetric Lamb wave also increases.

CHAPTER-4

INFLUENCE OF MICROSTRUCTURE, HETEROGENEITY AND INTERNAL FRICTION ON SH WAVES PROPAGATION IN A VISCOELASTIC LAYER OVERLYING A COUPLE STRESS SUBSTRATE[3]

4.1 INTRODUCTION

In the traditional approach, theory of seismic wave propagation was developed within the frame work of linear elasticity, but later developments showed that earth should be more correctly regarded as a dissipative medium. To encounter dissipation of energy considerations and to overcome the shortcomings of linear elasticity the near sub surface of earth is modelled as linearly viscoelastic material. The geological evidence of heterogeneity within the earth are provided by the wide variations of rocks erupted from volcanoes. The scattering of high frequency seismic waves also support the existence of small scale heterogeneity in the earth lithosphere. Hence, for characterising the internal microstructure of solid earth, heterogeneity and viscoelasticity of the material composition of the earth subsurface has to be taken into account.

In this problem, we have investigated shear horizontal wave propagation in a layered structure, consisting of granular macromorphic rock (Dionysos Marble) substrate underlying a viscoelastic layer of finite thickness. Dionysos Marble is a white fine-grained metamorphic marble with a saccharoidal microstructure. SH waves characteristics are affected by the material properties of both underlying substrate and the coating. Dispersion equation for propagation of SH wave in considered model is derived. The effects of microstructural parameter characteristic length of the substrate, along with heterogeneity, internal friction and thickness of viscoelastic layer are studied on the dispersion curves. Real and damping phase velocities of SH waves are studied against dimensionless wave number, for different combinations of various parameters involved in the problem.

[3] Contents of this chapter are published in SCI indexed journal, *Structural Engineering and Mechanics* (2016), **57**(4):703-716 with impact factor- 0.927

4.2 FORMULATION AND SOLUTION OF THE PROBLEM

Consider a layer of viscoelastic medium of thickness H, lying over a couple stress half space with microstructures, characterised by an additional material parameter l, characteristic length. The origin of the coordinate system $O(x, y, z)$ lies on the interfacial surface joining half space and layer of viscoelastic medium. Here, z-axis is pointing vertically downwards into the half space, the interface between layer and half space is given by $z = 0$ and the free surface of layer is $z = -H$. Here, we have assumed that two media are perfectly bonded to each other at the interface. For SH waves, displacement components and body forces are independent of y co-ordinate, so if (u, v, w) are the displacement co-ordinates of a point, then $u = w = 0$ and v is function of parameters x, z and t.

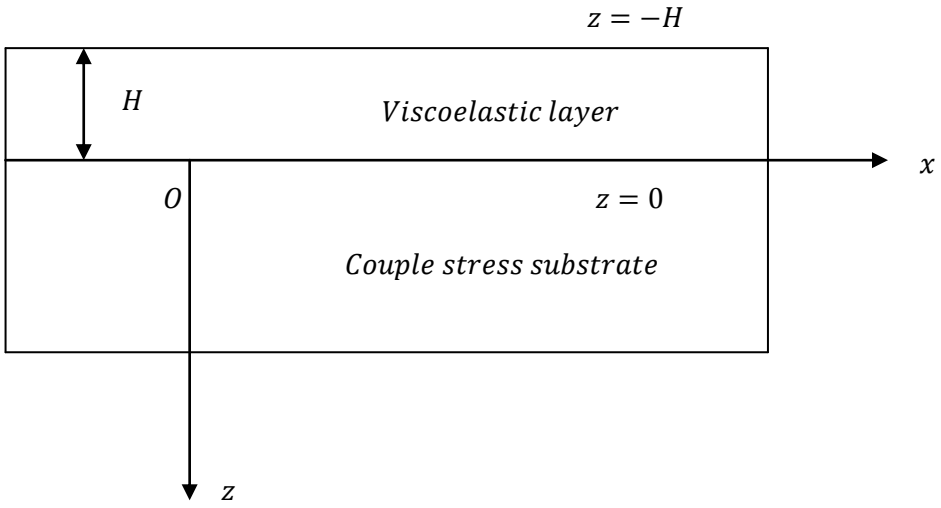

Figure 4.1 Geometry of the problem

4.2.1 Couple stress half space

The basic governing equation of motion and constitutive relations of couple stress theory for isotropic material in the absence of body forces (Hadjesfandiari and Dargush [46]) are given by

$$(\lambda + \mu + \eta\nabla^2)\nabla(\nabla.\vec{u}) + (\mu - \eta\nabla^2)\nabla^2\vec{u} = \rho\frac{\partial^2\vec{u}}{\partial t^2} \qquad (4.2.1.1)$$

where λ and μ are Lamé constants, $\eta = \mu l^2$ is couple-stress coefficient, l is characteristic length, ρ is the density of the material of elastic half space and $\vec{u}$ is the displacement vector. Let us assume that $\vec{u} = (0, v, 0)$ and $\frac{\partial}{\partial y} \equiv 0$

Imposing above said conditions, equation of motion becomes,

$$\left(\frac{\partial^2 v}{\partial x^2}+\frac{\partial^2 v}{\partial z^2}\right)-l^2\left(\frac{\partial^4 v}{\partial x^4}+\frac{\partial^4 v}{\partial z^4}+2\frac{\partial^4 v}{\partial x^2 \partial z^2}\right)=\frac{1}{C_2^2}\frac{\partial^2 v}{\partial t^2} \tag{4.2.1.2}$$

Where $C_2^2=\frac{\mu}{\rho}$

Let us assume the solution of above equation as

$$v=f(z)e^{-i(\omega t-\xi x)} \tag{4.2.1.3}$$

where ξ is the wave number, $\omega=\xi c$ is the angular frequency and c is the phase velocity. Eq. (4.2.1.3) reduces to

$$\frac{d^4 f}{dz^4}-S\frac{d^2 f}{dz^2}+Pf=0 \tag{4.2.1.4}$$

Where

$$S=2\xi^2+\frac{1}{l^2} \tag{4.2.1.5}$$

$$P=\xi^4+\frac{\xi^2}{l^2}-\frac{\omega^2}{l^2 C_2^2} \tag{4.2.1.6}$$

Since in the couple stress elastic half space amplitude of waves decreases with increase in depth, so solution of above differential equation becomes

$$f(z)=A_1 e^{-a_1 z}+B_1 e^{-b_1 z} \tag{4.2.1.7}$$

Where

$$a_1=\sqrt{\frac{S+\sqrt{S^2-4P}}{2}} \tag{4.2.1.8}$$

$$b_1=\sqrt{\frac{S-\sqrt{S^2-4P}}{2}} \tag{4.2.1.9}$$

Hence $v=(A_1 e^{-a_1 z}+B_1 e^{-b_1 z})e^{-i(\omega t-\xi x)}$ (4.2.1.10)

The constitutive relations for couple stress space are given by (Hadjesfandiari and Dargush [46])

$$\sigma_{ji}=\lambda u_{k,k}\delta_{ij}+\mu\left(u_{i,j}+u_{j,i}\right)-\eta\nabla^2\left(u_{i,j}-u_{j,i}\right) \tag{4.2.1.11}$$

$$\mu_{ji} = 4\eta\left(\omega_{i,j} - \omega_{j,i}\right) \tag{4.2.1.12}$$

where

$$\omega_i = \frac{1}{2}\epsilon_{ijk}\, u_{k,j}$$

Here, u_i are the displacement components, σ_{ji} is the non-symmetric force stress tensor, μ_{ji} is skew symmetric couple-stress tensor, δ_{ij} is Kronecker's delta and ϵ_{ijk} is permutation tensor and $i, j, k = 1, 2, 3$.

$$\sigma_{yz} = \mu\frac{\partial v}{\partial z} + \mu l^2\left(\frac{\partial^3 v}{\partial x^2 \partial z} + \frac{\partial^3 v}{\partial z^3}\right) \tag{4.2.1.13}$$

$$\mu_{xz} = 2\mu l^2\left(\frac{\partial^2 v}{\partial x^2} + \frac{\partial^2 v}{\partial z^2}\right) \tag{4.2.1.14}$$

Using Eq. (4.5) in Eq. (4.8), we get

$$\sigma_{yz} = \begin{bmatrix} \mu(-a_1 A_1 e^{-a_1 z} - b_1 B_1 e^{-b_1 z}) + \\ \mu l^2(a_1 A_1 \xi^2 e^{-a_1 z} + b_1 B_1 \xi^2 e^{-b_1 z} - a_1^3 A_1 e^{-a_1 z} - b_1^3 B_1 e^{-b_1 z}) \end{bmatrix} e^{-i(\omega t - \xi x)} \tag{4.2.1.15}$$

$$\mu_{xz} = 2\mu l^2[(a_1^2 A_1 e^{-a_1 z} + b_1^2 B_1 e^{-b_1 z}) - (A_1 e^{-a_1 z} + B_1 e^{-b_1 z})\xi^2] e^{-i(\omega t - \xi x)} \tag{4.2.1.16}$$

4.2.2 Heterogeneous viscoelastic layer

For the heterogeneity of the layer, we have assumed that properties of the medium change only in z-direction. For SH waves propagation in the x-direction and causing displacement in y-direction only, we shall assume that $\vec{u}_1 = (0, v_1, 0)$ and $\frac{\partial}{\partial y} \equiv 0$

Equation of motion in the absence of body forces and under the above mentioned assumptions (Ravindra [103]) is given by

$$\frac{\partial P_{xy}}{\partial x} + \frac{\partial P_{yz}}{\partial z} = \rho_1 \frac{\partial^2 v_1}{\partial t^2} \tag{4.2.2.1}$$

where

$$P_{xy} = \left(\mu_1 + \eta_1 \frac{\partial}{\partial t}\right)\frac{\partial v_1}{\partial x} \tag{4.2.2.2}$$

$$P_{yz} = \left(\mu_1 + \eta_1 \frac{\partial}{\partial t}\right)\frac{\partial v_1}{\partial z} \tag{4.2.2.3}$$

In the upper viscoelastic layer μ_1, η_1 and ρ_1 are assumed to be function of depth only and are given by

$$\left.\begin{aligned}\mu_1 &= \mu_0(1 - sin\alpha z)\\ \eta_1 &= \eta_0(1 - sin\alpha z)\\ \rho_1 &= \rho_0(1 - sin\alpha z)\end{aligned}\right\} \tag{4.2.2.4}$$

where μ_0, η_0, ρ_0 are the constant values of μ_1, η_1 and ρ_1 at the interface of layer and half space and α is an arbitrary constant having dimensions of inverse of length.

Using Eqs. (4.2.2.2) and (4.2.2.3) in Eq. (4.2.2.1), equation of motion for heterogeneous viscoelastic layer becomes

$$\left(\mu_1 + \eta_1 \frac{\partial}{\partial t}\right)\frac{\partial^2 v_1}{\partial x^2} + \frac{\partial}{\partial z}\left[\left(\mu_1 + \eta_1 \frac{\partial}{\partial t}\right)\frac{\partial v_1}{\partial z}\right] = \rho_1 \frac{\partial^2 v_1}{\partial t^2} \tag{4.2.2.5}$$

Now, assuming the solution

$$v_1 = v_L(z)e^{-i(\omega t - \xi x)} \tag{4.2.2.6}$$

Using the assumed solution in Eq. (4.2.2.5), we get

$$\frac{d^2 v_L}{dz^2} + \frac{1}{\overline{\mu_1}}(\overline{\mu_1})' \frac{dv_L}{dz} + \left(\frac{\rho_1 \omega^2}{\overline{\mu_1}} - \xi^2\right) v_L = 0 \tag{4.2.2.7}$$

where

$\overline{\mu_1} = \mu_1 - i\omega\eta_1$ and $(\overline{\mu_1})' = \frac{d\overline{\mu_1}}{dz}$

Taking $v_L(z) = \frac{Y_1(z)}{\sqrt{\overline{\mu_1}}}$, Eq. (4.2.2.7) reduces to

$$\frac{d^2 Y_1}{dz^2} + \left[\frac{1}{4(\overline{\mu_1})^2}\left(\frac{d\overline{\mu_1}}{dz}\right)^2 - \frac{1}{2\overline{\mu_1}}\frac{d^2\overline{\mu_1}}{dz^2} + \frac{\rho_1\omega^2}{\overline{\mu_1}} - \xi^2\right] Y_1 = 0 \tag{4.2.2.8}$$

Now $(\overline{\mu_1})' = \frac{d\overline{\mu_1}}{dz} = \frac{d}{dz}(\mu_1 - i\omega\eta_1)$, using Eq. (4.2.2.4), we get

$$(\overline{\mu_1})' = -\mu_o \alpha Cos(\alpha z) + i\omega\eta_o \alpha Cos(\alpha z) \tag{4.2.2.9}$$

$$(\overline{\mu_1})'' = \frac{d^2\overline{\mu_1}}{dz^2} = (\mu_o \alpha^2 Sin(\alpha z) - i\omega\eta_o \alpha^2 Sin(\alpha z)) \tag{4.2.2.10}$$

Using Eqs. (4.2.2.9) and (4.2.2.10) in (4.2.2.8), gives us

$$\frac{d^2Y_1}{dz^2} + \left[\frac{\alpha^2}{4} + \frac{\rho_0\omega^2}{\overline{\mu_0}} - \xi^2\right] Y_1 = 0, \tag{4.2.2.11}$$

where $\overline{\mu_0} = \mu_0 - i\omega\eta_0$

Solution to differential Eq. (4.2.2.11) is

$Y_1 = Acos(mz) + Bsin(mz)$, where A and B are the arbitrary constants

where

$$m^2 = \left(\frac{\alpha^2}{4} + \frac{\rho_0\omega^2}{\overline{\mu_0}} - \xi^2\right)$$

Hence $v_1 = v_L(z)e^{-i(\omega t - \xi x)} = \frac{Y_1(z)}{\sqrt{\overline{\mu_1}}} e^{-i(\omega t - \xi x)}$

$$v_1 = \frac{1}{\sqrt{\overline{\mu_0}}}(1 - sin\alpha z)^{-1/2}(Acos(mz) + Bsin(mz))e^{-i(\omega t - \xi x)} \tag{4.2.2.12}$$

Using Eq. (4.2.2.12) in Eqs. (4.2.2.2) and (4.2.2.3), we get

$$P_{xy} = \left(\mu_1 + \eta_1 \frac{\partial}{\partial t}\right)\frac{\partial}{\partial x}\left(\frac{1}{\sqrt{\overline{\mu_0}}}(1 - sin\alpha z)^{-1/2}(Acos(mz) + Bsin(mz))e^{-i(\omega t - \xi x)}\right)$$

$$P_{xy} = i\xi\sqrt{\overline{\mu_o}(1 - Sin(\alpha z))}(ACos(mz) + BSin(mz))e^{-i(\omega t - \xi x)} \tag{4.2.2.13}$$

$$P_{yz} = \left(\mu_1 + \eta_1 \frac{\partial}{\partial t}\right)\frac{\partial}{\partial z}\left(\frac{1}{\sqrt{\overline{\mu_0}}}(1 - sin\alpha z)^{-1/2}(Acos(mz) + Bsin(mz))e^{-i(\omega t - \xi x)}\right)$$

$$P_{yz} = \frac{\sqrt{\overline{\mu_o}}}{2\sqrt{(1 - Sin(\alpha z))}}\begin{bmatrix} 2m\{1 - Sin(\alpha z)\}\left(-ASin(mz) + BCos(mz)\right) + \\ \alpha Cos(\alpha z)(ACos(mz) + BSin(mz)) \end{bmatrix} e^{-i(\omega t - \xi x)} \tag{4.2.2.14}$$

4.3 BOUNDARY CONDITIONS

Boundary conditions to be satisfied at the free surface of the viscoelastic layer and at the interfacial surface between viscoelastic layer and couple stress half space are

(i) Top surface of the viscoelastic layer should be stress free that is

$$P_{yz} = \left(\mu_1 + \eta_1 \frac{\partial}{\partial t}\right)\frac{\partial v_1}{\partial z} = 0 \text{ at } z = -H$$

(ii) Displacement components should be continuous at the interfacial surface, that is

$v_1 = v$ at $z = 0$

(iii) The magnitude of shear component of the stress tensor of the viscoelastic layer should be equal to shear component of the stress tensor of couple stress substrate at the interface, that is, $P_{yz} = \sigma_{yz}$ at $z = 0$

(iv) Couple stresses of substrate should vanish the interface, that is

$\mu_{xz} = 0$ at $z = 0$

4.4 DERIVATION OF SECULAR EQUATION

Using above mentioned boundary conditions, we get following four equations

$$\begin{bmatrix} \sqrt{\overline{\mu_0}}[2m(1+sin(\alpha H))sin(mH) + \alpha cos(\alpha H)cos(mH)]A \\ +\sqrt{\overline{\mu_0}}[2m(1+sin(\alpha H))\,cos(mH) - \alpha cos(\alpha H)sin(mH)]B \end{bmatrix} = 0 \tag{4.4.1}$$

$$-\frac{A}{\sqrt{\overline{\mu_0}}} + A_1 + B_1 = 0 \tag{4.4.2}$$

$$\frac{\alpha\sqrt{\overline{\mu_0}}A}{2} + \sqrt{\overline{\mu_0}}mB + \mu a_1[1+(a_1^2-\xi^2)l^2]A_1 + \mu b_1[1+(b_1^2-\xi^2)l^2]B_1 = 0 \tag{4.4.3}$$

$$(a_1^2-\xi^2)A_1 + (b_1^2-\xi^2)B_1 = 0 \tag{4.4.4}$$

Eqs. (4.4.1)-(4.4.4) will have a non-trivial solution, if determinant of coefficients of unknowns A, B, A_1, B_1 vanishes. After applying this condition to the above system of equations, we obtain following determinant

$$\begin{vmatrix} T_1 & T_2 & 0 & 0 \\ \frac{-1}{\sqrt{\overline{\mu_0}}} & 0 & 1 & 1 \\ \frac{\alpha\sqrt{\overline{\mu_0}}}{2} & \sqrt{\overline{\mu_0}}m & \mu a_1[1+(a_1^2-\xi^2)l^2] & \mu b_1[1+(b_1^2-\xi^2)l^2] \\ 0 & 0 & (a_1^2-\xi^2) & (b_1^2-\xi^2) \end{vmatrix} = 0 \tag{4.4.5}$$

By solving this determinant, we obtain secular equations for the SH waves in an heterogeneous viscoelastic layer over a couple stress half space with microstructures as

$$\begin{Bmatrix} 2T_1\overline{\mu_0}m(a_1^2-b_1^2) + 2T_2\{\mu(\xi^2-a_1^2)(\xi^2-b_1^2)(a_1-b_1)l^2 \\ +\mu b_1(\xi^2-a_1^2) - \mu a_1(\xi^2-b_1^2)\} + T_2\overline{\mu_0}\alpha(b_1^2-a_1^2) \end{Bmatrix} = 0 \tag{4.4.6}$$

Where

$$T_1 = 2m\{1 + sin(\alpha H)\}\, sin(mH) + \alpha\, cos(\alpha H)\, cos(mH)$$

$$T_2 = 2m\{1 + sin(\alpha H)\}\, cos(mH) - \alpha cos(\alpha H) sin(mH)$$

Separating the real and imaginary parts of dispersion equation, we get real part of dispersion equation of SH waves as

$$\left.\begin{matrix} 2R_1(\mu_0 m_1 + \omega\eta_0 m_2)(a_1^2 - b_1^2) + 2I_1(\omega\eta_0 m_1 - \mu_0 m_2)(a_1^2 - b_1^2) \\ +2R_2 Q + \alpha(R_2\mu_0 + \omega\eta_0 I_2)(b_1^2 - a_1^2) \end{matrix}\right\} = 0 \qquad (4.4.7)$$

and imaginary part of dispersion equation of SH waves as

$$\left.\begin{matrix} 2R_1(\mu_0 m_2 - \omega\eta_0 m_1)(a_1^2 - b_1^2) + 2I_1(\mu_0 m_1 + \omega\eta_0 m_2)(a_1^2 - b_1^2) \\ +2I_2 Q + \alpha(I_2\mu_0 - R_2\omega\eta_0)(b_1^2 - a_1^2) \end{matrix}\right\} = 0 \qquad (4.4.8)$$

where

$$T_1 = R_1 + iI_1$$

$$T_2 = R_2 + iI_2$$

$$m = m_1 + im_2$$

$$Q = \mu(\xi^2 - a_1^2)(\xi^2 - b_1^2)(a_1 - b_1)l^2 + \mu b_1(\xi^2 - a_1^2) - \mu a_1(\xi^2 - b_1^2)$$

$$R_1 = 2(1 + sin(\alpha H))(m_1 S_1 - m_2 S_2) + \alpha\, cos(\alpha H)\, E_1$$

$$I_1 = 2(1 + sin(\alpha H))(m_1 S_2 + m_2 S_1) - \alpha\, cos(\alpha H)\, E_2$$

$$R_2 = 2(1 + sin(\alpha H))(m_1 E_1 + m_2 E_2) - \alpha\, cos(\alpha H)\, S_1$$

$$I_2 = 2(1 + sin(\alpha H))(m_2 E_1 - m_1 E_2) - \alpha\, cos(\alpha H)\, S_2$$

$$S_1 = sin(m_1 H) cosh(m_2 H)$$

$$S_2 = cos(m_1 H) sinh(m_2 H)$$

$$E_1 = cos(m_1 H) cosh(m_2 H)$$

$$E_2 = sin(m_1 H) sinh(m_2 H)$$

$$m_1 = r^{\frac{1}{2}} cos\left(\frac{\theta}{2}\right)$$

$$m_2 = r^{\frac{1}{2}} sin\left(\frac{\theta}{2}\right)$$

$$F_1 = \frac{\rho_0 \omega^3 \eta_0}{\mu_0^2 + \omega^2 \eta_0^2}$$

$$F_2 = \frac{\alpha^2}{4} - \xi^2 + \frac{\rho_0 \omega^2 \mu_0}{\mu_0^2 + \omega^2 \eta_0^2}$$

$$r = (F_1^2 + F_2^2)^{\frac{1}{2}}$$

$$tan(\theta) = \left(\frac{F_1}{F_2}\right)$$

4.5 NUMERICAL RESULTS AND DISCUSSION

(i) For viscoelastic layer the various material parameters (Gubbins [44]) used, are

ρ_0	$4705\ kg/m^3$
μ_0	$1.987 \times 10^{10}\ N/m^2$
$\frac{\mu_0}{\eta_0}$	$10^6\ s^{-1}$
$\beta_1 = \sqrt{\frac{\mu_0}{\rho_0}}$	$2055\ m/s$

Table 4.1 Physical data for viscoelastic material

(ii) The material properties for couple stress half space made of Dionysos marble (Vardoulakis and Georgiadis [135]), are

μ	$30.5 \times 10^9\ N/m^2$
ρ	$2717\ kg/m^3$
C_2	$3350\ m/s$

Table 4.2 Physical data for Dionysos marble

To find the impact of characteristic length, different cases of characteristic length (l), comparable with the internal cell size of granular macromorphic rock ($O(10^{-4})$) such as $l = 0.0001\ m$, $l = 0.0004\ m$, $l = 0.0008\ m$ are considered.

4.5.1 Effects of heterogeneity parameter

To study the role of heterogeneity parameter on the characteristics of SH waves in viscoelastic layer, dispersion curves are provided for three different values of heterogeneity parameter (αH=0.18, 0.54 and 0.72 for the curves R1, R2 and R3 respectively), by keeping

fixed values of $H = 0.09\,m$, characteristic length parameter $l = 0.0004\,m$ and friction parameter $\mu_1/\eta_1 = 10^6\,s^{-1}$. From Fig. 4.2, it can be observed that normalized real phase velocity decreases with the increase in normalized wave number before becoming asymptotically closer to 1, for all the considered values of heterogeneity parameter. It can be further seen that with the increase in heterogeneity parameter, real phase velocity decreases. Similar kind of trends, as seen for real phase velocity are also observed for normalized damping phase velocity of SH waves (Fig. 4.3). A closed survey of the demonstrated results shows that damping phase velocity is more sensitive to heterogeneity parameter (αH).

4.5.2 Effects of friction parameter

Dispersion curves, to demonstrate the role of friction parameter on SH waves in the viscoelastic layer are provided for three different values of friction parameter $\mu_1/\eta_1 = 7 \times 10^5\,s^{-1}, 10 \times 10^5\,s^{-1}, 80 \times 10^5\,s^{-1}$, by keeping fixed value of heterogeneity parameter $\alpha H = 0.54$ and characteristic length parameter $l = 0.0004\,m$. It is observed from Figs. 4.4 and 4.5 that normalized real phase velocity tends to decrease with the increase in friction parameter, but has an inverse impact on the normalized damping phase velocity and in both the cases effects are seen for the normalized wave number greater than 1.5.

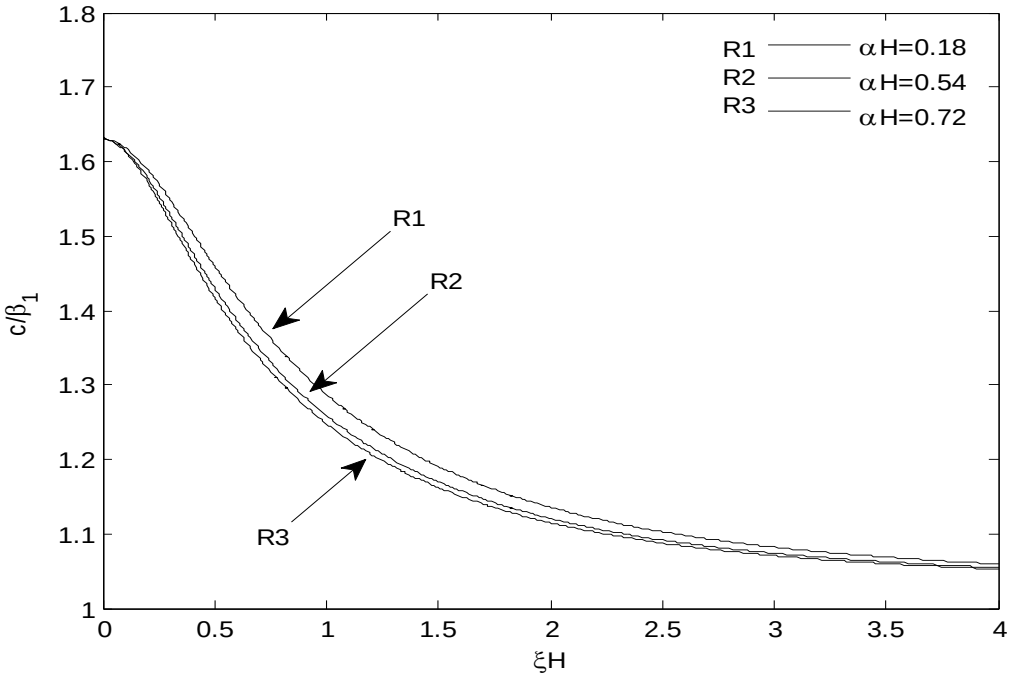

Figure 4.2 Variation of normalized real phase velocity (c/β_1) of SH waves against normalized wave number (ξH) for different values of heterogeneity parameter (αH)

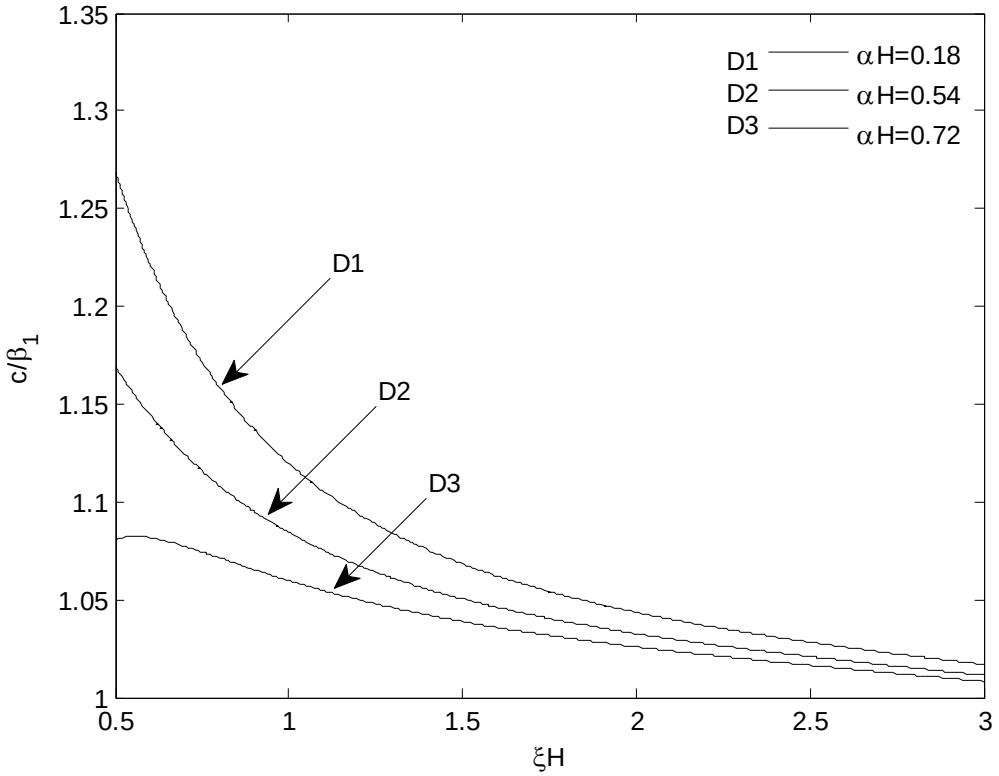

Figure 4.3 Variation of normalized damping phase velocity (c/β_1) of SH waves against normalized wave number (ξH) for different values of heterogeneity parameter (αH)

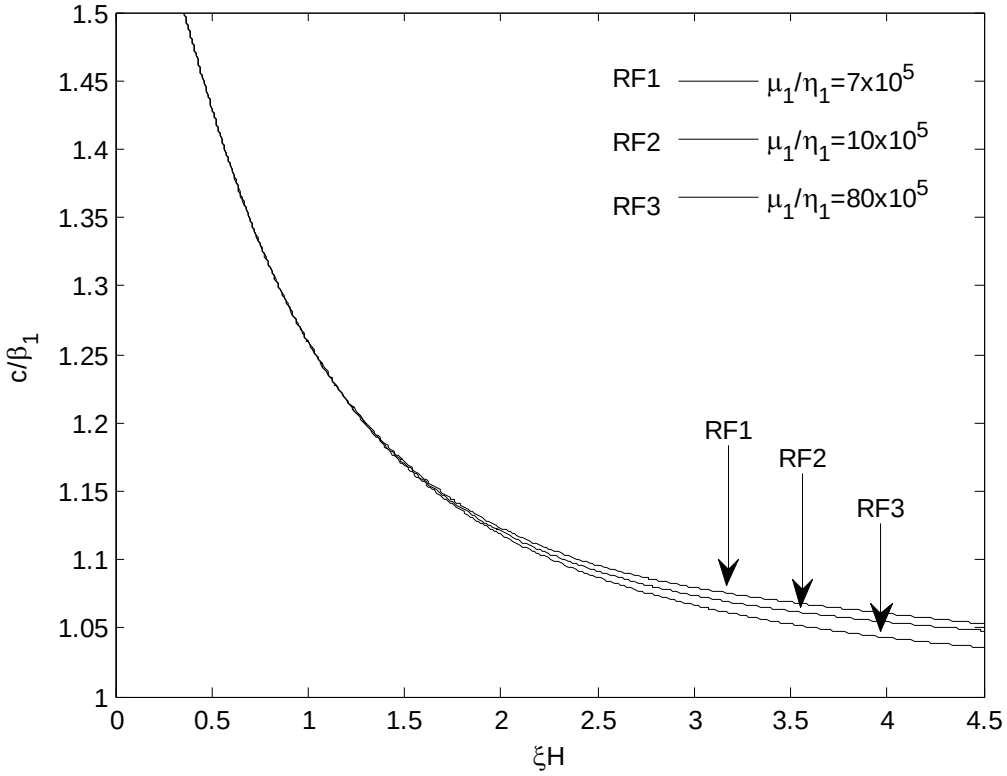

Figure 4.4 Variation of normalized real phase velocity (c/β_1) of SH waves against normalized wave number (ξH) for different values of internal friction parameter (μ_1/η_1)

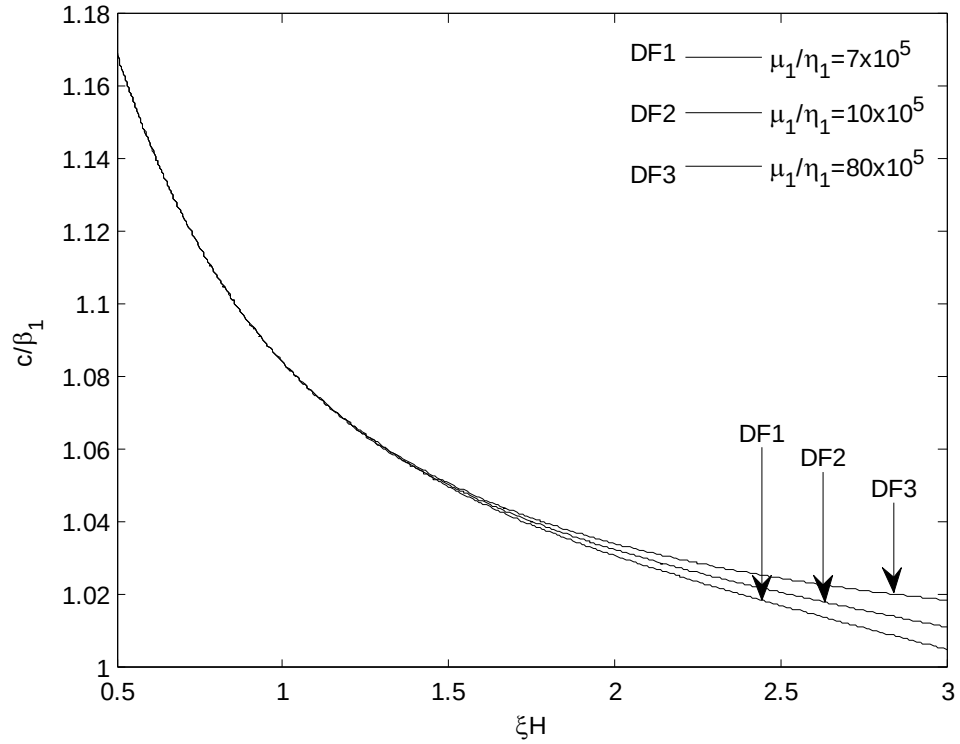

Figure 4.5 Variation of normalized damping phase velocity (c/β_1) of SH waves against normalized wave number (ξH) for different values of internal friction parameter (μ_1/η_1)

4.5.3 Effects of thickness of viscoelastic layer

The influence of thickness(H), of viscoelastic layer on normalized real and damping phase velocities of propagation of SH waves are shown in Figs. 4.6 and 4.7. Fig. 4.6, shows the variation in normalized real phase velocity(c/β_1), against the normalized wave number(ξH), for three different values of thickness, $H = 0.04\ m, 0.06\ m$ and $0.09\ m$ keeping fixed value of heterogeneity parameter $\alpha H = 0.54$, friction parameter $\mu_1/\eta_1 = 10^6 s^{-1}$ and characteristic length parameter $l = 0.0004\ m$. It is observed that with the increase in thickness parameter H, normalized real phase velocity decreases. Normalized damping velocity of SH waves increases with increase in this parameter (Fig. 4.7) and again in both the cases, results are more prominent for wave number (ξH) greater than 1.5.

4.5.4 Effects of internal microstructure of the substrate

For observing the effects of internal microstructure of the underlying substrate, the variation in normalized real and damping phase velocities (c/β_1), against the normalized wave number (ξH), are provided in Figs. 4.8 and 4.9, for three different values of characteristic length parameter $l = 0.0001\ m$, $l = 0.0004\ m$, $l = 0.0008\ m$, keeping fixed values of heterogeneity parameter $\alpha H = 0.54$, thickness of viscoelastic layer $H = 0.09\ m$ and friction parameter $\mu_1/\eta_1 = 10^6\ s^{-1}$. It can be observed that both real (Fig. 4.8) and damping (Fig. 4.9) phase velocities of SH waves, increase with the increase in characteristic length (l) of the material.

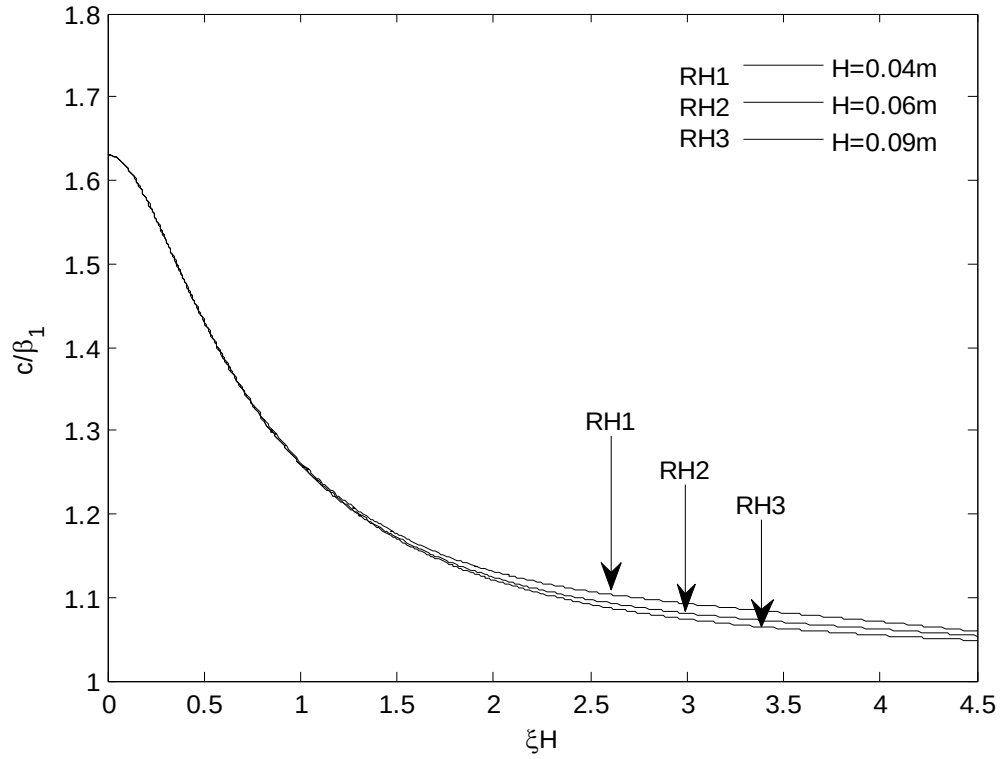

Figure 4.6 Variation of normalized real phase velocity (c/β_1) of SH waves against normalized wave number (ξH) for varying thickness of viscoelastic layer (H)

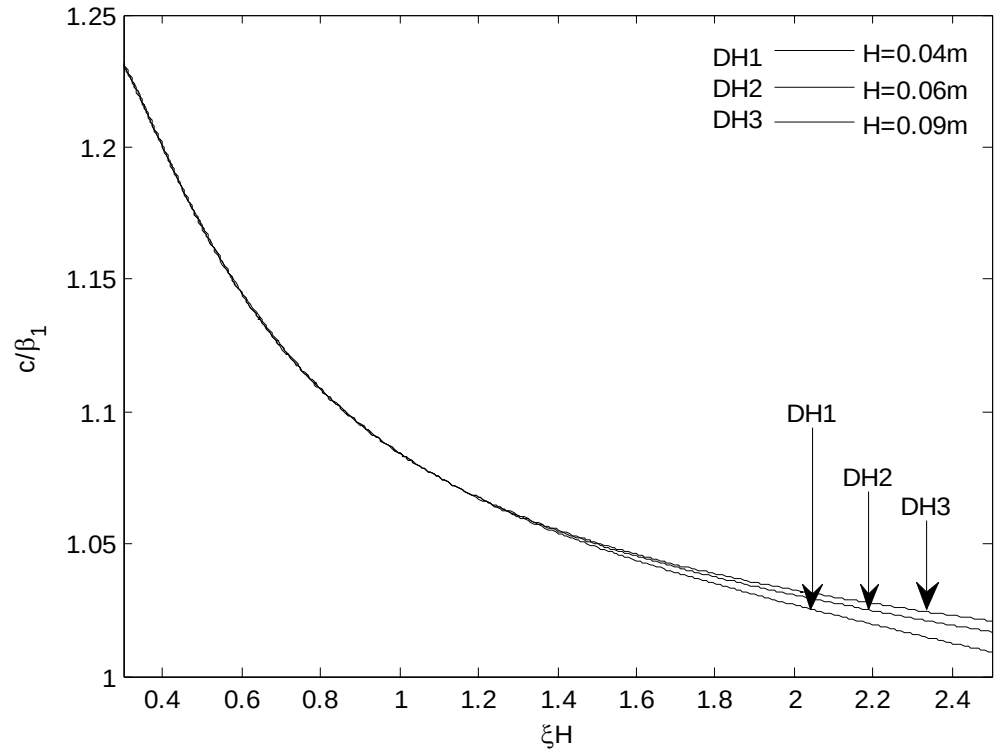

Figure 4.7 Variation of normalized damping phase velocity (c/β_1) of SH waves against normalized wave number (ξH) for varying thickness of viscoelastic layer (H).

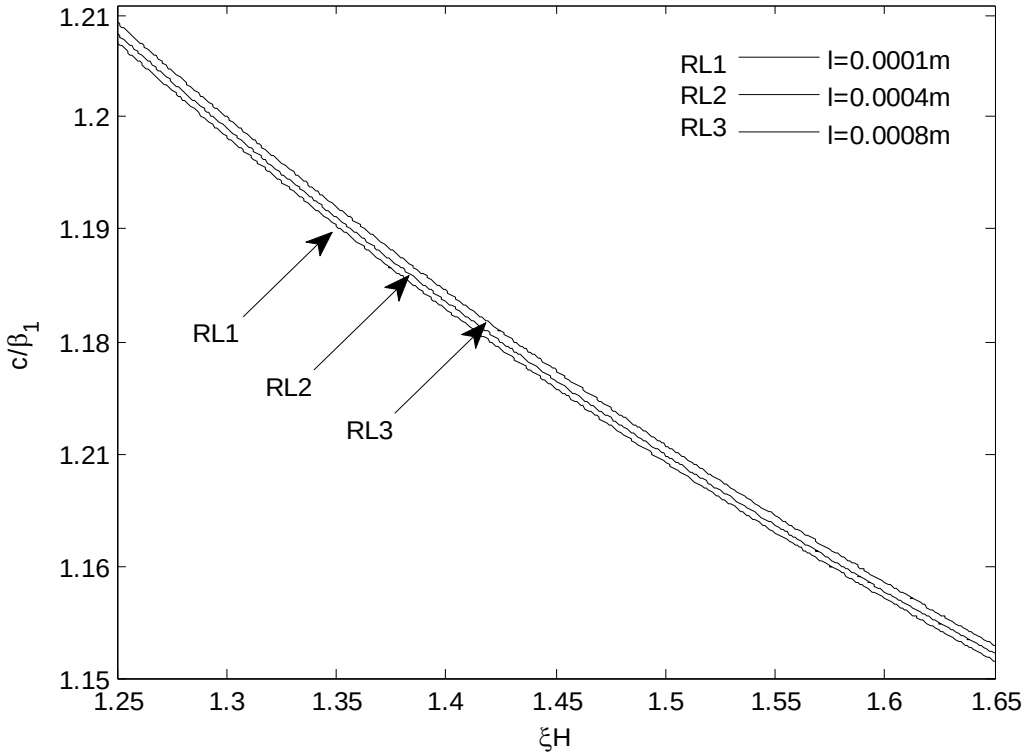

Figure 4.8 Variation of normalized real phase velocity (c/β_1) of SH waves against normalized wave number (ξH) for different values of characteristic length parameter (l)

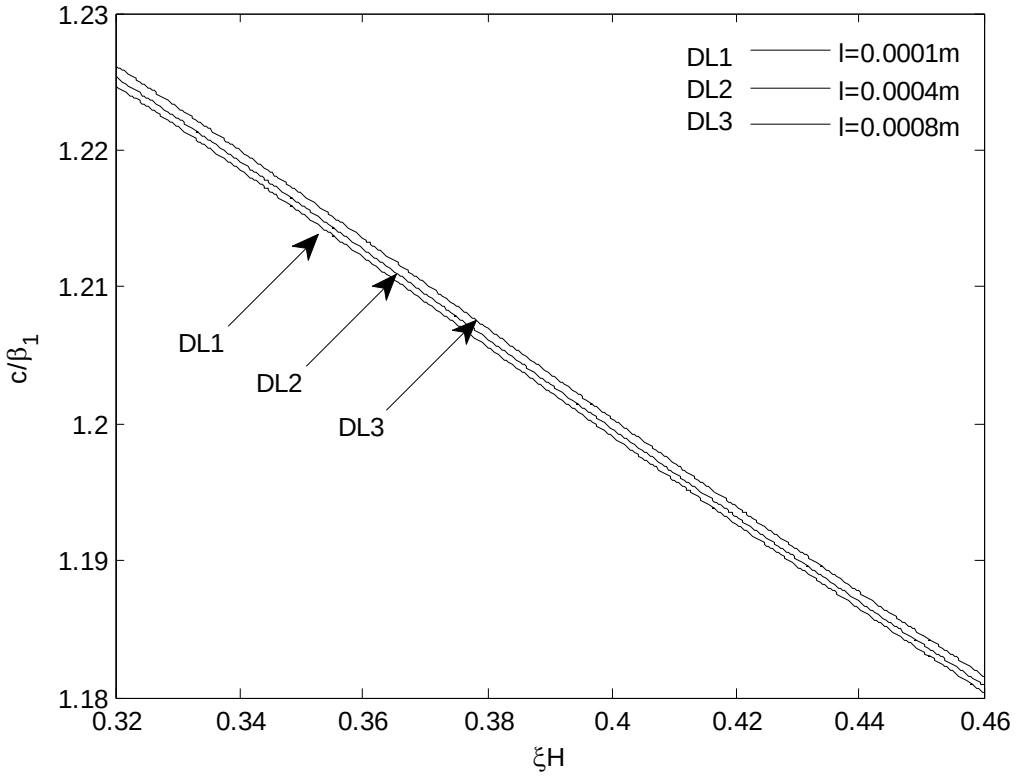

Figure 4.9 Variation of normalized damping phase velocity (c/β_1) of SH waves against normalized wave number (ξH) for different values of characteristic length parameter (l)

4.6 CONCLUSION

The propagation of SH waves is studied in viscoelastic layer overlying a couple stress elastic half space. It is observed that the microstructural parameter characteristic length, heterogeneity, internal friction and thickness of layer have significant effects on the propagation of SH waves. The numerical results are represented graphically for various combinations of parameters involved in the problem. Following conclusions can be drawn from the present analysis

- Increase in characteristic length parameter involved in couple stress theory results in increase of phase velocity of the SH waves. The study has been made for both real and damping phase velocity.

- Heterogeneity parameter involved in viscoelastic layer has prominent effects on the phase velocity profiles of SH waves. Both real and damped phase velocities decrease with the increase in this parameter.

- Real phase velocity is observed to be decreasing with the increase in both internal friction parameter and thickness of the viscoelastic layer for the wave number greater than 1.5. On the other side, these two parameters have an inverse effect on damping phase velocity for the same range.

The theoretical consideration of study concerning microstructural effects of the substrate and effects of other parameters of viscoelastic layer on propagation of SH waves, may find possible applications in seismology, exploration geophysics, non destructive testing techniques and in designing chemical and biochemical sensors coated with surface bound receptive layers, possessing viscoelastic properties which are used to detect compounds in the liquid or gases.

CHAPTER-5

DISPERSION OF SH WAVES IN A VISCOELASTIC LAYER IMPERFECTLY BONDED WITH A COUPLE STRESS SUBSTRATE[4]

5.1 INTRODUCTION

SH waves in a layered structure for a perfectly bonded interface between two media are studied in context of couple stress theory in chapter-4, but this condition is difficult to achieve in reality. Due to certain reasons like thermal mismatch or some faults during manufacturing process, cracks or defects may appear at the interface which leads to an imperfect interface between two media. Components of displacement field are not continuous at the common boundary of two media in case of imperfect interface. The difference in displacement fields is assumed to depend linearly upon traction vector. These imperfections at the common boundary may affect the propagation of SH waves.

Keeping in mind various factors affecting the dispersion of SH waves like nature of interface between two media, properties of both half space and coated layer, here we intend to extend the study of SH waves in a viscoelastic layer lying over a couple stress substrate with imperfect interface between them. To study the effects of microstructures of substrate on the propagation of SH waves, same model as adopted in chapter-4, comprising of granular macromorphic rock (Dionysos Marble) exhibiting the properties of a couple stress solid underlying heterogeneous viscoelastic layer is employed. Couple stress theory is applied for observing the effects of microstructures of the material of substrate in terms of characteristic length and other parameters of viscoelastic layer on the propagation of SH waves. Dispersion equation of SH waves in a viscoelastic layer overlying a couple stress substrate with imperfect interface between them has been obtained. Dispersion equations for propagation of SH waves with perfectly bonded interface and slippage interface between two media are also obtained as particular cases. Effects of degree of imperfectness of the interface are studied on the phase velocity of SH waves. Dispersion curves are plotted and effects of material properties of both couple stress substrate and viscoelastic layer are studied.

[4] Communicated to SCI indexed journal

5.2 FORMULATION AND SOLUTION OF THE PROBLEM

Consider a layer of viscoelastic medium of thickness *H*, lying over a couple stress substrate with microstructures. The interface between two media is assumed to be imperfect. The origin of the coordinate system $O(x, y, z)$ lies on the interfacial surface joining substrate and layer of viscoelastic medium. Here, $z-$ axis is pointing vertically downwards into the half space, the interface between layer and half space is given by $z = 0$ and the free surface of layer is at $z = -H$. For SH waves, displacement components and body forces are independent of y co-ordinate, so if (u, v, w) are the displacement co-ordinates of a point, then $u = w = 0$ and v is function of parameters x, z and t.

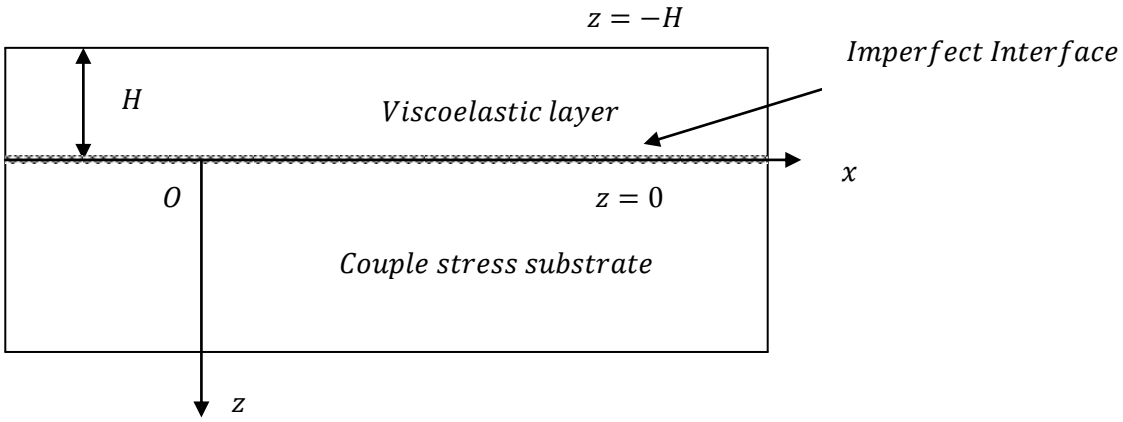

Figure 5.1 Geometry of the problem

5.3 BOUNDARY CONDITIONS

Boundary conditions to be satisfied at the free surface of the viscoelastic layer and at the interfacial surface between viscoelastic layer and couple stress half space are

(i) Top surface of viscoelastic layer should be stress free, that is

$$P_{yz} = \left(\mu_1 + \eta_1 \frac{\partial}{\partial t}\right)\frac{\partial v_1}{\partial z} = 0 \text{ at } z = -H.$$

(ii) The difference in displacement fields is assumed to depend linearly upon traction vector that is

$$P_{yz} = G(v - v_1) \text{ at } z = 0$$

where G measures the degree of imperfectness at the interface, above equation can also be written as

$$\left(\mu_1 + \eta_1 \frac{\partial}{\partial t}\right) \frac{\partial v_1}{\partial z} = G(v - v_1) \text{ at } z = 0$$

(iii) The magnitude of shear stresses of both couple stress substrate and viscoelastic layer should be equal at the interface that is $P_{yz} = \sigma_{yz}$ at $z = 0$, hence

$$\left(\mu_1 + \eta_1 \frac{\partial}{\partial t}\right) \frac{\partial v_1}{\partial z} = \mu \frac{\partial v}{\partial z} + \mu l^2 \left(\frac{\partial^3 v}{\partial x^2 \partial z} + \frac{\partial^3 v}{\partial z^3}\right) \text{ at } z = 0$$

(iv) Couple stress tensor μ_{xz} should vanish at the interface, that is $\mu_{xz} = 0$ at $z = 0$, so we get

$$2\mu l^2 \left(\frac{\partial^2 v}{\partial x^2} + \frac{\partial^2 v}{\partial z^2}\right) = 0 \text{ at } z = 0$$

5.4 DERIVATION OF SECULAR EQUATION

Using Eqs. (4.2.1.10), (4.2.1.15), (4.2.1.16), (4.2.2.12), (4.2.2.14) of chapter-4 and imposing above mentioned boundary conditions and we get following four equations

$$\begin{bmatrix} \sqrt{\overline{\mu_0}}\{2m(1 + sin(\alpha H))sin(mH) + \alpha cos(\alpha H)cos(mH)\}A + \\ \sqrt{\overline{\mu_0}}\{2m(1 + sin(\alpha H))\, cos(mH) - \alpha cos(\alpha H)sin(mH)\}B \end{bmatrix} = 0 \quad (5.4.1)$$

$$-\left(\frac{\sqrt{\overline{\mu_0}}\alpha}{2} + \frac{G}{\sqrt{\overline{\mu_0}}}\right) A - \sqrt{\overline{\mu_0}} mB + GA_1 + GB_1 = 0 \quad (5.4.2)$$

$$\frac{\alpha\sqrt{\overline{\mu_0}}A}{2} + \sqrt{\overline{\mu_0}} mB + \mu a_1[1 + (a_1^2 - \xi^2)l^2]A_1 + \mu b_1[1 + (b_1^2 - \xi^2)l^2]B_1 = 0 \quad (5.4.3)$$

$$(a_1^2 - \xi^2)A_1 + (b_1^2 - \xi^2)B_1 = 0 \quad (5.4.4)$$

5.4.1 SH waves in a viscoelastic layer over a couple stress half space with imperfect interface

Eqs. (5.4.1) to (5.4.4) will have a non-trivial solution, if determinant of coefficients of unknowns A, B, A_1, B_1 vanishes. Applying this condition to the above system of equations, we obtain following determinant

$$\begin{vmatrix} T_1 & T_2 & 0 & 0 \\ -\left(\frac{\sqrt{\overline{\mu_0}}\alpha}{2}+\frac{G}{\sqrt{\overline{\mu_0}}}\right) & -\sqrt{\overline{\mu_0}}m & G & G \\ \frac{\alpha\sqrt{\overline{\mu_0}}}{2} & \sqrt{\overline{\mu_0}}m & \mu a_1[1+(a_1^2-\xi^2)l^2] & \mu b_1[1+(b_1^2-\xi^2)l^2] \\ 0 & 0 & (a_1^2-\xi^2) & (b_1^2-\xi^2) \end{vmatrix} = 0 \quad (5.4.1.1)$$

By solving this determinant, we obtain secular equation for the SH waves in heterogeneous viscoelastic layer over a couple stress half space with imperfect interface between them as

$$(-2T_1\overline{\mu_0}m + T_2\overline{\mu_0}\alpha)\big(Q + G(b_1^2 - a_1^2)\big) + 2T_2QG = 0 \quad (5.4.1.2)$$

Where

$T_1 = [2m\{1 + sin(\alpha H)\}sin(mH) + \alpha\, cos(\alpha H)\, cos(mH)]$,

$T_2 = [2m\{1 + sin(\alpha H)\}cos(mH) - \alpha cos(\alpha H)sin(mH)]$

$Q = \mu(\xi^2 - a_1^2)(\xi^2 - b_1^2)(a_1 - b_1)l^2 + \mu b_1(\xi^2 - a_1^2) - \mu a_1(\xi^2 - b_1^2)$

Now, separating the real and imaginary parts of dispersion equation in Eq. (5.4.1.2), we get real part of dispersion equation of SH waves as

$$\begin{Bmatrix} -2R_1\mu_0 m_1 - 2R_1\omega\eta_0 m_2 - 2I_1\omega\eta_0 m_1 + \\ 2I_1\mu_0 m_2 + \alpha(R_2\mu_0 + \omega\eta_0 I_2) \end{Bmatrix}\big(Q + G(b_1^2 - a_1^2)\big) + 2R_2QG = 0 \quad (5.4.1.3)$$

and imaginary part of dispersion equation of SH waves as

$$\begin{Bmatrix} 2R_1\omega\eta_0 m_1 - 2R_1\mu_0 m_2 - 2I_1\mu_0 m_1 - \\ 2I_1\omega\eta_0 m_2 + \alpha(I_2\mu_0 - R_2\omega\eta_0) \end{Bmatrix}\big(Q + G(b_1^2 - a_1^2)\big) + 2I_2QG = 0 \quad (5.4.1.4)$$

5.4.2 SH waves in a viscoelastic layer over a couple stress half space with perfectly bonded interface

If in Eq. (5.4.1.2), $G \to \infty$, we get dispersion equation for SH waves in a viscoelastic layer over a couple stress half space with perfectly bonded interface between them and this is same as obtained in chapter-4, Eq. (4.4.6)

$$(-2T_1\overline{\mu_0}m + T_2\overline{\mu_0}\alpha)(b_1^2 - a_1^2) + 2T_2Q = 0 \quad (5.4.2.1)$$

5.4.3 SH waves in a viscoelastic layer over a couple stress half space with slip interface

If in Eq. (5.4.1.2), $G \to 0$, we get secular equation for SH waves in a viscoelastic layer over a couple stress half space for slippage interface between them

$$(-2T_1\overline{\mu_0}m + T_2\overline{\mu_0}\alpha)Q = 0 \qquad (5.4.3.1)$$

Parameters involved in Eqs. (5.4.1.2), (5.4.1.3), (5.4.1.4), (5.4.2.1) and (5.4.3.1) are all defined in section-4.4 of chapter-4.

5.5 NUMERICAL RESULTS AND DISCUSSION

(i) For viscoelastic layer the various material parameters (Gubbins [44]) used, are

$$\rho_0 = 4705\ kg/m^3, \mu_0 = 1.987 \times 10^{10}\ N/m^2, \frac{\mu_0}{\eta_0} = 10^6\ s^{-1}, \beta_1^2 = \frac{\mu_0}{\rho_0}.$$

(ii) The material properties for couple stress half space made of Dionysos marble (Vardoulakis and Georgiadis [135]), are $\mu = 30.5 \times 10^9\, N/m^2$, Density = $\rho = 2717\, kg/m^3$, the value of shear velocity comes out to be, $C_2 = 3350\, m/s$. To find the impact of characteristic length, again three different cases of characteristic length (l), comparable with the internal cell size of granular macromorphic rock which is of the order 10^{-4}, such as $l = 0.0001\, m$, $l = 0.0004\, m$, $l = 0.0008\, m$ are considered.

5.5.1 Effects of degree of imperfectness at the interface

To study the role of degree of imperfectness of the interface on the propagation of SH waves in the viscoelastic layer over a couple stress substrate, dispersion curves are provided in Fig. 5.2 by using Eq. (5.4.1.3) which is real part of Eq. (5.4.1.2) and real part of Eq. (5.4.2.1) (which is limiting case of Eq. (5.4.1.3) as $G \to \infty$) for different values G, and by keeping fixed values of other parameters as $\alpha H = 0.54$, characteristic length parameter $l = 0.0004\, m$ and friction parameter $\mu_1/\eta_1 = 10^6\, s^{-1}$. It can be observed that SH waves are dispersive and real phase velocity (c/β_1) of SH waves decreases sharply with the increase in wave number (ξH) before becoming asymptotically constant. It can be observed from the profiles that an increase in the value of parameter G, leads to increase in phase velocity of SH waves for any fixed value of dimensionless wave number (ξH). Since imperfectness is inversely proportional to G, so an increase in imperfectness adversely affects the phase velocity and phase velocity is maximum when interface is perfectly bonded ($G \to \infty$).

5.5.2 Effects of heterogeneity parameter

Role of heterogeneity parameter on the real phase velocity of SH waves in the viscoelastic layer is studied in Fig. 5.3, again by plotting Eq. (5.4.1.3). Dispersion curves are provided for three different values of heterogeneity parameter (αH=0.18, 0.54 and 0.72 for the curves R1, R2 and R3 respectively) and by keeping fixed values of other parameters as $H = 0.09m$, characteristic length parameter $l = 0.0004\, m$ and friction parameter $\mu_1/\eta_1 = 10^6\, s^{-1}$ and the value of $G = 2 \times 1.987 \times 10^{10}$ which measures degree of imperfectness at the interface. In Fig. 5.3 non dimensional phase velocity (c/β_1) of SH waves is plotted against non dimensional wave number (ξH) and it can be observed that with the increasing value of heterogeneity parameter (αH) real phase velocity of SH waves decreases.

5.5.3 Effects of friction parameter

To demonstrate the role of friction parameter on SH waves in the viscoelastic layer dispersion curves are provided in Fig. 5.4, for three different values of friction parameter $\mu_1/\eta_1 = 7 \times 10^5\, s^{-1}, 10 \times 10^5\, s^{-1}, 80 \times 10^5\, s^{-1}$, by keeping fixed value of heterogeneity parameter $\alpha H = 0.54$, characteristic length parameter $l = 0.0004\, m$ and $G = 2 \times 1.987 \times 10^{10}$. Here, non dimensional real phase velocity of SH waves tends to decrease with the increasing value of friction parameter (μ_1/η_1) and these results are visible for the wave number greater than 1.

5.5.4 Effects of thickness of viscoelastic layer

Fig. 5.5, shows the variation in non dimensional real phase velocity (c/β_1), against non dimensional wave number (ξH), for three different values of thickness, $H = 0.04\, m, 0.06\, m,$ and $0.09\, m$ of viscoelastic layer keeping fixed value of heterogeneity parameter $\alpha H = 0.54$, friction parameter $\mu_1/\eta_1 = 10^6\, s^{-1}$, characteristic length parameter $l = 0.0004\, m$ and $G = 2 \times 1.987 \times 10^{10}$. It is observed that with the increasing value of thickness of viscoelastic layer over the couple stress substrate, real phase velocity of SH waves also increases.

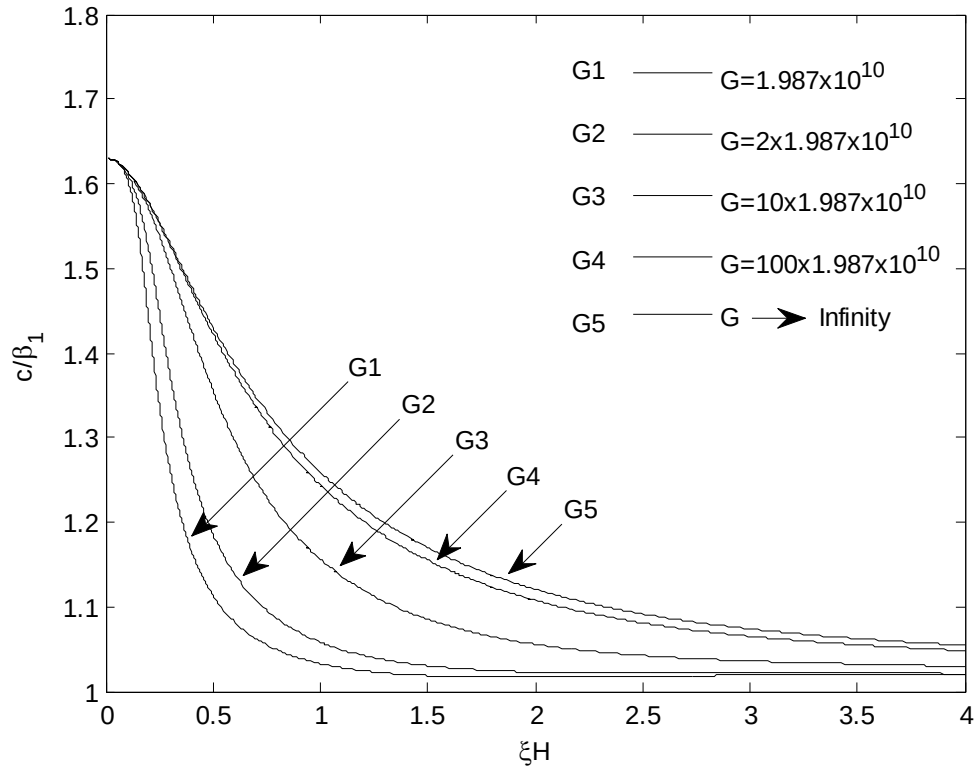

Figure 5.2 Real phase velocity profiles of SH waves with wave number for different values of parameter G, measuring imperfectness at the interface

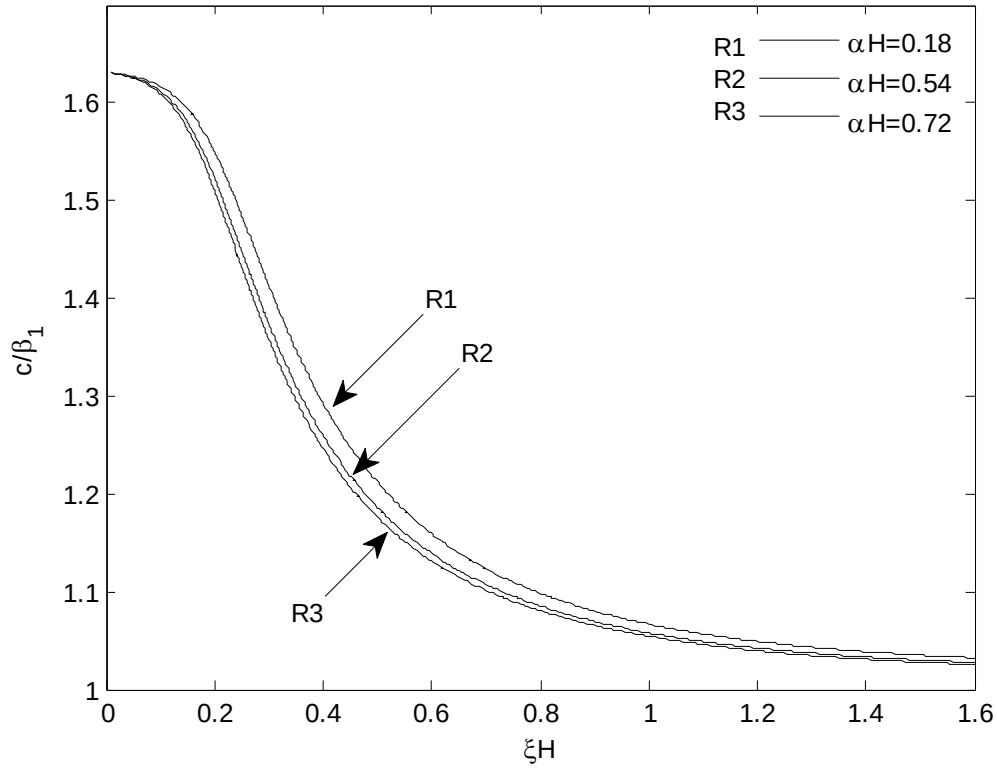

Figure 5.3 Real phase velocity profiles of SH waves with wave number for different values of parameter αH

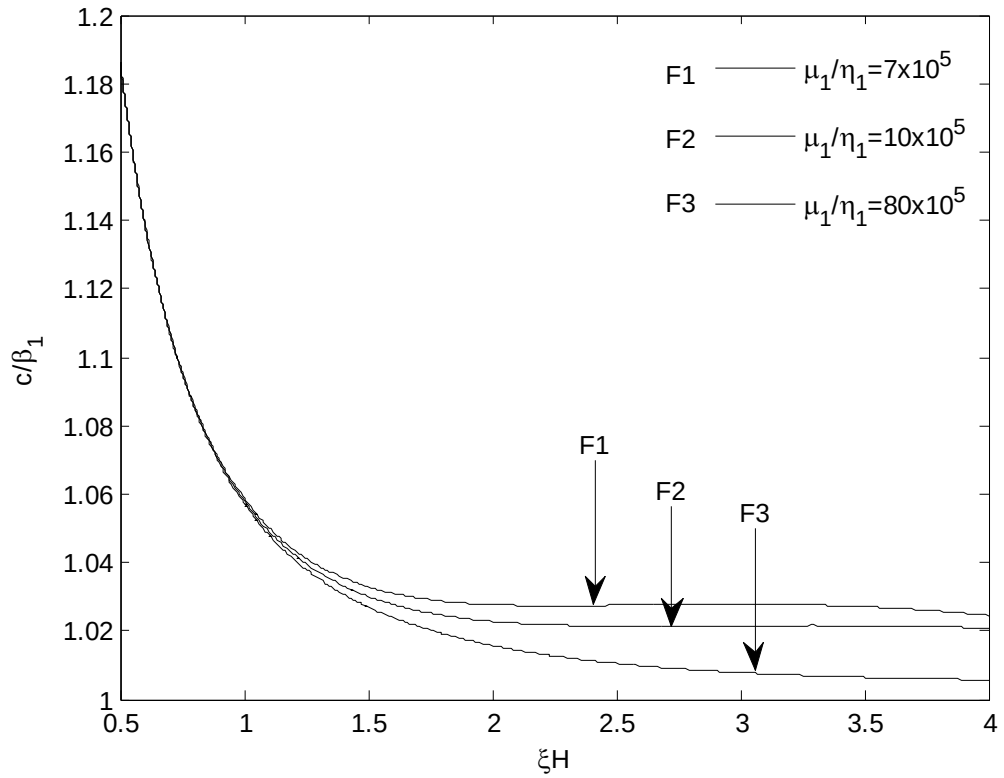

Figure 5.4 Real phase velocity profiles of SH waves with wave number for different values of parameter μ_1/η_1

5.5.5 Effects of internal microstructure of the substrate

For observing the effects of internal microstructure of the underlying substrate, the variation in normalized real phase velocity (c/β_1), against the normalized wave number (ξH), is shown in Fig. 5.6, for three different values of characteristic length parameter $l = 0.0001\,m, 0.0004\,m$ and $0.0008\,m$, keeping fixed values of heterogeneity parameter $\alpha H = 0.54$, friction parameter $\mu_1/\eta_1 = 10^6\,s^{-1}$ and $G = 2 \times 1.987 \times 10^{10}$. It can be observed that real phase velocity of SH waves increases with the increase in characteristic length (l) of the material.

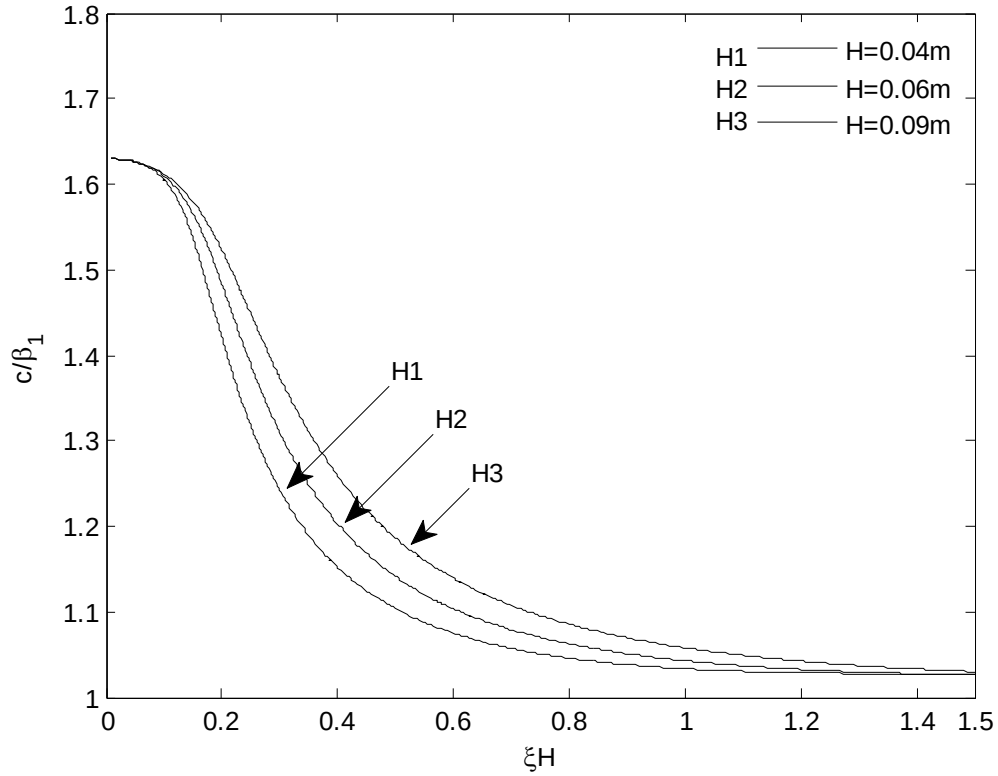

Figure 5.5 Real phase velocity profiles of SH waves with wave number for different values of parameter *H*

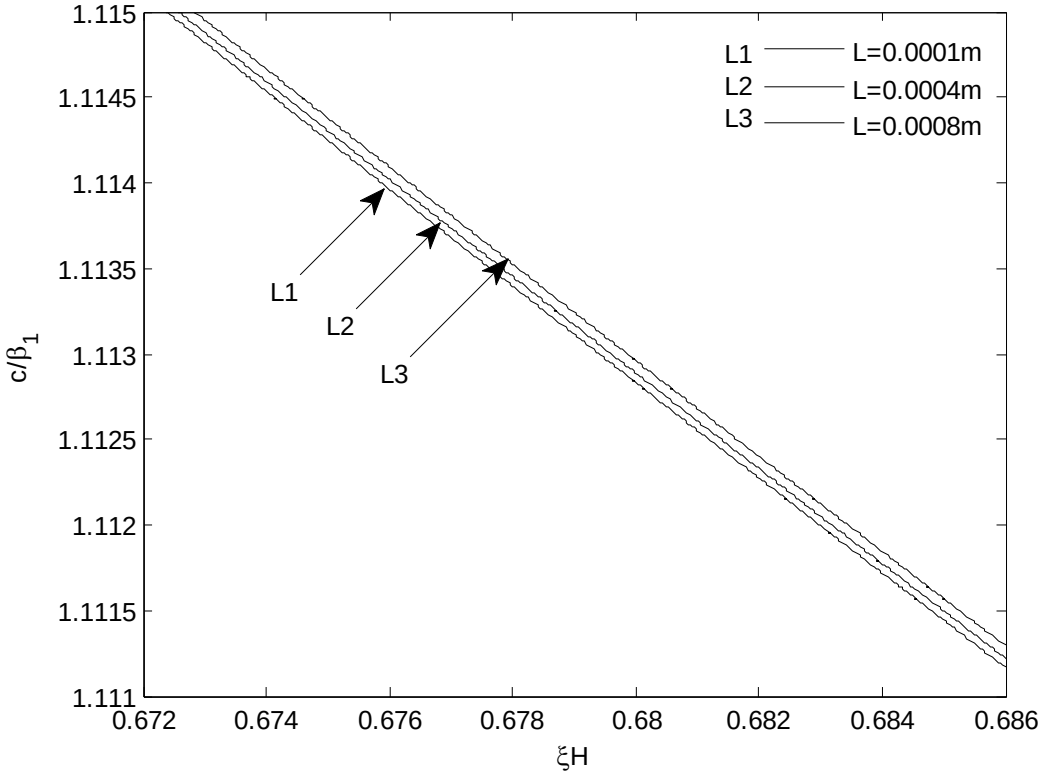

Figure 5.6 Real phase velocity profiles of SH waves with wave number for different values of parameter *l*

5.6 CONCLUSION

The propagation of SH waves is studied in a viscoelastic layer bonded imperfectly with a couple stress substrate. Analytical results for the perfectly bonded interface and slip interface are also observed as particular cases. The numerical results are presented graphically. Following major findings are drawn from the present study

1. SH waves have shown dispersion in the considered model and initially, SH wave velocity decreases sharply with the increase in the value of wave number, then it becomes asymptotically constant for the higher values of wave number.

2. Imperfectness factor at the interface between two media has a significant effect on the phase velocity of SH waves. It is observed that with the decreasing value of imperfectness at the interface, phase velocity of SH waves increases and phase velocity is highest when interface becomes perfectly bonded.

3. Both friction and heterogeneity parameters of viscoelastic layer have an adverse effect on the phase velocity of SH waves and phase velocity decreases with the increasing value of both these parameters.

4. It is observed that with the increasing value of thickness of viscoelastic layer over a couple stress substrate, phase velocity of SH waves also increases.

5. It is observed that characteristic length (l) which is measuring internal microstructure of the material of underlying substrate favours phase velocity of SH waves. Phase velocity increases with the increase in characteristic length (l) of the material of underlying couple stress substrate.

For the interfaces involving imperfections, the study carried out in this chapter is more realistic and logical. Further, the consideration of microstructural effects on the propagation of SH waves may provide possible applications in the fields of non-destructive testing techniques, semiconductor industry, seismology or geomechanics engineering.

CHAPTER-6

EFFECTS OF MICROSTRUCTURE AND LIQUID LOADING ON VELOCITY DISPERSION OF LEAKY RAYLEIGH WAVES AT LIQUID SOLID INTERFACE[5]

6.1 INTRODUCTION

It is interesting to study the changes in the profiles of Rayleigh type waves when homogeneous elastic half space is loaded with liquid. This study becomes more application oriented when the material of half space exhibits internal microstructures. Keeping this in view, we have applied the consistent couple stress theory to study the impact of characteristic length parameter and liquid loadings on the behaviour of leaky Rayleigh waves in a couple stress elastic solid half space loaded with homogeneous inviscid liquid layer of finite thickness (H) or a liquid half-space.

The study of leaky Rayleigh waves generated at the interface of solid half space with liquid layer is of great importance for quick scanning and imaging of large civil engineering structures. Equations of couple stress theory are solved and dispersion equations are obtained for the propagation of leaky Rayleigh waves in a couple stress elastic half space loaded with liquid layer of finite thickness or liquid half space. Dispersion equation for propagation of Rayleigh waves in a couple stress elastic half space without any loadings is also obtained as a special case. Phase velocity of leaky Rayleigh waves is studied for three different values of characteristic length (l) which are of the order of internal cell size of the material. Effects of thickness of liquid layer are also studied.

6.2 FORMULATION OF THE PROBLEM

Consider a couple stress elastic solid half space loaded with homogeneous inviscid liquid layer of finite thickness (H) or a liquid half space. It is assumed that that there is no reflection from the inner layers of the liquid medium. The origin of the coordinate system (x, y, z) lies on the interfacial surface joining solid half space and liquid medium. It is assumed that z-axis of the coordinate system is pointing vertically downwards into solid half space and wave is

[5] Communicated to SCI indexed journal

assumed to propagate in the direction of x-axis. All the particles along a line parallel to y-axis are assumed to be equally displaced, thus there is no variation in various fields of either media in the direction of y-axis.

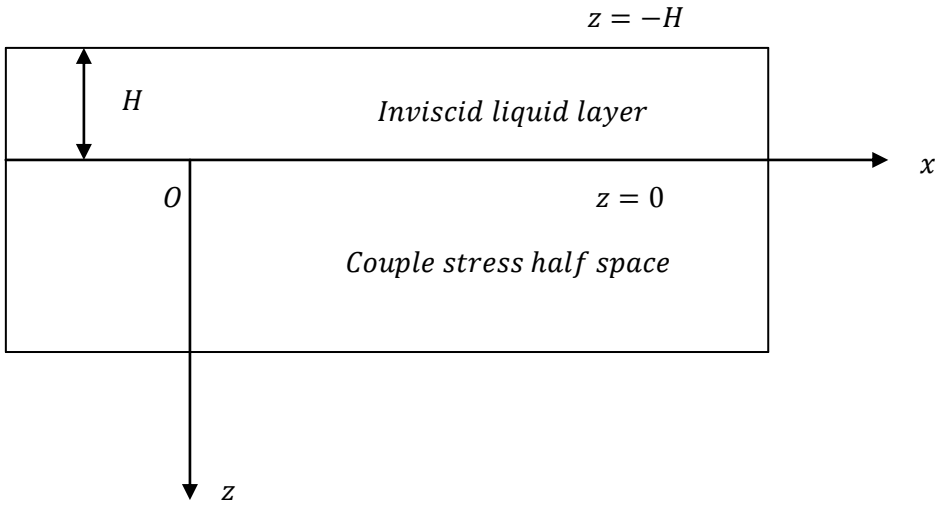

Figure 6.1 Geometry of the problem

Basic governing equations of consistent couple stress elasticity for isotropic material in the absence of body forces and constitutive relations are given in Eqs. (2.2.1), (2.2.4) and (2.2.5) of chapter-2.

In order to solve the equation given in (2.2.1), we confine our discussion to two dimensional medium so, we take $\vec{u} = (u, 0, w)$ and we introduce potential functions, ϕ and $\vec{\psi} = (0, \psi, 0)$ in the solid which are defined by

$$u = \frac{\partial \phi}{\partial x} - \frac{\partial \psi}{\partial z} \text{ and } w = \frac{\partial \phi}{\partial z} + \frac{\partial \psi}{\partial x} \tag{6.2.1}$$

where ϕ and ψ are potential function of longitudinal and shear waves in the solid half-space. Substituting Eqs. (6.2.1) into Eq. (2.2.1), we obtain two decoupled equations in terms of potential functions as

$$\nabla^2 \phi = \frac{1}{C_1^2} \frac{\partial^2 \phi}{\partial t^2} \tag{6.2.2}$$

$$\nabla^2 \psi - l^2 \nabla^4 \psi = \frac{1}{C_2^2} \frac{\partial^2 \psi}{\partial t^2} \tag{6.2.3}$$

where $C_1^2 = \frac{(\lambda + 2\mu)}{\rho}$, $C_2^2 = \frac{\mu}{\rho}$ are the dilatational and shear waves speed, respectively in classical theory of elasticity.

In the liquid medium, we have

$$u_L = \frac{\partial \phi_L}{\partial x} - \frac{\partial \psi_L}{\partial z} \text{ and } w_L = \frac{\partial \phi_L}{\partial z} + \frac{\partial \psi_L}{\partial x} \quad (6.2.4)$$

Here ϕ_L and ψ_L are the scalar and vector potential, u_L and w_L are x and z components of the particle displacement in the liquid medium.

Because the inviscid liquid does not support the shear motion, therefore shear modulus of liquid vanishes that is $\mu_L = 0$ and hence $\psi_L = 0$. The potential function ϕ_L and stresses σ_{ij}^L in case of liquid medium are given by

$$\nabla^2 \phi_L = \frac{1}{C_L^2} \frac{\partial^2 \phi_L}{\partial t^2} \quad (6.2.5)$$

$$\sigma_{ij}^L = \lambda_L \left(\frac{\partial u_L}{\partial x} + \frac{\partial w_L}{\partial z} \right) \delta_{ij} = \lambda_L \left(\frac{\partial^2 \phi_L}{\partial x^2} + \frac{\partial^2 \phi_L}{\partial z^2} \right) \quad (6.2.6)$$

where $C_L^2 = \frac{\lambda_L}{\rho_L}$, C_L is the velocity of sound in the liquid, λ_L is the bulk modulus, ρ_L is the density of the liquid.

6.3 BOUNDARY CONDITIONS

The boundary conditions to be satisfied at the solid liquid interface are:

(i) Continuity of normal component of stress tensor at the interface z = 0, that is $\sigma_{zz} = \sigma_{zz}^L$ that is $\lambda \left(\frac{\partial u}{\partial x} + \frac{\partial w}{\partial z} \right) + 2\mu \frac{\partial w}{\partial z} = \lambda_L \left(\frac{\partial u_L}{\partial x} + \frac{\partial w_L}{\partial z} \right)$

(ii) Since liquid does not support the shear motion so, the tangential component of the stress tensor of couple stress half space should be equal to zero, which implies $\sigma_{zx} = 0$, at z = 0 that is

$$\mu \left(\frac{\partial u}{\partial z} + \frac{\partial w}{\partial x} \right) - \mu l^2 \left(\frac{\partial^3 u}{\partial x^2 \partial z} - \frac{\partial^3 w}{\partial x^3} + \frac{\partial^3 u}{\partial z^3} - \frac{\partial^3 w}{\partial z^2 \partial x} \right) = 0 \text{ at z = 0}$$

(iii) The continuity of the normal component of the displacement field of both media, at the interface z = 0, that is $w = w_L$

(iv) Couple stress tensor, μ_{zy} should vanish at the interface z = 0, that is $\mu_{zy} = 0$, that is

$$2\eta \left(\frac{\partial^2 u}{\partial z^2} - \frac{\partial^2 w}{\partial z \partial x} \right) = 0 \text{ at z = 0}$$

6.4 FORMAL SOLUTION OF THE PROBLEM

We assume the solution of the form

$$\phi = f(z) e^{i\xi(x-ct)} \quad (6.4.1)$$

$$\psi = g(z) e^{i\xi(x-ct)} \quad (6.4.2)$$

$$\phi_L = \bar{\phi}_L(z) e^{i\xi(x-ct)} \quad (6.4.3)$$

where c is the phase velocity, ξ is the wave number. Now using the solution given in Eqs. (6.4.1) to (6.4.3) in the Eqs. (6.2.2), (6.2.3) and (6.2.5), we obtain following three differential equations

$$\frac{d^2 f(z)}{dz^2} - \left(\xi^2 - \frac{\xi^2 c^2}{C_1^2}\right) f(z) = 0 \tag{6.4.4}$$

$$\frac{d^4 g(z)}{dz^4} - \left(2\xi^2 + \frac{1}{l^2}\right)\frac{d^2 g(z)}{dz^2} + \left(\xi^4 + \frac{\xi^2}{l^2}\left(1 - \frac{c^2}{C_2^2}\right)\right) g(z) = 0 \tag{6.4.5}$$

$$\frac{d^2 \bar{\phi}_L(z)}{dz^2} - \left(\xi^2 - \frac{\xi^2 c^2}{C_L^2}\right) \bar{\phi}_L(z) = 0 \tag{6.4.6}$$

By solving these differential equations, we get following expressions for $f(z), g(z)$ and $\bar{\phi}_L(z)$

$$f(z) = (A_1 e^{-\alpha z} + A_2 e^{\alpha z}) \tag{6.4.7}$$

$$g(z) = \left(B_1 e^{-\alpha z} + B_2 e^{-\beta z} + B_3 e^{\alpha z} + B_4 e^{\beta z}\right) \tag{6.4.8}$$

$$\bar{\phi}_L(z) = (D_1 e^{\gamma z} + D_2 e^{-\gamma z}) \tag{6.4.9}$$

where

$$a^2 = \xi^2 \left(1 - \frac{c^2}{C_1^2}\right)$$

$$(\alpha^2 + \beta^2) = 2\xi^2 + \frac{1}{l^2}$$

$$\alpha^2 \beta^2 = \xi^4 + \frac{\xi^2}{l^2}\left(1 - \frac{c^2}{C_2^2}\right)$$

$$\gamma^2 = \xi^2 \left(1 - \frac{c^2}{C_L^2}\right)$$

Hence solutions are given by

$$\phi = (A_1 e^{-\alpha z} + A_2 e^{\alpha z}) e^{i\xi(x-ct)} \tag{6.4.10}$$

$$\psi = \left(B_1 e^{-\alpha z} + B_2 e^{-\beta z} + B_3 e^{\alpha z} + B_4 e^{\beta z}\right) e^{i\xi(x-ct)} \tag{6.4.11}$$

$$\phi_L = (D_1 e^{\gamma z} + D_2 e^{-\gamma z}) e^{i\xi(x-ct)} \tag{6.4.12}$$

These solutions consist of pairs of partial waves propagating along positive and negative z-directions with A_1, A_2, B_1, B_2, B_3, B_4, D_1, D_2 being unknown amplitudes. These forms of formal solution are appropriate for the description of wave propagation in infinite elastic media.

For wave propagation in half space, we choose the partial waves satisfying the radiation condition that all field variables must be bounded for location deep within the solid. Thus for

propagation in the half space $z \geq 0$ underlying a liquid layer of finite thickness (H) or a liquid half space, we choose our solutions as

$$\phi = A_1 e^{-az} e^{i\xi(x-ct)} \tag{6.4.13}$$

$$\psi = \left(B_1 e^{-\alpha z} + B_2 e^{-\beta z}\right) e^{i\xi(x-ct)} \tag{6.4.14}$$

$$\phi_L = \begin{cases} D_1 \text{Sinh}\{\gamma(z+H)\} e^{i\xi(x-ct)}, & \text{for the liquid layer}, -H \leq z \leq 0 \\ D_1 e^{\gamma z} e^{i\xi(x-ct)} & \text{for the liquid half} - \text{space} \end{cases} \tag{6.4.15}$$

6.5 DERIVATION OF DISPERSION EQUATIONS

6.5.1 Leaky Rayleigh waves in a couple stress elastic half space loaded with inviscid liquid layer of finite thickness

We derive the dispersion relations for leaky Rayleigh surface waves propagating in a couple stress elastic half space underlying a liquid layer of finite thickness in context of couple stress theory. Solid half space extends in the positive z-direction and liquid layer of finite thickness (H) or liquid half-space in negative z-direction. By applying the required interfacial boundary conditions at z = 0 given in section 6.3, we obtain the following set of four homogeneous equations in four unknowns A_1, B_1, B_2 and D_1

$$\mu\left[\left(\frac{C_1^2}{C_2^2}(a^2-\xi^2)\right)+2\xi^2\right]A_1 - 2\mu\alpha i\xi B_1 - 2\mu\beta i\xi B_2 - \lambda_L \text{Sinh}(\gamma H)(\gamma^2-\xi^2)D_1 = 0 \tag{6.5.1.1}$$

$$-2\mu i a\xi A_1 + \mu[l^2(\xi^2-\alpha^2)^2 - (\xi^2+\alpha^2)]B_1 + \mu[l^2(\xi^2-\beta^2)^2 - (\xi^2+\beta^2)]B_2 = 0 \tag{6.5.1.2}$$

$$-aA_1 + i\xi B_1 + i\xi B_2 - \gamma D_1 \text{Cosh}(\gamma H) = 0 \tag{6.5.1.3}$$

$$\mu l^2(\alpha\xi^2 - \alpha^3)B_1 + \mu l^2(\beta\xi^2 - \beta^3)B_2 = 0 \tag{6.5.1.4}$$

For non trivial solution of above four equations, we take the determinant of the coefficient matrix of above four equations equal to zero

$$\begin{vmatrix} \mu P & -2\mu\alpha i\xi & -2\mu\beta i\xi & -\lambda_L \text{Sinh}(\gamma H)(\gamma^2-\xi^2) \\ -2ia\xi & [l^2(\xi^2-\alpha^2)^2 - (\xi^2+\alpha^2)] & [l^2(\xi^2-\beta^2)^2 - (\xi^2+\beta^2)] & 0 \\ -a & i\xi & i\xi & -\gamma \text{Cosh}(\gamma H) \\ 0 & (\alpha\xi^2-\alpha^3) & (\beta\xi^2-\beta^3) & 0 \end{vmatrix} = 0$$

By solving this determinant, we obtain following dispersion equation for leaky Rayleigh waves in an elastic half space loaded with liquid layer of finite thickness (H) in context of consistent couple stress theory

$$\begin{bmatrix} \left(\mu\gamma P - a\lambda_L \tanh(\gamma H) K_\gamma\right)\left\{\beta K_\beta (l^2 K_\alpha^2 - S_\alpha) - \alpha K_\alpha \left(l^2 K_\beta^2 - S_\beta\right)\right\} \\ -4a\alpha\beta\gamma\mu\left(K_\alpha - K_\beta\right)\xi^2 - 2a\lambda_L \tanh(\gamma H)\xi^2 K_\gamma\left(-\alpha K_\alpha + \beta K_\beta\right) \end{bmatrix} = 0 \qquad (6.5.1.5)$$

where

$$P = 2\xi^2 - \frac{C_1^2}{C_2^2}(\xi^2 - a^2)$$

$$K_\alpha = (\xi^2 - \alpha^2)$$

$$K_\beta = (\xi^2 - \beta^2)$$

$$K_\gamma = (\xi^2 - \gamma^2)$$

$$S_\alpha = (\xi^2 + \alpha^2)$$

$$S_\beta = (\xi^2 + \beta^2)$$

6.5.2 Rayleigh waves in a stress free couple stress elastic half space

If we assume $\lambda_L \to 0$, Eq. (6.5.1.5) reduces to the dispersion equation for Rayleigh waves in stress free homogeneous solid elastic half space under couple stress theory

$$P\left[\beta K_\beta (l^2 K_\alpha^2 - S_\alpha) - \alpha K_\alpha \left(l^2 K_\beta^2 - S_\beta\right)\right] - 4a\alpha\beta\left(K_\alpha - K_\beta\right)\xi^2 = 0 \qquad (6.5.2.1)$$

6.5.3 Leaky Rayleigh waves in a couple stress elastic half space loaded with inviscid liquid half space

Again by applying the required interfacial boundary conditions mentioned in section 6.3, at z = 0, we obtain the following set of four homogeneous equations in four unknowns A_1, B_1, B_2 and D_1 for the Rayleigh waves in a couple stress elastic half space under the loading of inviscid liquid half space

$$\mu\left[\left(\frac{C_1^2}{C_2^2}(a^2 - \xi^2)\right) + 2\xi^2\right]A_1 - 2\mu\alpha i\xi B_1 - 2\mu\beta i\xi B_2 - \lambda_L(\gamma^2 - \xi^2)D_1 = 0 \qquad (6.5.3.1)$$

$$-2\mu i a\xi A_1 + \mu[l^2(\xi^2-\alpha^2)^2 - (\xi^2+\alpha^2)]B_1 + \mu[l^2(\xi^2-\beta^2)^2 - (\xi^2+\beta^2)]B_2 = 0$$

(6.5.3.2)

$$-aA_1 + i\xi B_1 + i\xi B_2 - \gamma D_1 = 0 \quad (6.5.3.3)$$

$$\mu l^2(\alpha\xi^2 - \alpha^3)B_1 + \mu l^2(\beta\xi^2 - \beta^3)B_2 = 0 \quad (6.5.3.4)$$

For non trivial solution of above four homogeneous equations, we take the determinant of the coefficient matrix equal to zero

$$\begin{vmatrix} \mu P & -2\mu\alpha i\xi & -2\mu\beta i\xi & -\lambda_L(\gamma^2-\xi^2) \\ -2ia\xi & [l^2(\xi^2-\alpha^2)^2 - (\xi^2+\alpha^2)] & [l^2(\xi^2-\beta^2)^2 - (\xi^2+\beta^2)] & 0 \\ -a & i\xi & i\xi & -\gamma \\ 0 & (\alpha\xi^2-\alpha^3) & (\beta\xi^2-\beta^3) & 0 \end{vmatrix} = 0 \quad (6.5.3.5)$$

By solving this determinant, we obtain the following dispersion equation for leaky Rayleigh waves in a homogeneous solid elastic half space loaded with inviscid liquid half space in context of consistent couple stress theory

$$\begin{bmatrix} (\mu\gamma P - a\lambda_L K_\gamma)\{\beta K_\beta(l^2K_\alpha^2 - S_\alpha) - \alpha K_\alpha(l^2K_\beta^2 - S_\beta)\} \\ -4a\alpha\beta\gamma\mu(K_\alpha - K_\beta)\xi^2 - 2a\lambda_L\xi^2 K_\gamma(-\alpha K_\alpha + \beta K_\beta) \end{bmatrix} = 0 \quad (6.5.3.6)$$

In Eq. (6.5.1.5) if $H \to \infty$, that is liquid layer changes to liquid half space, then $\tanh(\gamma H) \to 1$, and this Eq. (6.5.1.5) reduces to the Eq. (6.5.3.6) for leaky Rayleigh waves in a homogeneous solid elastic half space under the loading of liquid half space .

6.6 NUMERICAL RESULTS AND DISCUSSIONS

The material of the solid elastic half space is assumed to have properties similar to cortical bone and various material parameters related to it are given in section-3.5 of chapter-3. The liquid medium used is inviscid liquid with $C_L = 1.5 \times 10^3\, m/s$ and density $\rho_L = 1000$ kg/m^3. Here to study the impact of characteristic length on leaky Rayleigh waves, three values of characteristic length parameter (l) are considered. Graphs are plotted using Eq. (6.5.1.5).

6.6.1 Effects of thickness of liquid layer

Fig. 6.2, shows the trend of non dimensional leaky Rayleigh wave velocity (c/C_2) with non dimensional wave number (ξH) in a couple stress elastic half space loaded with inviscid

liquid layer of finite thickness (H). Here, characteristic length ($l = 0.00003\, m$) of the material is kept fixed and thickness of the liquid layer is variable $H = 0.002\, m, 0.003\, m$ and $0.01\, m$. It can be observed that for the small values of wave number the phase velocity of Rayleigh waves is high, which decreases sharply with the increase in wave number and then becomes almost constant with the higher values of wave number. It shows that Rayleigh waves are dispersive in case of couple stress model, which is in agreement with the findings of Gazis *et al.* [40], Ottosen *et al.* [96], Georgiadis and Velgaki [42] and is contrary to the case of linear theory of classical elasticity. It clearly depicts the impact of characteristic length parameter (l), which was absent in the classical model. Here, in Fig. 6.2, the effect of liquid loadings is not visible for the given value of characteristic length ($l = 0.00003\, m$). Fig. 6.3, is taken with the same values of all the parameters as involved in Fig. 6.2, but with small variation in wave number for depicting the effects of liquid loadings by taking thickness of liquid layer as $H = 0.002\, m, 0.003\, m$ and $0.01\, m$ for H1, H2 and H3 profiles respectively. In Fig. 6.3, it can be seen that with the increase in the value of thickness of liquid layer (H), phase velocity of Rayleigh waves is decreasing.

To further study the impact of thickness of liquid layer on the propagation of leaky Rayleigh waves in homogeneous elastic half space, Figs. 6.4-6.5 are plotted with different values of characteristic length. These figures are again drawn for three different values of thickness, $H = 0.002\, m$ for the curve H1, $H = 0.003\, m$ for H2 and for curve H3, we take $H = 0.01\, m$. In Fig. 6.4, characteristic length is $l = 0.0001\, m$ and for Fig. 6.5, the value of characteristic length parameter is $l = 0.0003\, m$. It can be observed that for the small values of wave number, phase velocity of leaky Rayleigh waves is almost same in all three cases of liquid loadings, but as the wave number increases the effects are clearly visible. Similar pattern in profiles is observed, profiles are again suppressed under the increasing liquid loadings (H) in each case, which indicates the effect of liquid loading. Though the basic trend of profiles in all three Figs. 6.3 to 6.5 is same but results become significant with the increasing value of characteristic length.

6.6.2 Effects of microstructure of couple stress half space

Figs. 6.6, 6.7 and 6.8, show the effects of characteristic length parameter on the non dimensional phase velocity (c/C_2) profile of leaky Rayleigh waves against non dimensional wave number (ξH). These figures are drawn by considering three different values of characteristic length parameter, for L1 profile characteristic length is $l = 0.00003\, m$, for L2 profile it is $l = 0.0001\, m$ and for L3 the value is $l = 0.0003\, m$. Thickness of liquid layer is

kept as $H = 0.002\ m$ for the Fig. 6.6, $H = 0.003\ m$ for Fig. 6.7 and $H = 0.01\ m$ for Fig. 6.8. As, material of the half space is assumed to have properties similar to cortical bone and internal cell size of cortical bone varies from 10 to 500 μm (Vavva *et al*. [137]). Here, all the considered values of characteristic length parameter (l), lies within this specified range of internal cell size of the material. From Figs. 6.6 to 6.8, it can be observed that phase velocity of leaky Rayleigh waves increases with the increase in characteristic length (l) of the material. It can also be seen that effects of characteristic length (l) are more visible with the decreasing value of thickness of liquid loadings (H).

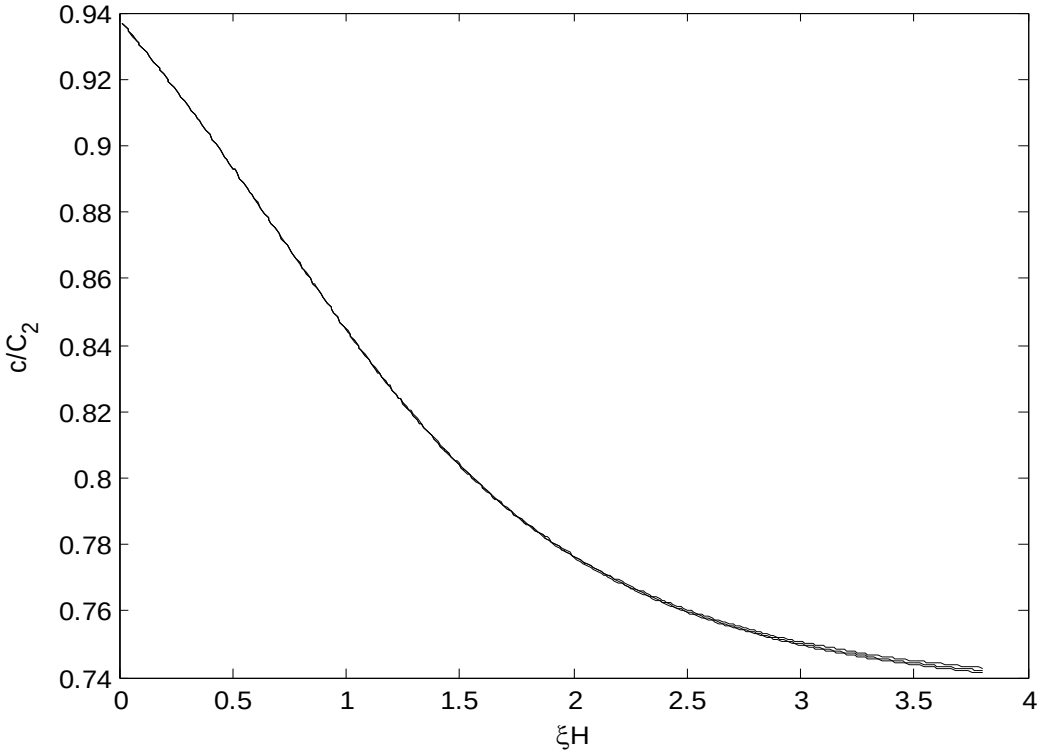

Figure 6.2 Phase velocity profile of leaky Rayleigh waves in elastic half space, loaded with liquid layer of finite thickness (H), when ($l = 0.00003\ m$)

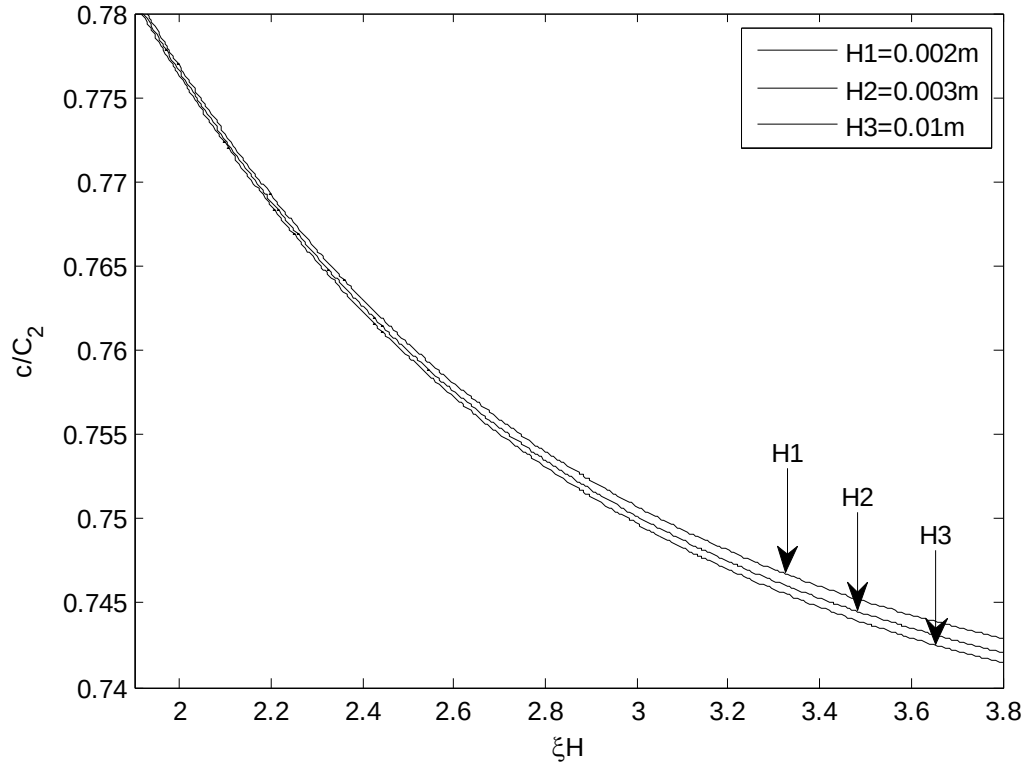

Figure 6.3 Phase velocity profile of leaky Rayleigh waves in an elastic half space with wave number, under the loading of liquid layer with thickness $H = 0.002\ m, 0.003\ m$ and $0.01\ m$ for $H1, H2$ and $H3$ curves respectively, when ($l = 0.00003\ m$)

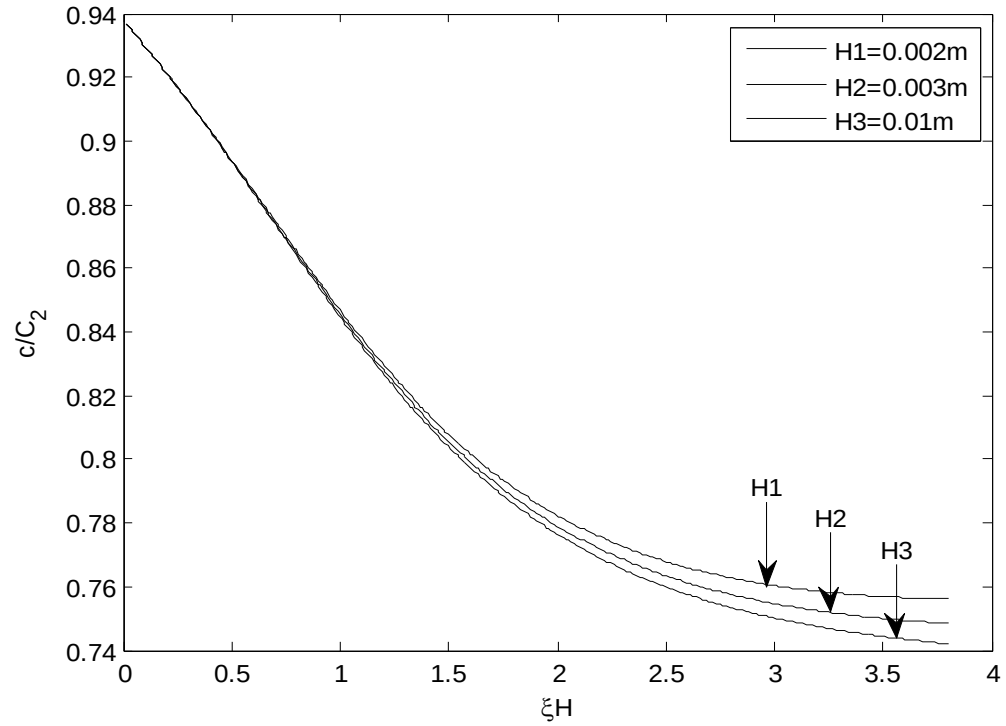

Figure 6.4 Phase velocity profile of leaky Rayleigh waves in an elastic half space with wave number, under the loading of liquid layer with thickness $H = 0.002\ m, 0.003\ m$ and $0.01\ m$ for $H1, H2$ and $H3$ curves respectively, when ($l = 0.0001\ m$)

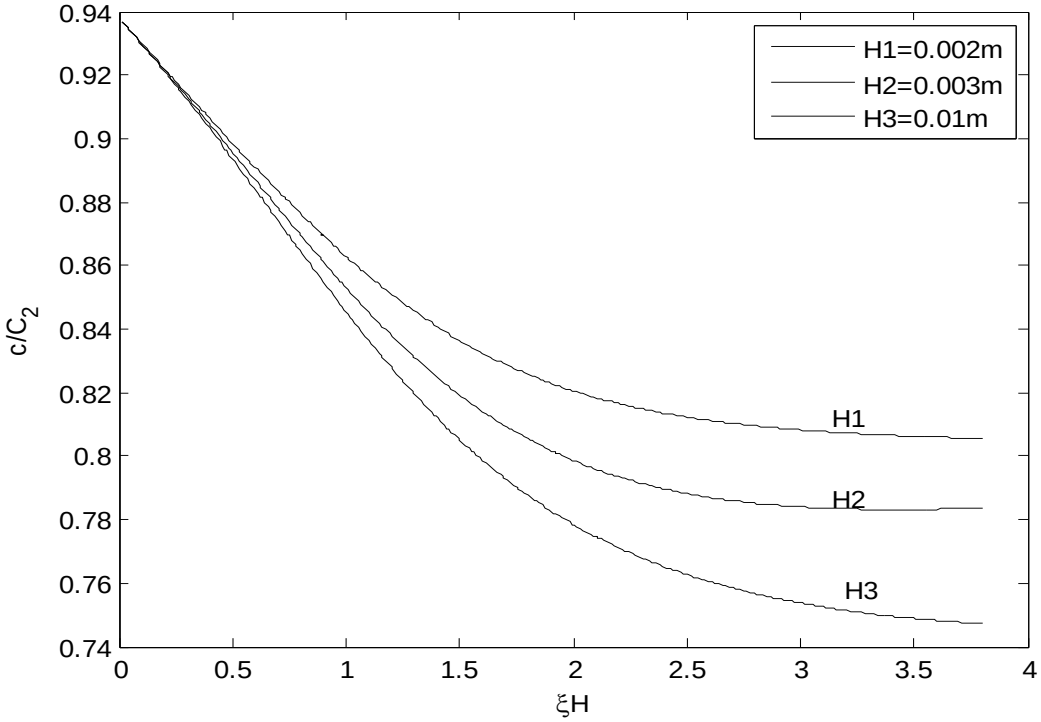

Figure 6.5 Phase velocity profile of leaky Rayleigh waves in an elastic half space with wave number, under the loading of liquid layer with thickness $H = 0.002\ m, 0.003\ m$ and $0.01\ m$ for $H1, H2$ and $H3$ curves respectively, when ($l = 0.0003\ m$)

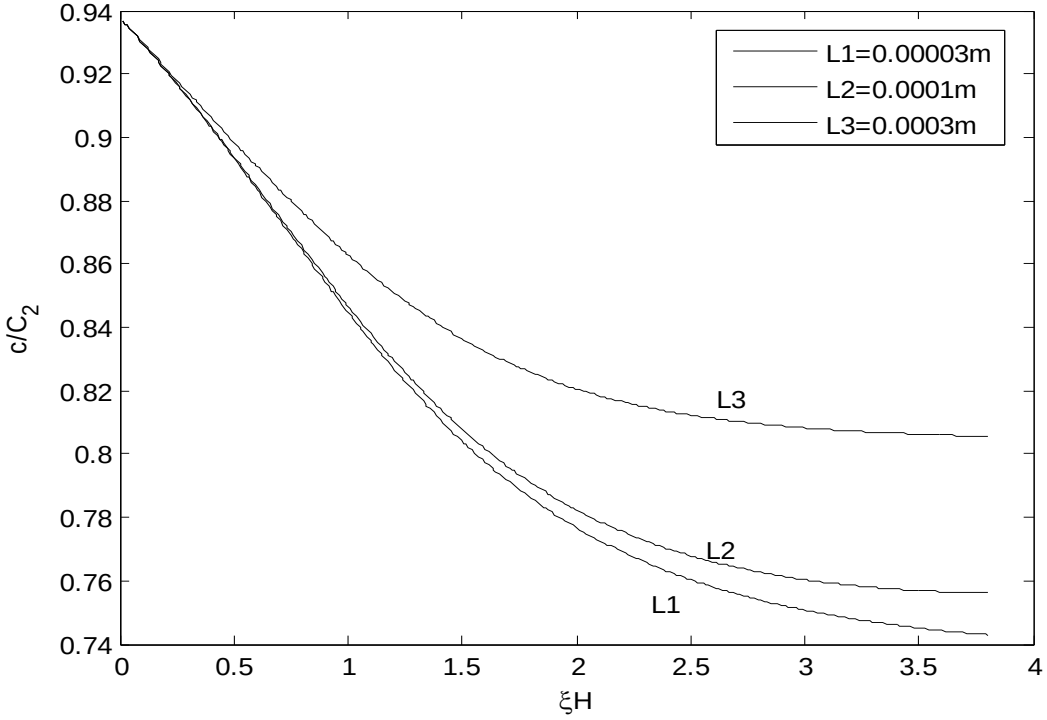

Figure 6.6 Phase velocity profile of leaky Rayleigh waves in an elastic half space with wave number, under loading of liquid layer with characteristic length $l = 0.00003\ m, 0.0001\ m$ and $0.0003\ m$ for $L1, L2$ and $L3$ curves respectively, when ($H = 0.002\ m$)

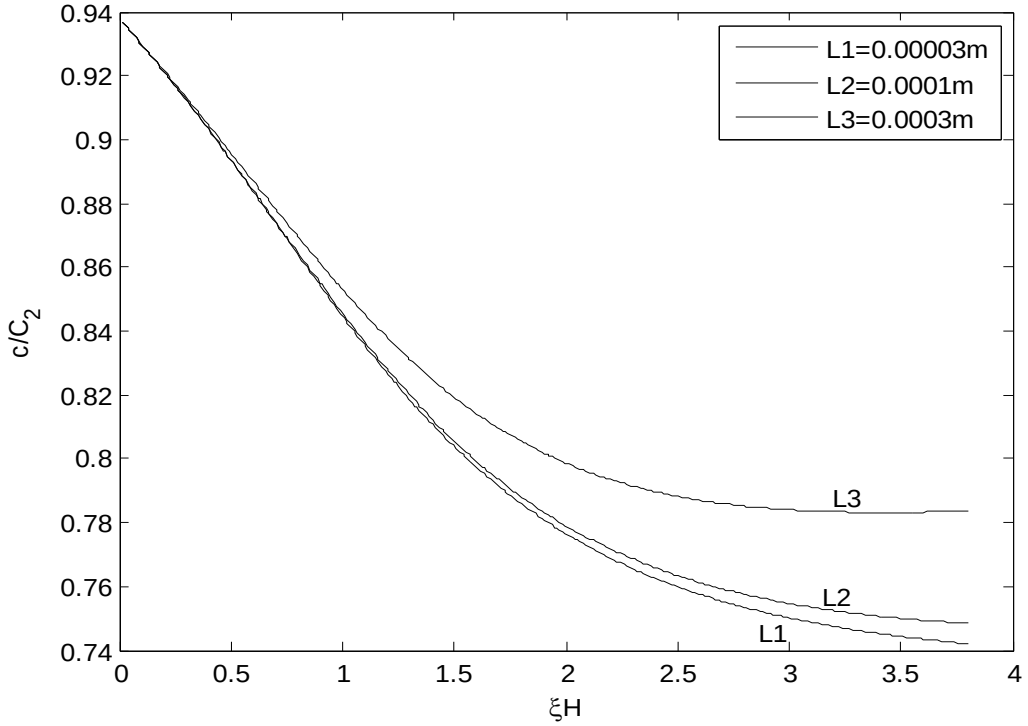

Figure 6.7 Phase velocity profile of leaky Rayleigh waves in an elastic half space with wave number, under loading of liquid layer with characteristic length $l = 0.00003\ m, 0.0001\ m$ and $0.0003\ m$ for $L1, L2$ and $L3$ curves respectively, when ($H = 0.003\ m$)

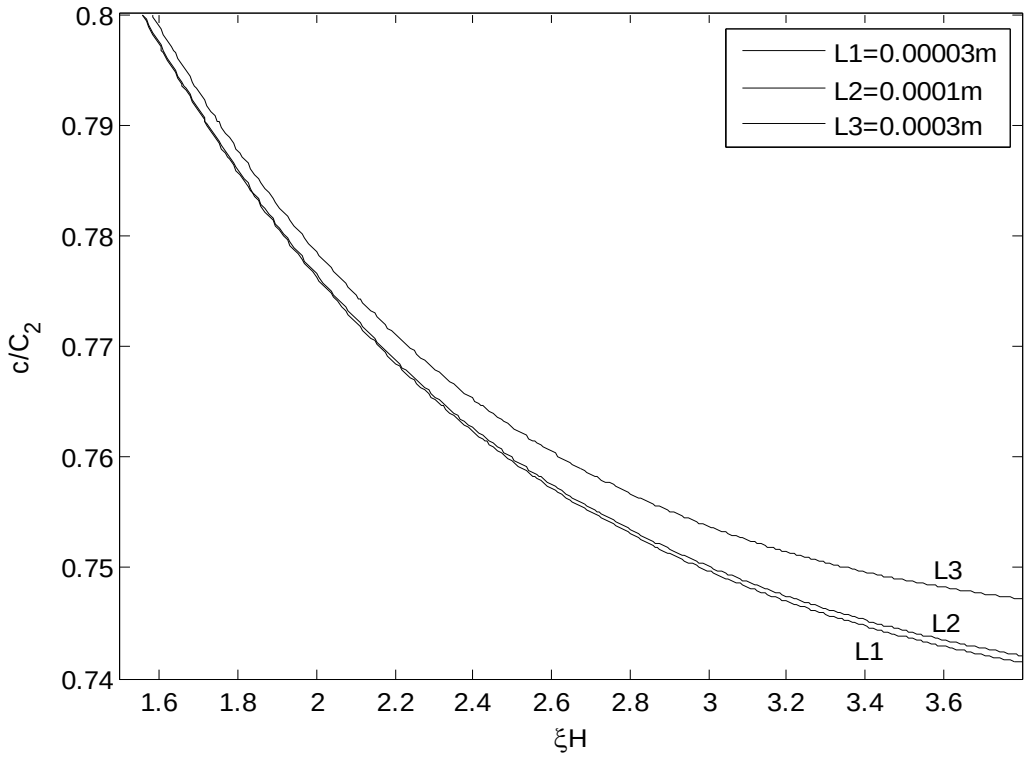

Figure 6.8 Phase velocity profile of leaky Rayleigh waves in an elastic half space with wave number, under loading of liquid layer with characteristic length $l = 0.00003\ m, 0.0001\ m$ and $0.0003\ m$ for $L1, L2$ and $L3$ curves respectively, when ($H = 0.01\ m$)

6.7 CONCLUSION

Couple stress theory involving characteristic length parameter has been applied to study the behaviour of leaky Rayleigh wave propagation in a homogeneous solid elastic half space loaded with homogeneous inviscid liquid layer. Different combinations of characteristic length parameter in comparison to cell size of the considered material are taken. Following observations can be made from the present analysis

(i) Dispersion equations are obtained for the propagation of leaky Rayleigh waves in a couple stress elastic half space loaded with liquid layer of finite thickness or liquid half space. Dispersion equation for the propagation of Rayleigh waves in a couple stress half space without any liquid loadings is also obtained as a particular case using couple stress theory.

(ii) Rayleigh type waves at the solid liquid interface are found to be dispersive in this considered model.

(iii) The effect of liquid loading is observed by taking three different values of thickness of liquid layer. It is observed that phase velocity of Rayleigh waves decreases with the increase in the thickness of liquid layer.

(iv) Effects of characteristic length parameter (l) are also studied by considering three different values of this parameter in comparison with the internal cell size of the material. It can be seen that with the increase in the characteristic length of the material, phase velocity of Rayleigh waves also increases.

The applications of these waves range from geophysics to non destructive testing of structures. A metallic structure surrounded by liquid is a natural occurring phenomenon in the fields like oil exploration or under water NDT applications. The properties of leaky Rayleigh waves like velocity, dispersion are affected by material properties of both loaded liquid and underlying solid half space. Material properties of solid can be indirectly obtained by studying the profiles of leaky Rayleigh waves.

CHAPTER 7

DISPERSION OF RAYLEIGH WAVES IN A MICROSTRUCTURAL COUPLE STRESS SUBSTRATE LOADED WITH LIQUID LAYER UNDER THE EFFECTS OF GRAVITY[6]

7.1 INTRODUCTION

Seeing the importance of Rayleigh waves to the fields of geophysics and seismology, here we have extended our work to study the effects of gravity together with microstructures of substrate on propagation of leaky Rayleigh waves. The effects of gravity on wave propagation were firstly studied by Bromwich [12] by treating gravitational force as a body force. Love ([77], [78]) studied the effects of gravity on various problems of wave propagation. He concluded that Rayleigh wave velocity gets significantly affected due to the presence of gravitational field, when the wavelength of waves is large. Bhattacharyya and De [9] studied surface wave propagation in viscoelastic media under the influence of gravity. They derived wave velocity equations and investigated particular surface waves like Rayleigh, Love and Stoneley waves. They also showed that their results are in agreement with classical results when the effects of gravity and viscosity are neglected.

We have used consistent couple stress theory proposed by Hadjesfandiari and Dargush [46] and followed the model of gravity given in Bhattacharyya and De [9] to study the impact of characteristic length parameter, gravity and liquid loadings on velocity dispersion of leaky Rayleigh waves propagating in a couple stress half space under the effects of gravity and loaded with homogeneous inviscid liquid layer of finite thickness (H) or a liquid half space. Dispersion relations for leaky Rayleigh waves in couple stress half space loaded with inviscid liquid layer of finite thickness or a liquid half space under the effects of gravity are derived.

7.2 FORMULATION AND SOLUTION OF THE PROBLEM

Consider a layer of inviscid liquid of finite thickness (H) or a liquid half space lying over a couple stress half space under the effects of gravity (g). It is assumed that that there is no reflection from the inner layers of the liquid medium. The origin of the coordinate system

[6] Communicated to SCI indexed journal

(x, y, z) lies on the interfacial surface joining solid half space and liquid medium. It is assumed that z-axis of the coordinate system is pointing vertically downwards into solid half space and wave is assumed to propagate in the direction of x-axis. All the particles along a line parallel to y-axis are assumed to be equally displaced, thus there is no variation in the fields of either media in the direction of y-axis.

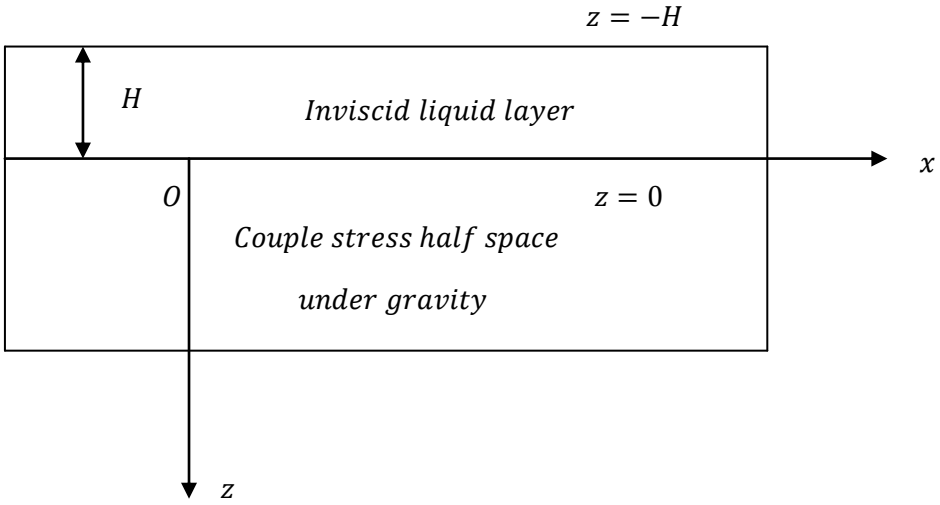

Figure 7.1 Geometry of the problem

7.2.1 Couple stress substrate under gravity

The basic governing equations of motion of couple stress theory (Hadjesfandiari and Dargush [46]) following Bhattacharyya and De [9] for the effects of gravity, are given by

$$\frac{(\lambda+2\mu)}{\rho}\left(\frac{\partial^2 u}{\partial x^2}+\frac{\partial^2 v}{\partial x\partial y}+\frac{\partial^2 w}{\partial x\partial z}\right)-\frac{\mu}{\rho}(1-l^2\nabla^2)\left(\frac{\partial^2 v}{\partial x\partial y}-\frac{\partial^2 u}{\partial y^2}-\frac{\partial^2 u}{\partial z^2}+\frac{\partial^2 w}{\partial z\partial x}\right)+g\frac{\partial w}{\partial x}=\frac{\partial^2 u}{\partial t^2} \quad (7.2.1.1)$$

$$\frac{(\lambda+2\mu)}{\rho}\left(\frac{\partial^2 u}{\partial x\partial y}+\frac{\partial^2 v}{\partial y^2}+\frac{\partial^2 w}{\partial y\partial z}\right)-\frac{\mu}{\rho}(1-l^2\nabla^2)\left(\frac{\partial^2 u}{\partial x\partial y}-\frac{\partial^2 v}{\partial x^2}-\frac{\partial^2 v}{\partial z^2}+\frac{\partial^2 w}{\partial z\partial y}\right)+g\frac{\partial w}{\partial y}=\frac{\partial^2 v}{\partial t^2} \quad (7.2.1.2)$$

$$\frac{(\lambda+2\mu)}{\rho}\left(\frac{\partial^2 u}{\partial x\partial z}+\frac{\partial^2 v}{\partial y\partial z}+\frac{\partial^2 w}{\partial z^2}\right)-\frac{\mu}{\rho}(1-l^2\nabla^2)\left(\frac{\partial^2 u}{\partial x\partial z}-\frac{\partial^2 w}{\partial x^2}-\frac{\partial^2 w}{\partial y^2}+\frac{\partial^2 v}{\partial y\partial z}\right)-g\left(\frac{\partial u}{\partial x}+\frac{\partial v}{\partial y}\right)=\frac{\partial^2 w}{\partial t^2} \quad (7.2.1.3)$$

where (u, v, w) are the displacement components and g is gravity, l is characteristic length parameter λ, μ are Lame constants, ρ is the density of material. We confine our discussion to two-dimensional medium so, we take $\vec{u} = (u, 0, w)$ and $\frac{\partial}{\partial y} \equiv 0$, in this case Eq. (7.2.1.2) will be identically satisfied.

The constitutive relations for couple stress half space are given by

$$\sigma_{ji} = \lambda u_{k,k}\delta_{ij} + \mu\left(u_{i,j} + u_{j,i}\right) - \eta\nabla^2\left(u_{i,j} - u_{j,i}\right) \quad (7.2.1.4)$$

$$\mu_{ji} = 4\eta\left(\omega_{i,j} - \omega_{j,i}\right), \text{ where } \omega_i = \frac{1}{2}\epsilon_{ijk}\, u_{k,j} \quad (7.2.1.5)$$

Here, σ_{ji} is the non-symmetric force stress tensor, μ_{ji} is skew symmetric couple stress tensor, δ_{ij} is Kronecker's delta, $\eta = \mu l^2$ is couple stress coefficient, ϵ_{ijk} is permutation tensor.

Now we introduce potential functions ϕ and $\vec{\psi} = (0, \psi, 0)$ in the solid such that $\vec{u} = \nabla\phi + \nabla \times \vec{\psi}$, so we get

$$u = \frac{\partial\phi}{\partial x} - \frac{\partial\psi}{\partial z} \text{ and } w = \frac{\partial\phi}{\partial z} + \frac{\partial\psi}{\partial x} \quad (7.2.1.6)$$

where ϕ and ψ are potential function of longitudinal and shear waves in the solid half space. Using these values of potential functions, Eqs. (7.2.1.1) and (7.2.1.3) get reduced to

$$\frac{\partial}{\partial x}\left[C_1^2\left(\frac{\partial^2\phi}{\partial x^2} + \frac{\partial^2\phi}{\partial z^2}\right) - \frac{\partial^2\phi}{\partial t^2} + g\frac{\partial\psi}{\partial x}\right] - \frac{\partial}{\partial z}\left[C_2^2(1 - l^2\nabla^2)\left(\frac{\partial^2\psi}{\partial x^2} + \frac{\partial^2\psi}{\partial z^2}\right) - \frac{\partial^2\psi}{\partial t^2} - g\frac{\partial\phi}{\partial x}\right] = 0 \quad (7.2.1.7)$$

$$\frac{\partial}{\partial z}\left[C_1^2\left(\frac{\partial^2\phi}{\partial x^2} + \frac{\partial^2\phi}{\partial z^2}\right) - \frac{\partial^2\phi}{\partial t^2} + g\frac{\partial\psi}{\partial x}\right] + \frac{\partial}{\partial x}\left[C_2^2(1 - l^2\nabla^2)\left(\frac{\partial^2\psi}{\partial x^2} + \frac{\partial^2\psi}{\partial z^2}\right) - \frac{\partial^2\psi}{\partial t^2} - g\frac{\partial\phi}{\partial x}\right] = 0 \quad (7.2.1.8)$$

where

$C_1^2 = \frac{(\lambda+2\mu)}{\rho}$, $C_2^2 = \frac{\mu}{\rho}$ are dilatational and shear wave speed.

This gives us two partial differential equations as

$$C_1^2\left(\frac{\partial^2\phi}{\partial x^2} + \frac{\partial^2\phi}{\partial z^2}\right) + g\frac{\partial\psi}{\partial x} = \frac{\partial^2\phi}{\partial t^2} \quad (7.2.1.9)$$

$$C_2^2(1 - l^2\nabla^2)\left(\frac{\partial^2\psi}{\partial x^2} + \frac{\partial^2\psi}{\partial z^2}\right) - g\frac{\partial\phi}{\partial x} = \frac{\partial^2\psi}{\partial t^2} \quad (7.2.1.10)$$

We consider the solution as

$$\phi = f(z)\mathrm{e}^{i\xi(x-ct)} \quad (7.2.1.11)$$

$$\psi = h(z)\mathrm{e}^{i\xi(x-ct)} \quad (7.2.1.12)$$

Using given two solutions in Eqs. (7.2.1.9) and (7.2.1.10), we get following two differential equations

$$\frac{d^2f(z)}{dz^2} - \left(\xi^2 - \frac{\xi^2 c^2}{C_1^2}\right) f(z) + \frac{gi\xi}{C_1^2} h(z) = 0 \tag{7.2.1.13}$$

$$\frac{d^4h(z)}{dz^4} - \left(2\xi^2 + \frac{1}{l^2}\right)\frac{d^2h(z)}{dz^2} + \left(\xi^4 + \frac{\xi^2}{l^2}\left(1 - \frac{c^2}{C_2^2}\right)\right) h(z) + \frac{gi\xi}{l^2 C_2^2} f(z) = 0 \tag{7.2.1.14}$$

By solving Eqs. (7.2.1.13) and (7.2.1.14), we get following differential equation in terms of only one function $f(z)$

$$\frac{d^6f(z)}{dz^6} - (P_1 + P_2)\frac{d^4f(z)}{dz^4} + (P_1P_2 + P_3)\frac{d^2f(z)}{dz^2} - (P_1P_3 - P_4) f(z) = 0 \tag{7.2.1.15}$$

Where

$$P_1 = \xi^2\left(1 - \frac{c^2}{C_1^2}\right)$$

$$P_2 = \left(2\xi^2 + \frac{1}{l^2}\right)$$

$$P_3 = \xi^4 + \frac{\xi^2}{l^2} - \frac{\xi^2 c^2}{l^2 C_2^2}$$

$$P_4 = \frac{g^2\xi^2}{l^2 C_1^2 C_2^2}$$

By solving Eq. (7.2.1.15), we get

$$f(z) = m_1 e^{-t_{11}z} + m_2 e^{-t_{22}z} + m_3 e^{-t_{33}z} \tag{7.2.1.16}$$

$$\phi = (m_1 e^{-t_{11}z} + m_2 e^{-t_{22}z} + m_3 e^{-t_{33}z})\mathrm{e}^{i\xi(x-ct)} \tag{7.2.1.17}$$

where m_1, m_2 and m_3 are constants and

$$t_{11} = \sqrt{2a - a_1}$$

$$t_{22} = \sqrt{-a - b\sqrt{3} - a_1}$$

$$t_{33} = \sqrt{-a + b\sqrt{3} - a_1}$$

$$2a - a_1 > 0$$

$$-a - b\sqrt{3} - a_1 > 0$$

$$-a + b\sqrt{3} - a_1 > 0$$

$$a = r^{\frac{1}{3}} Cos\left(\frac{\theta}{3}\right)$$

$$b = r^{\frac{1}{3}} Sin\left(\frac{\theta}{3}\right)$$

$$r = \sqrt{-H_1^3}$$

$$tan\theta = \frac{-\sqrt{-G_1^2 - 4H_1^3}}{G_1}$$

$$G_1 = a_3 - 3a_1a_2 + 2a_1^3$$

$$H_1 = a_2 - a_1^2$$

$$G_1^2 + 4H_1^3 < 0$$

$$a_1 = \frac{-(P_1 + P_2)}{3}$$

$$a_2 = \frac{P_1P_2 + P_3}{3}$$

$$a_3 = P_4 - P_1P_3$$

Using Eq. (7.2.1.16) in Eq. (7.2.1.13), we get

$$h(z) = \begin{Bmatrix} \alpha_1 m_1 \left[-t_{11}^2 + \left(1 - \frac{c^2}{C_1^2}\right)\xi^2\right] e^{-t_{11}z} + \\ \alpha_1 m_2 \left[-t_{22}^2 + \left(1 - \frac{c^2}{C_1^2}\right)\xi^2\right] e^{-t_{22}z} + \alpha_1 m_3 \left[-t_{33}^2 + \left(1 - \frac{c^2}{C_1^2}\right)\xi^2\right] e^{-t_{33}z} \end{Bmatrix} \quad (7.2.1.18)$$

where $\alpha_1 = \frac{C_1^2}{gi\xi}$

$$\psi = \begin{Bmatrix} \alpha_1 m_1 \left[-t_{11}^2 + \left(1 - \frac{c^2}{C_1^2}\right)\xi^2\right] e^{-t_{11}z} + \\ \alpha_1 m_2 \left[-t_{22}^2 + \left(1 - \frac{c^2}{C_1^2}\right)\xi^2\right] e^{-t_{22}z} + \\ \alpha_1 m_3 \left[-t_{33}^2 + \left(1 - \frac{c^2}{C_1^2}\right)\xi^2\right] e^{-t_{33}z} \end{Bmatrix} e^{i\xi(x-ct)} \quad (7.2.1.19)$$

$$\psi = [m_1\beta_1 e^{-t_{11}z} + m_2\beta_2 e^{-t_{22}z} + m_3\beta_3 e^{-t_{33}z}]e^{i\xi(x-ct)} \quad (7.2.1.20)$$

where

$$\beta_1 = \alpha_1 \left[-t_{11}^2 + \left(1 - \frac{c^2}{C_1^2}\right)\xi^2\right] = \frac{C_1^2}{gi\xi}\left[-t_{11}^2 + \left(1 - \frac{c^2}{C_1^2}\right)\xi^2\right]$$

$$\beta_2 = \alpha_1 \left[-t_{22}^2 + \left(1 - \frac{c^2}{C_1^2}\right)\xi^2\right] = \frac{C_1^2}{gi\xi}\left[-t_{22}^2 + \left(1 - \frac{c^2}{C_1^2}\right)\xi^2\right]$$

$$\beta_3 = \alpha_1 \left[-t_{33}^2 + \left(1 - \frac{c^2}{C_1^2}\right)\xi^2\right] = \frac{C_1^2}{gi\xi}\left[-t_{33}^2 + \left(1 - \frac{c^2}{C_1^2}\right)\xi^2\right]$$

7.2.2 Inviscid liquid layer

Equation of motion for inviscid liquid layer is

$$\lambda_L \nabla(\nabla.\vec{u}_L) = \rho_L \frac{\partial^2 \vec{u}_L}{\partial t^2} \quad (7.2.2.1)$$

where

$\vec{u}_L = (u_L, v_L, w_L)$ are displacement components in liquid layer, λ_L is the bulk modulus, ρ_L is the density of the liquid.

In the liquid medium, we have

$$u_L = \frac{\partial \phi_L}{\partial x} - \frac{\partial \psi_L}{\partial z} \text{ and } w_L = \frac{\partial \phi_L}{\partial z} + \frac{\partial \psi_L}{\partial x} \quad (7.2.2.2)$$

Here ϕ_L and ψ_L are the scalar and vector potential functions, u_L and w_L are x and z components of the particle displacement in the liquid medium.

Because the inviscid liquid does not support the shear motion, therefore shear modulus of liquid vanishes that is $\mu_L = 0$ and hence $\psi_L = 0$. Using these conditions in Eq. (7.2.2.1), we get

$$\nabla^2 \phi_L = \frac{1}{C_L^2}\frac{\partial^2 \phi_L}{\partial t^2} \quad (7.2.2.3)$$

and stresses σ_{ij}^L in case of liquid medium are given by

$$\sigma_{ij}^L = \lambda_L \left(\frac{\partial u_L}{\partial x} + \frac{\partial w_L}{\partial z}\right)\delta_{ij} \quad (7.2.2.4)$$

where $C_L^2 = \frac{\lambda_L}{\rho_L}$, C_L is the velocity of sound in the liquid.

We assume the solution of type

$$\phi_L = \bar{\phi}_L(z)\mathrm{e}^{i\xi(x-ct)} \tag{7.2.2.5}$$

Using this solution in Eq. (7.2.2.3), we get following solution

$$\phi_L = (m_4 e^{t_{44}z} + m_5 e^{-t_{44}z})\mathrm{e}^{i\xi(x-ct)} \tag{7.2.2.6}$$

where

$$t_{44}^2 = \xi^2\left(1 - \frac{c^2}{C_L^2}\right)$$

For propagation of Rayleigh waves in the half space $z \geq 0$ underlying a liquid layer of finite thickness (H) or a liquid half space, we choose the solution as

$$\phi_L = \begin{cases} m_4 \mathrm{Sinh}\{t_{44}(z+H)\}\mathrm{e}^{i\xi(x-ct)}, & \text{for the liquid layer, } -H \leq \mathrm{z} \leq 0 \\ m_4 e^{t_{44}z}\mathrm{e}^{i\xi(x-ct)} & \text{for the liquid half space} \end{cases} \tag{7.2.2.7}$$

7.3 BOUNDARY CONDITIONS

The boundary conditions to be satisfied at the solid liquid interface are:

(i) Continuity of normal component of stress tensor at the interface z = 0, that is $\sigma_{zz} = \sigma_{zz}^L$ that is $\lambda\left(\frac{\partial u}{\partial x} + \frac{\partial w}{\partial z}\right) + 2\mu\frac{\partial w}{\partial z} = \lambda_L\left(\frac{\partial u_L}{\partial x} + \frac{\partial w_L}{\partial z}\right)$

(ii) Since liquid does not support the shear motion so, the tangential component of the stress tensor of couple stress half space should be equal to zero, which implies $\sigma_{zx} = 0$, at z = 0 that is

$\mu\left(\frac{\partial u}{\partial z} + \frac{\partial w}{\partial x}\right) - \mu l^2\left(\frac{\partial^3 u}{\partial x^2 \partial z} - \frac{\partial^3 w}{\partial x^3} + \frac{\partial^3 u}{\partial z^3} - \frac{\partial^3 w}{\partial z^2 \partial x}\right) = 0$ at z = 0

(iii) The continuity of the normal components of the displacement field of both media at the interface z = 0, that is $w = w_L$

(iv) Couple stress tensor, μ_{zy} should vanish at the interface z = 0, that is $\mu_{zy} = 0$, that is

$2\eta\left(\frac{\partial^2 u}{\partial z^2} - \frac{\partial^2 w}{\partial z \partial x}\right) = 0$ at z = 0

7.4 DERIVATION OF SECULAR EQUATION

7.4.1 Rayleigh waves in a couple stress elastic half space loaded with inviscid liquid half space under gravity

Using boundary conditions given in section (7.3), together with Eqs. (7.2.1.17), (7.2.1.20) and (7.2.2.7), we get following four equations

$$\mu\left\{\frac{C_1^2}{C_2^2}(t_{11}^2-\xi^2)+2\xi^2-2\beta_1 t_{11} i\xi\right\}m_1+\mu\left\{\frac{C_1^2}{C_2^2}(t_{22}^2-\xi^2)+2\xi^2-2\beta_2 t_{22} i\xi\right\}m_2+$$

$$\mu\left\{\frac{C_1^2}{C_2^2}(t_{33}^2-\xi^2)+2\xi^2-2\beta_3 t_{33} i\xi\right\}m_3-\lambda_L(t_{44}^2-\xi^2)m_4=0 \qquad (7.4.1.1)$$

$$(\beta_1 i\xi-t_{11})m_1+(\beta_2 i\xi-t_{22})m_2+(\beta_3 i\xi-t_{33})m_3-t_{44}m_4=0 \qquad (7.4.1.2)$$

$$(\beta_1 t_{11}\xi^2-\beta_1 t_{11}^3)m_1+(\beta_2 t_{22}\xi^2-\beta_2 t_{22}^3)m_2+(\beta_3 t_{33}\xi^2-\beta_3 t_{33}^3)m_3=0 \qquad (7.4.1.3)$$

$$\{l^2(\xi^4+t_{11}^4-2t_{11}^2\xi^2)\beta_1-2t_{11}i\xi-\beta_1\xi^2-\beta_1 t_{11}^2\}m_1+\{l^2(\xi^4+t_{22}^4-2t_{22}^2\xi^2)\beta_2-$$
$$2t_{22}i\xi-\beta_2\xi^2-\beta_2 t_{22}^2\}m_2+\{l^2(\xi^4+t_{33}^4-2t_{33}^2\xi^2)\beta_3-2t_{33}i\xi-\beta_3\xi^2-\beta_3 t_{33}^2\}m_3=0$$

(7.4.1.4)

For non trivial solution of the above four homogeneous linear equations, determinant of coefficient matrix should vanish. By imposing this condition we get following determinant

$$\begin{vmatrix} E_1 & E_2 & E_3 & -\lambda_L(t_{44}^2-\xi^2) \\ \beta_1 i\xi-t_{11} & \beta_2 i\xi-t_{22} & \beta_3 i\xi-t_{33} & -t_{44} \\ \beta_1 t_{11}\xi^2-\beta_1 t_{11}^3 & \beta_2 t_{22}\xi^2-\beta_2 t_{22}^3 & \beta_3 t_{33}\xi^2-\beta_3 t_{33}^3 & 0 \\ F_1 & F_2 & F_3 & 0 \end{vmatrix}=0 \qquad (7.4.1.5)$$

where

$$E_1=\mu\left\{\frac{C_1^2}{C_2^2}(t_{11}^2-\xi^2)+2\xi^2-2\beta_1 t_{11} i\xi\right\}$$

$$E_2=\mu\left\{\frac{C_1^2}{C_2^2}(t_{22}^2-\xi^2)+2\xi^2-2\beta_2 t_{22} i\xi\right\}$$

$$E_3=\mu\left\{\frac{C_1^2}{C_2^2}(t_{33}^2-\xi^2)+2\xi^2-2\beta_3 t_{33} i\xi\right\}$$

$$F_1=\{l^2(\xi^4+t_{11}^4-2t_{11}^2\xi^2)\beta_1-2t_{11}i\xi-\beta_1\xi^2-\beta_1 t_{11}^2\}$$

$$F_2=\{l^2(\xi^4+t_{22}^4-2t_{22}^2\xi^2)\beta_2-2t_{22}i\xi-\beta_2\xi^2-\beta_2 t_{22}^2\}$$

$$F_3=\{l^2(\xi^4+t_{33}^4-2t_{33}^2\xi^2)\beta_3-2t_{33}i\xi-\beta_3\xi^2-\beta_3 t_{33}^2\}$$

By solving this determinant, we get following dispersion equation for leaky Rayleigh waves in a couple stress substrate loaded with liquid half space under the effect of gravity

$$\begin{Bmatrix} \lambda_L(t_{44}^2-\xi^2)\begin{bmatrix}(-t_{11}+\beta_{11}\xi)(U_1+V_{11})+(t_{22}-\beta_{22}\xi)(U_2+V_{22})\\ +(-t_{33}+\xi\beta_{33})(U_3+V_{33})\end{bmatrix} \\ -t_{44}\mu\begin{bmatrix}\left(\frac{C_1^2}{C_2^2}(t_{11}^2-\xi^2)+2\xi^2-2\beta_{11}t_{11}\xi\right)(U_1+V_{11})- \\ \left(\frac{C_1^2}{C_2^2}(t_{22}^2-\xi^2)+2\xi^2-2\beta_{22}t_{22}\xi\right)(U_2+V_{22})+ \\ \left(\frac{C_1^2}{C_2^2}(t_{33}^2-\xi^2)+2\xi^2-2\beta_{33}t_{33}\xi\right)(U_3+V_{33})\end{bmatrix} \end{Bmatrix}=0 \qquad (7.4.1.6)$$

Where

$$\beta_1=\frac{\beta_{11}}{i}\ ,\beta_2=\frac{\beta_{22}}{i}\ ,\beta_3=\frac{\beta_{33}}{i}$$

7.4.2 Rayleigh waves in a couple stress elastic half space loaded with inviscid liquid layer of finite thickness under gravity

Using boundary conditions mentioned in section (7.3), together with Eqs. (7.2.1.17), (7.2.1.20) and (7.2.2.7), we get following four equations

$$\mu\left\{\frac{C_1^2}{C_2^2}(t_{11}^2-\xi^2)+2\xi^2-2\beta_1t_{11}i\xi\right\}m_1+\mu\left\{\frac{C_1^2}{C_2^2}(t_{22}^2-\xi^2)+2\xi^2-2\beta_2t_{22}i\xi\right\}m_2+$$
$$\mu\left\{\frac{C_1^2}{C_2^2}(t_{33}^2-\xi^2)+2\xi^2-2\beta_3t_{33}i\xi\right\}m_3-\lambda_L(t_{44}^2-\xi^2)Sinh(t_{44}H)m_4=0 \qquad (7.4.2.1)$$

$$(\beta_1i\xi-t_{11})m_1+(\beta_2i\xi-t_{22})m_2+(\beta_3i\xi-t_{33})m_3-t_{44}Cosh(t_{44}H)m_4=0 \qquad (7.4.2.2)$$

$$(\beta_1t_{11}\xi^2-\beta_1t_{11}^3)m_1+(\beta_2t_{22}\xi^2-\beta_2t_{22}^3)m_2+(\beta_3t_{33}\xi^2-\beta_3t_{33}^3)m_3=0 \qquad (7.4.2.3)$$

$$\{l^2(\xi^4+t_{11}^4-2t_{11}^2\xi^2)\beta_1-2t_{11}i\xi-\beta_1\xi^2-\beta_1t_{11}^2\}m_1+\{l^2(\xi^4+t_{22}^4-2t_{22}^2\xi^2)\beta_2-$$
$$2t_{22}i\xi-\beta_2\xi^2-\beta_2t_{22}^2\}m_2+\{l^2(\xi^4+t_{33}^4-2t_{33}^2\xi^2)\beta_3-2t_{33}i\xi-\beta_3\xi^2-\beta_3t_{33}^2\}m_3=0$$

(7.4.2.4)

For non-trivial solution of the above four homogeneous linear equations, determinant of four unknown coefficients $m_1\ ,m_2\ ,m_3\ ,m_4$ must be zero. By imposing this condition we get following determinant

$$\begin{vmatrix} E_1 & E_2 & E_3 & -\lambda_L(t_{44}^2-\xi^2)Sinh(t_{44}H) \\ \beta_1i\xi-t_{11} & \beta_2i\xi-t_{22} & \beta_3i\xi-t_{33} & -t_{44}Cosh(t_{44}H) \\ \beta_1t_{11}\xi^2-\beta_1t_{11}^3 & \beta_2t_{22}\xi^2-\beta_2t_{22}^3 & \beta_3t_{33}\xi^2-\beta_3t_{33}^3 & 0 \\ F_1 & F_2 & F_3 & 0 \end{vmatrix}=0$$

(7.4.2.5)

By solving this determinant, we get following dispersion equation for Rayleigh waves in a couple stress substrate loaded with inviscid liquid layer of finite thickness under the effect of gravity as

$$\left\{\begin{array}{l} \lambda_L(t_{44}^2-\xi^2)tanh(t_{44}H)\begin{bmatrix}(-t_{11}+\beta_{11}\xi)(U_1+V_{11})+\\(t_{22}-\beta_{22}\xi)(U_2+V_{22})+\\(-t_{33}+\xi\beta_{33})(U_3+V_{33})\end{bmatrix}- \\ t_{44}\mu\begin{bmatrix}\left(\frac{C_1^2}{C_2^2}(t_{11}^2-\xi^2)+2\xi^2-2\beta_{11}t_{11}\xi\right)(U_1+V_{11})-\\\left(\frac{C_1^2}{C_2^2}(t_{22}^2-\xi^2)+2\xi^2-2\beta_{22}t_{22}\xi\right)(U_2+V_{22})+\\\left(\frac{C_1^2}{C_2^2}(t_{33}^2-\xi^2)+2\xi^2-2\beta_{33}t_{33}\xi\right)(U_3+V_{33})\end{bmatrix} \end{array}\right\}=0 \qquad (7.4.2.6)$$

In Eq. (7.4.2.6) if $H \to \infty$, that is liquid layer changes to liquid half space, then $\tanh(t_{44}H) \to 1$, and this Eq. (7.4.2.6) reduces to the Eq. (7.4.1.6) for leaky Rayleigh waves in a homogeneous solid elastic half space under the loading of liquid half space with effects of gravity.

7.5 NUMERICAL RESULTS AND DISCUSSION

Couple stress half space is assumed to have properties similar to cortical bone given in table (2.1) of chapter-2. The values of bulk longitudinal and shear velocities comes out to be $C_1 = 4063\, m/s$, $C_2 = 1846\, m/s$ respectively. The liquid medium used is inviscid liquid with $C_L = 1.5 \times 10^3\, m/s$ and density $\rho_L = 1000\, kg/m^3$. Here to study the impact of characteristic length, three values of characteristic length (l), $l = 0.0001\, m$, $l = 0.0002\, m$, $l = 0.0003\, m$ are considered. Dispersion equation in Eq. (7.4.2.6) is plotted below graphically.

7.5.1 Effects of Gravity

Fig. 7.2 shows the general trend of non dimensional phase velocity (c/C_2) of Rayleigh waves with non dimensional wave number (ξH) in a couple stress substrate with characteristic length parameter $l = 0.0001\, m$ under the combined effects of gravity $g = 9.8\, m/sec^2$ and liquid loadings $H = 0.002\, m$. Rayleigh waves are observed to be dispersive in the considered model. It is observed that Rayleigh wave velocity is higher for small wave number range and then it decreases down with the increasing values of the wave number and for the higher values of wave number it becomes almost constant.

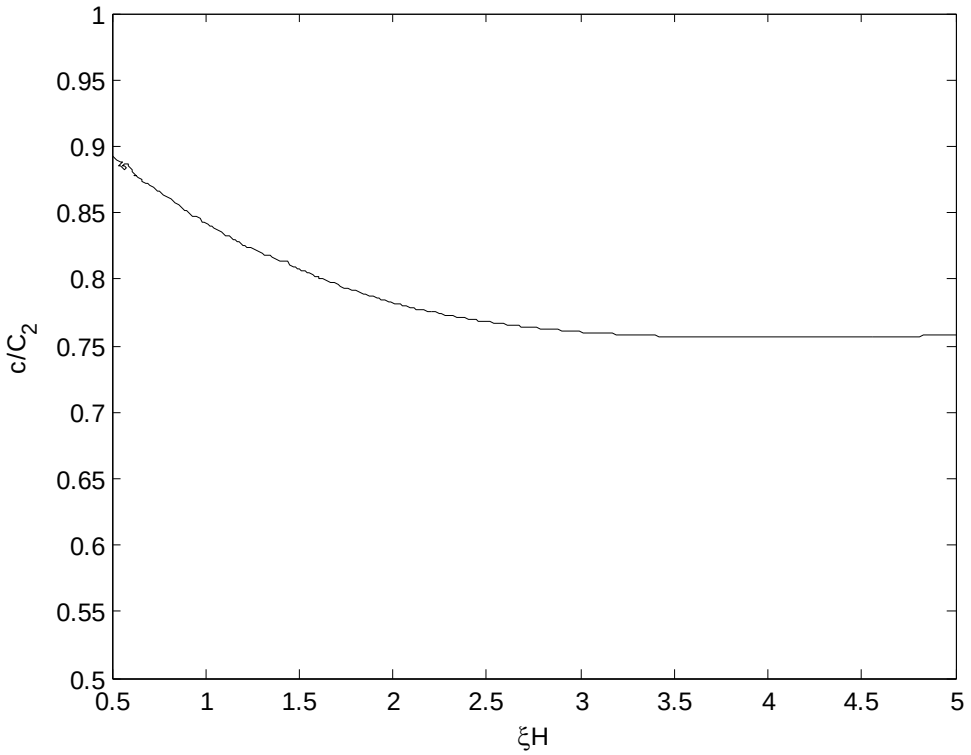

Figure 7.2 Phase velocity profile of Rayleigh waves in a couple stress substrate with wave number under the effect of gravity and liquid loadings

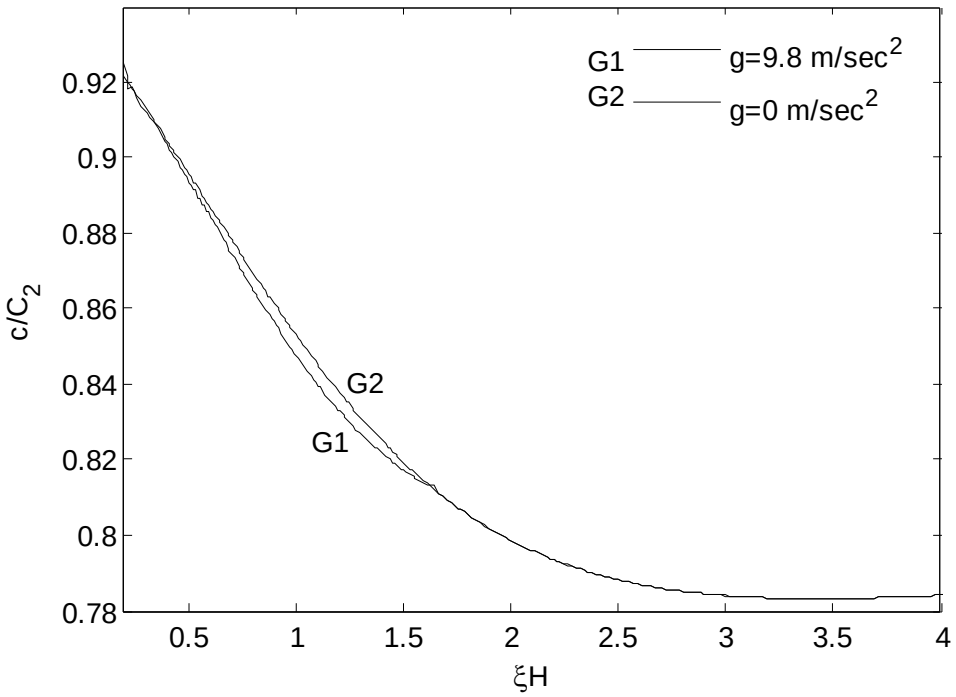

Figure 7.3 Phase velocity profile of Rayleigh waves in a couple stress substrate with wave number under liquid loadings, showing effects of gravity

Fig. 7.3 shows the effects of gravity on Rayleigh wave velocity in a couple stress half space loaded with liquid layer of finite thickness. Here, the value of characteristic length parameter is $l = 0.0002\ m$ and the thickness of liquid layer is $H = 0.002\ m$. Comparison is made by taking gravity parameter $g = 9.8\ m/sec^2$ for G1 curve and $g = 0.0\ m/sec^2$ for G2 curve. It is observed that Rayleigh waves propagate with lower phase velocity under the effects of gravity. This trend is observed only for lower values of wave number ($upto\ \xi H = 1.6$), no such difference is observed for the higher values of wave number. This finding is quite similar to one observed by Love ([77], [78]).

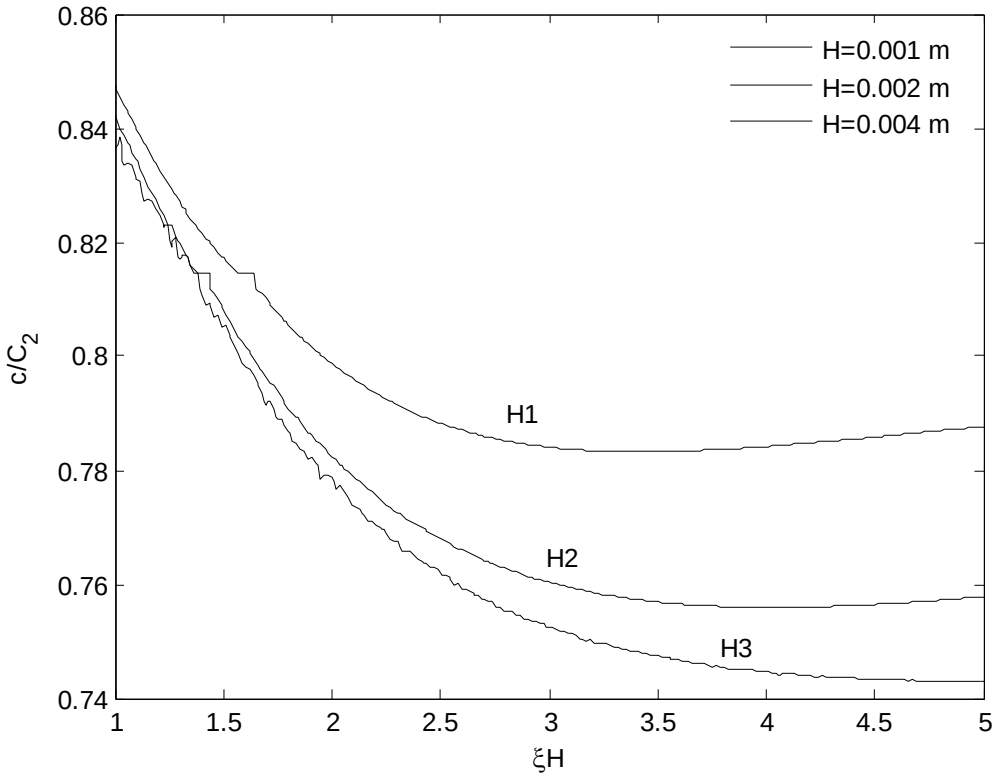

Figure 7.4 Phase velocity profile of Rayleigh waves in a couple stress substrate with wave number under gravity, showing effects of thickness of liquid layer

7.5.2 Effects of thickness of liquid layer

Effects of thickness of liquid layer on phase velocity of Rayleigh waves are shown in Fig. 7.4. For the curves in Fig. 7.4 the value of gravity $g = 9.8\ m/sec^2$, characteristic length parameter $l = 0.0001\ m$ and the value of thickness of liquid layer are $H = 0.001\ m, 0.002\ m, 0.004\ m$ for $H1, H2$ and $H3$ curves respectively. Form the figure it is clear that thickness of liquid layer has a prominent effect on phase velocity of Rayleigh waves and it is seen that increasing value of thickness of liquid layer has an adverse affect on

phase velocity of Rayleigh waves. Phase velocity is found to be decreasing with the increasing value of thickness of liquid layer.

7.5.3 Effects of characteristic length of couple stress half space

Fig. 7.5 shows the effects of microstructural parameter characteristic length (l) of the underlying couple stress substrate on phase velocity of Rayleigh waves in the presence of both gravity and liquid loadings. The values of the various parameters are $H = 0.002\, m, g = 9.8\, m/sec^2$ and values of characteristic length parameter are $l = 0.0001\, m, 0.0002\, m, 0.0003\, m$ for the curves $L1$, $L2$ and $L3$ respectively. From the figure it can be concluded that increasing value of characteristic length favours phase velocity of Rayleigh waves. For a same wave number the value of phase velocity is going higher with the increasing value of characteristic length parameter (l).

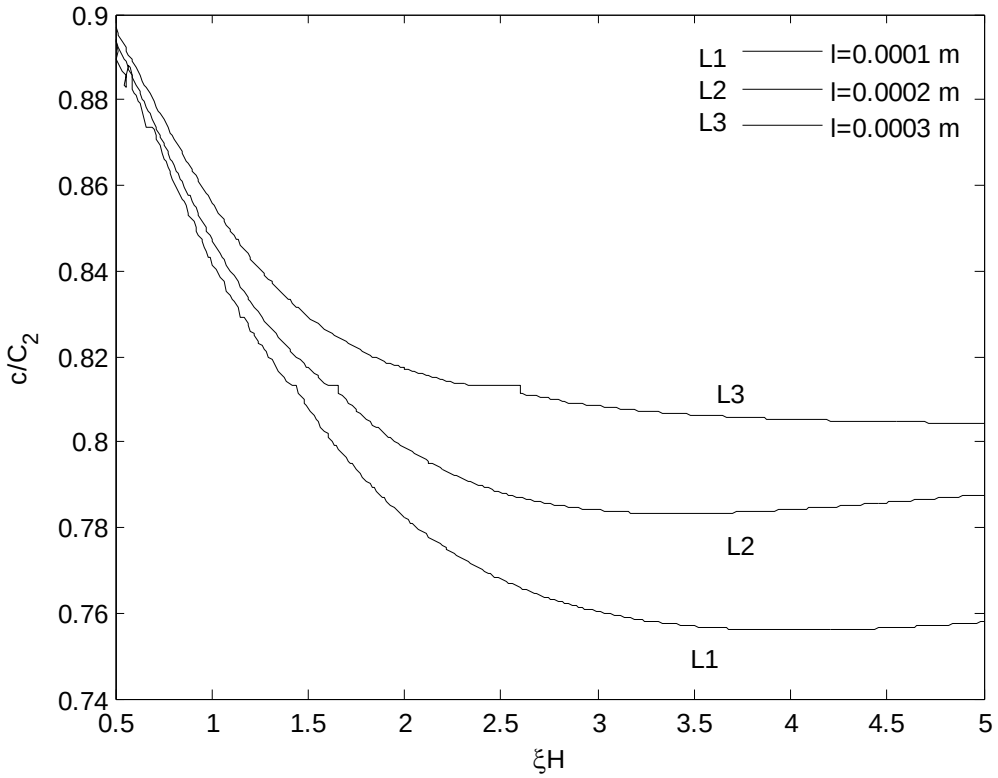

Figure 7.5 Phase velocity profile of Rayleigh waves in a couple stress substrate with wave number, under the joint effects of liquid loadings and gravity, showing effects of microstructural parameter characteristic length

7.6 CONCLUSION

Couple stress theory has been applied to study the behaviour of Rayleigh wave propagation in a couple stress half space loaded with homogeneous inviscid liquid layer under the effects of gravity. Following observations can be made from the present analysis

(1) Rayleigh waves are found to be dispersive in nature, under the model considered in the problem. It can be observed that for the small values of wave number the phase velocity of Rayleigh waves is high, which decreases with the increase in wave number and then becomes almost constant for the higher values of wave numbers.

(2) It is found that gravity has minor effect on the propagation of Rayleigh wave velocity and these are visible only for the lower values wave number. Phase velocity of Rayleigh waves decreases due to the presence of gravity as compared to phase velocity during propagation of these waves in same couple stress substrate with same conditions, but in the absence of gravity.

(3) The effect of liquid loading is observed by taking three different values of thickness of liquid layer and it is found that thickness of liquid layer has notable effects on phase velocity of Rayleigh waves. It is observed that phase velocity of Rayleigh waves decreases with the increase in the thickness of liquid layer.

(4) Effects of microstructural parameter involved in couple stress theory which measures internal microstructures of the material are also studied and it is found that characteristic length parameter also has profound effects on Rayleigh wave velocity. Study has been made by considering three different values of characteristic length parameter and it is observed that for a same wave number the value of phase velocity is higher with the increasing value of characteristic length parameter.

SUGGESTION FOR FUTURE WORK

Following suggestions have been made for the extension and further use of the present research work:

- Couple stress theory can be further used to explore the propagation of some other type of elastic waves like Stoneley waves, Longitudinal waves etc. to find the effects of internal microstructures of the material.
- The applicability of theory can further be explored in the problems involving moving loads, stress analysis and beams. The effects of internal characteristic length parameter of the material can be calculated in these problems.
- There is a scope of solving problems of refection and transmission of waves using this theory. This research work can be further extended to explore the effects of thermally or electrically conducting inviscid or viscous fluid loadings.
- The effects of anisotropy can also be considered on various problems discussed above.
- The models presented here can be further extended to theory of non linear elasticity.

The study concerning microstructural effects of material on the solution of these problems, can propose some modifications in the literature based on classical theory of elasticity and results generated from the solution of above mentioned problems may find some possible applications in seismology, exploration geophysics, non destructive testing techniques or in some other branches of engineering.

BIBLIOGRAPHY

1. Ahmad, F., Kiyani, N., Yousaf, F., Shams, M. (2002), "Guided waves in fluid loaded transversely isotropic plate", *Mathematical problems in Engineering*, 8(2):151-159.

2. Ahmed, S.M., Abo-dahab, S.M. (2012), "Influence of initial stress and gravity field on propagation of rayleigh and stoneley waves in a thermoelastic orthotropic granular medium", Article ID 245965, DOI:10.1155/2012/245965

3. Akgoz, B., Civalek, O. (2013), "Modeling and analysis of micro-sized plates resting on elastic medium using the modified couple stress theory", *Meccanica*, 48:863–873.

4. Banks, H.T., Hu, S., Kenz, Z.R. (2011), "A brief review of elasticity and viscoelasticity for solids", *Advances in Applied Mathematics and Mechanics*, 3(1):1-51.

5. Bardet, J.P., Vardoulakis, I. (2001), "The asymmetry of stress in granular media", *International Journal of Solids and Structures*, 38: 353–367.

6. Benatar, A., Rittel, D., Yarin, A.L. (2003), "Theoretical and experimental analysis of longitudinal wave propagation in cylindrical viscoelastic rods", *Journal of the Mechanics and Physics of Solids*, 51:1413 – 1431.

7. Bernstein, I., Zerrad, E., Zhou, Q., Biswas, A., Melikechi, N. (2015), "Dispersive optical solitons with Schrödinger-Hirota equation by traveling wave hypothesis", *Optoelectronics and Advanced Materials – Rapid Communications*, 9(5-6):792-797.

8. Bhattacharya, S.N. (1970), "Exact solution of SH-wave equation for inhomogeneous media", *Bulletin of the Seismological Society of America*, 60(6):1847–1859.

9. Bhattacharyya, S., De, S.N. (1977), "Surface waves in viscoelastic media under the influence of gravity", *Australian Journal of Physics*, 30:347-353.

10. Bokhari, A.H., Kara, A.H., Zaman, F.D. (2007), "Exact solutions of some general nonlinear wave equations in elasticity", *Nonlinear Dynamics*, 48:49–54.

11. Borcherdt, R.D. (2009), "Viscoelastic waves in layered media", Cambridge University Press, New York.

12. Bromwich, T.J.I'A. (1898), "On the influence of gravity on elastic waves, and, in particular, on the vibrations of elastic globe", *Proceedings of the London Mathematical Society,* 30:98-120.

13. Carcione, J.M. (1990), "Wave propagation in anisotropic linear viscoelastic media: theory and simulated wave fields", *Geophysical Journal International,* 101:739-750.

14. Carcione, J.M., Kosloff, D., Kosloff, R. (1988), "Wave propagation simulation in a linear viscoelastic medium", *Geophysical Journal International,* 95:597-611

15. Cauchy, A.L. (1823), "Researches sur 1' equilibre et le movement interieur des corps solids ou fluids, elastiques ou non-elastiques" Bulletin des sciences par 1 a Societe Philomatique de Paris, 9-13.

16. Chakraborty, M. (1985), "Reflection and transmission of SH waves from an inhomogeneous half space", *Proceedings of the Indian National Science Academy,* 51(A)-4:716-723.

17. Chattopadhyay, A., Gupta, S., Singh, A.K., Sahu, S.A. (2010), "Propagation of SH waves in an irregular non homogeneous monoclinic crustal layer over a semi-infinite monoclinic medium", *Applied Mathematical Sciences,* 4(44):2157-2170.

18. Chaudhary, S., Kaushik, V.P., Tomar, S.K. (2010), "Transmission of plane SH-waves through a monoclinic layer embedded between two different self-reinforced elastic solid half spaces", *International Journal of Applied Mathematics and Mechanics* 6(19):22-43.

19. Chen, W., Li, X. (2014), "A new modified couple stress theory for anisotropic elasticity and microscale laminated Kirchhoff plate model", *Archive of Applied Mechanics,* 84: 323–341.

20. Chirita, S., Ciarletta, M., Tibullo, V. (2013), "Rayleigh SurfaceWaves on a Kelvin-Voigt viscoelastic half-space", *Journal of Elasticity,* DOI: 10.1007/s10659-013-9447-0.

21. Chugh, S., Madan, D.K., Singh, K. (2011), "Static deformation of an orthotropic elastic layered medium due to a non uniform discontinuity along a very long strike-slip fault" *International Journal of Engineering, Science and Technology,* 3(1):69-86.

22. Cosserat, E., Cosserat, F. (1909), "Théorie des corps déformables (Theory of deformable bodies)" A. Hermann et Fils, Paris.

23. Cui, J., Du, J., Wang, J. (2013), "Study on SH Waves in Piezoelectric Structure with an imperfectly bonded viscoelastic layer", Joint UFFC, EFTF and PFM Symposium 1017-1020.

24. Das, T.K., Mukherjee, A., Sengupta, P.R. (1992), "Couple-stress effect on the propagation of waves in a thermo-visco-elastic layer", *Proceedings of the Indian National Science Academy,* 58A(2):141-150.

25. Das, T.K., Sengupta, P.R., Debnath, L. (1991), "Thermo-Visco-Elastic Rayleigh waves under the influence of couple stress and gravity", *International Journal of Mathematics and Mathematical Sciences,* 14(3):553-560.

26. Debnath, L., Roy, P.P. (1988), "Propagation of edge waves in a thinly layered laminated medium with stress couples under initial stresses", *Journal of Applied Mathematics and Simulation,* 1:271-286.

27. Destrade, M. (2003), "Rayleigh waves in symmetry planes of crystals: explicit secular equations and some explicit wave speeds", *Mechanics of Materials,* 35: 931–939.

28. Destrade, M. (2007), "Seismic Rayleigh waves on an exponentially graded, orthotropic half-space", *Proceedings of the Royal Society A,* 463:495–502.

29. Du, J., Jin, X., Wang, J., Ningbo, China, P.R. (2007), "Love wave propagation in layered magneto-electro", *Acta Mechanica,* 192:169–189.

30. Eringen, A.C. (1966), "Linear theory of micropolar elasticity", *Journal of Mathematics and Mechanics,* 15:909-924.

31. Eringen, A.C. (1968), "Theory of micropolar elasticity" In: Liebowitz, H. (Ed.), Fracture, vol. 2. Academic Press, New York, 662–729.

32. Eringen, A.C. (1999), "Microcontinuum Field Theories I: Foundations and Solids", Springer-Verlag, New York.

33. Eringen, A.C., Suhubi, E.S. (1964), "Nonlinear theory of simple micro-elastic solids—I", *International Journal of Engineering Science,* 2:189–203.

34. Fatemi, J., Vankeulen, F., Onck, P.R. (2002), "Generalized continuum theories: Application to stress analysis in bone", *Meccanica* 37**:** 385–396.

35. Firestone, F.A., Ling, D.S. (1945), "Propagation of Waves in Plates", Technical Report, Sperry Products, Danbury, CT, USA.

36. Firestone, F.A., Ling, D.S. (1954), "Method and means for generating and utilizing vibration waves in plates", USA, Patent.

37. Frederick, C.L., Worlton, D.C. (1962), "Ultrasonic thickness measurements with Lamb waves", *Journal of Nondestructive Testing,* 20: 51–55.

38. Gaur, A.M., Rana, D.S. (2014), "Shear wave propagation in piezoelectric-piezoelectric composite layered structure", *Latin American Journal of Solids and Structures*, 11(13):2483-2496.

39. Gazis, D.C. (1958), "Exact analysis of the plane-strain vibrations of thick-walled hollow cylinders", *Journal of the Acoustical Society of America*, 30:786–794.

40. Gazis, D.C., Herman, R., Wallis, R.F. (1960), "Surface elastic waves in cubic crystal", *Physical Review*, 119:533–544.

41. Georgiadis, H.G., Vardoulakis, I., Velgaki, E.G. (2004), "Dispersive Rayleigh-wave propagation in microstructured solids characterized by dipolar gradient elasticity", *Journal of Elasticity*, 74:17–45.

42. Georgiadis, H.G., Velgaki, E.G. (2003), "High-frequency Rayleigh waves in materials with micro-structure and couple-stress effects", *International Journal of Solids and Structures*, 40:2501-2520.

43. Graff, K.F. (1991) "Wave motion in elastic solids", Dover Publications, New York.

44. Gubbins, D. (1990), "Seismology and Plate Tectonics" Cambridge University Press, Cambridge.

45. Gupta, S., Majhi, D.K., Kundu, S., Vishwakarma, S.K. (2013), "Propagation of Love waves in non-homogeneous substratum over initially stressed heterogeneous half-space", *Applied Mathematics and Mechanics (English Edition),* 34(2):249–258.

46. Hadjesfandiari, A.R., Dargush, G.F. (2011), "Couple stress theory for solids", *International Journal of Solids and Structures*, 48:2496-2510.

47. Hadjesfandiari, A.R., Dargush, G.F. (2012), "Boundary element formulation for plane problems in couple stress elasticity", *International Journal for Numerical Methods in Engineering*, 89:618–636.

48. Hadjesfandiari, A.R., Dargush, G.F. (2013), "Fundamental solutions for isotropic size-dependent couple stress elasticity", *International Journal of Solids and Structures*, 50:1253–1265.

49. Hassan, W., Nagy, P.B. (1998), "On the anomalously low attenuation of the leaky Rayleigh wave in a fluid filled cylindrical cavity", *Journal of Acoustical Society of America*, 104:1246-1255.

50. He, Y., Gao, J., Chen, Z. (2015), "On the comparison of properties of rayleigh waves in elastic and viscoelastic media", *International journal of numerical analysis and modeling*, 12(2): 254-267.

51. Hussain, T., Ahmad, F. (2014), "Existence of zero group velocity modes in an incompressible plate", *Archives of Mechanics*, 66(1):55–65.

52. Jasiuk, I., Ostoja-Starzewski, M. (1995), "Planar Cosserat elasticity of materials with holes and intrusions", *Applied Mechanics Reviews*, 48(11):S11–S18

53. Kakar, R. (2015), "SH-wave propagation in a heterogeneous layer over an inhomogeneous isotropic elastic half-space", *Earthquakes and Structures*, 9(2):305-320.

54. Kakar, R., Kakar, S. (2014), "Electro-magneto-thermoelastic surface waves in non-homogeneous orthotropic granular half space", *Geomechanics and Engineering*, **7**(1): 1-36.

55. Kaur, T., Sharma, S.K., Singh, A.K. (2016), "Effect of reinforcement, gravity and liquid loading on Rayleigh-type wave propagation", *Meccanica*, DOI:10.1007/s11012-016-0379-1.

56. Kaushik, V.P., Chopra, S.D. (1984), "Transmission and reflection of inhomogeneous plane SH- waves at an interface between two horizontally and vertically heterogeneous

viscoelastic solids", *Proceedings of the Indian National Science Academy*, 50(A)-4:291-311.

57. Kocaturk, T., Akbas, S.D. (2013), "wave propagation in a microbeam based on the modified couple stress theory", *Structural Engineering and mechanics,* 46(3):417-431.

58. Koiter, W.T., (1964), "Couple stresses in the theory of elasticity, I and II", *Koninklijke Nederlandse Akademie van Wetenschappen, Series B* 67:17–44.

59. Kumar, R., Ahuja, S., Garg, S.K. (2014), "Rayleigh waves in isotropic microstretch thermoelastic diffusion solid half space", *Latin American Journal of Solids and Structures,* 11:299 – 319.

60. Kumar, R., Chawla, V. (2011), "Wave propagation at the imperfect boundary between transversely isotropic thermodiffusive elastic layer and half-space", *Journal of Engineering Physics and Thermophysics*, 84(5):1192-2000.

61. Kumar, R., Kansal, T. (2008), "Effect of rotation on Rayleigh waves in an isotropic generalized thermoelastic diffusive half space", *Archives of Mechanics*, 60(5):421–443.

62. Kumar, R., Kansal, T. (2008), "Propagation of Rayleigh waves on free surface of transversely isotropic generalized thermoelastic diffusion", *Applied Mathematics and Mechanics (English Edition)*, 29(11):1451–1462.

63. Kumar, R., Partap, G. (2006), "Rayleigh Lamb waves in micropolar isotropic elastic plate", *Applied Mathematics and Mechanics*, 27(8):1049–1059.

64. Kumar, R., Singh, B. (2000), "Reflection of plane waves at a planar viscoelastic micropolar interface", *Indian Journal of Pure and Applied Mathematics*, 31(3):287-303.

65. Kumar, S., Sharma, J.N., Sharma, Y.D. (2011), "Generalized thermoelastic waves in microstretch plates loaded with fluid of varying temperature", *International Journal of Applied Mechanics*, 3:1-24.

66. Kundu, S., Gupta, S., Chattopadhyay, A., Majhi, D.K. (2013), "Love Wave Propagation in Porous Rigid Layer Lying over an Initially Stressed Half-Space", *International Journal of Applied Physics and Mathematics*, 3(2):140-142.

67. Lakes, R.S. (1991), "Experimental micro mechanics methods for conventional and negative poisson's ratio cellular solids as cosserat continua", *Journal of Engineering Materials and Technology*, 113:148-155.

68. Lakes, R.S., Yoon, H.S., Katz, J.L. (1986), "Ultrasonic wave propagation and attenuation in wet bone", *Journal Biomedical Engineering*, 8:143-148.

69. Lamb, H. (1917), "On waves in an elastic plate", *Proceedings of the Royal Society of London*, 114-128

70. Lamkanfi, E., Declercq, N.F., Paepegem, W.V., Degrieck, J. (2007), "Finite element analysis of transmission of leaky Rayleigh waves at the extremity of a fluid-loaded thick plate", *Journal of Applied Physics*, 101:114907.

71. Lee, J.S., Kim, H.W., Kim, Y.Y., Jeon, B.C., Cho, S.H. (2009), "Damage Detection in a Plate by Using Beam-Focused Shear-Horizontal Wave Magnetostrictive Patch Transducers", 50th AIAA/ASME/ASCE/AHS/ASC Structures, Structural Dynamics, and Materials Conference
17th. 4 - 7 May, Palm Springs, California.

72. Liao, W. (2011), "A computational method to estimate the unknown coefficient in a wave equation using boundary measurements", *Inverse Problems in Science and Engineering*, 19(6):855-877.

73. Liao, W. (2011), "A numerical method to identify the acoustic coefficients in a two-dimensional wave equation", Proceedings of the 4th IEEE International Conference on Computer Science and Information Technology, 4:395 - 399.

74. Liu, H., Yang, J.L., Liu, K.X. (2007), "Love waves in layered graded composite structures with imperfectly bonded interface", *Chinese Journal of Aeronautics* 20:210-214.

75. Liu, K., Liu, Y. (2004), "Propagation characteristic of Rayleigh waves in orthotropic fluid saturated porous media", *Journal of Sound and Vibration*, 271:1-13.

76. Lord, R. (1887), "On waves propagating along the plane surface of an elastic solid", *Proceedings of the London Mathematical Society*, 17:4-11.

77. Love, A.E.H. (1911), “A treatise on the mathematical theory of elasticity” Cambridge University Press, Cambridge. Dover Publications, New York, First American Printing 1944.

78. Love, A.E.H. (1911), “Some problems of Geodynamics”, Cambridge University Press, London.

79. Lubarda, V.A. (2003), “Circular inclusions in anti-plane strain couple stress elasticity”, *International Journal of Solids and Structures*, 40: 3827-3851.

80. Lubarda, V.A., Markenscoff, X. (2000), “Conservation integrals in couple stress elasticity”, *Journal of the Mechanics and Physics of Solids*, 48: 553–564.

81. Ma, T.C., Scott, R.A., Yang, W.H. (1980), “Harmonic wave propagation in an infinite viscoelastic medium with a periodic array of cylindrical elastic fibers”, *Journal of Sound and Vibration*, 69(2): 251-264.

82. Madan, D.K., Singh, K., Aggarwal, R., Gupta, A. (2005), “Displacements and stresses in an anisotropic medium due to non-uniform slip along a very long strike-slip fault”, *ISET Journal of Earthquake Technology*, 42(1):1-11.

83. Mindlin, R.D. (1963), “Influence of couple-stresses on stress concentration”, *Experimental Mechanics*, 3:1–7.

84. Mindlin, R.D. (1964), “Micro-structure in linear elasticity”, *Archive for Rational Mechanics and Analysis*, 16:51–78.

85. Mindlin, R.D. (1965), “Second gradient of strain and surface-tension in linear elasticity”, *International Journal of Solids and Structures*, 1:417-438.

86. Mindlin, R.D., Eshel, N.N. (1968), “On first strain-gradient theories in linear elasticity”, *International Journal of Solids and Structures*, 4:109-124.

87. Mindlin, R.D., Tiersten, H.F. (1962), “Effects of couple-stresses in linear elasticity”, *Archive for Rational Mechanics and Analysis*, 11:415–448.

88. Nayfeh, A.H., Nagy, P.B. (1997), “Excess attenuation of leaky Lamb waves due to viscous fluid loading”, *Journal of the Acoustical Society of America*, 101 (5):2649-2658.

89. Nayfeh, A.H., Nasser, S.N. (1971), "Thermoelastic waves in solids with relaxation", *Acta Mechanica*, 12:53–69.

90. Nie, G., An, Z., Liu, J. (2009), "SH-guided waves in layered piezoelectric/piezomagnetic plates", *Progress in Natural Science*, 19:811–816.

91. Novotny, O. (1999) Seismic surface waves. Lecture notes for post-graduate studies, Universidade Federal Da Bahia, Centro De Pesquisa Em Geofisica E Geologia, Salvador, Bahia.

92. Nowacki, W. (1974), "Micropolar Elasticity", International Center for Mechanical Sciences, Courses and Lectures No. 151, Udine, Springer-Verlag, Wien-New York.

93. Nowacki, W. (1986), "Theory of Asymmetric Elasticity", Pergamon Press,Oxford.

94. Osborne, M.F.M., Hart, S.D. (1945), "Transmission, reflection and guiding of an exponential pulse by a steel plate in water, I: theory", *Journal of the Acoustical Society of America*, 17: 1–18.

95. Otero, J.A., Calas, H., Ramos, R.R., Castillero, J.B., Aguiar, A.R., Monsivais, G. (2011), "Dispersion relations for SH waves on a magnetoelectroelastic heterostructure with imperfect interfaces", *Journal of mechanics of materials and structures*, 6(7-8):969-994.

96. Ottosen, N.S., Ristinmaa, M., Ljung, C. (2000), "Rayleigh waves by the indeterminate couple-stress theory", *European Journal of Mechanics-A/Solids*, 19:929–947.

97. Pagneux, V., Maurel, A. (2001), "Determination of Lamb mode eigenvalues", *Journal of the Acoustical Society of America*, 110 (3):1307-1314

98. Pathania, S., Sharma, J.N., Pathania, V., Sharma, P.K. (2010), "Generalized thermoelastic waves in anisotropic plates sandwiched between viscous liquid layers", *International Journal of Applied Mathematics and Mechanics*, 7 (5):62-88.

99. Petcher, P.A., Burrows, S.E., Dixon, S. (2014), "Shear horizontal (SH) ultrasound wave propagation around smooth corners", *Ultrasonics*, 54:997–1004.

100. Plona, T.J., Behravesh, M., Mayer, W.G. (1975), "Rayleigh and Lamb waves at liquid-solid boundaries", *Ultrasonics*, 13:171-174.

101. Qi, Q. (1994), "Attenuated Leaky Lamb Waves", *Journal of Acoustical Society of America*, 95:3222–3231.

102. Qingzeng, M.A., Jingpin, J., Ping, H.U., Xi, Z., Bin, W.U., Cunfu, H.E. (2014), "Excitation and detection of shear horizontal waves with electromagnetic acoustic transducers for nondestructive testing of plates", *Chinese Journal of Mechanical Engineering*, 27(2):428-436.

103. Ravindra, R. (1968), "Usual assumptions in the treatment of wave propagation in heterogeneous elastic media", *Pure and Applied Geophysics* 70(1):12–17.

104. Reinhardt, H.W., Dally, J.W. (1970), "Some characteristics of Rayleigh waves interaction with surface flaws", *Materials Evaluation*, 28:213-220.

105. Sahu, S.A., Saroj, P.K., Dewangan, N. (2014), "SH-waves in viscoelastic heterogeneous layer over half-space with self-weight", *Archive of Applied Mechanics*, 84:235-245.

106. Schoch V.A., (1952), "Der schalldurchgang durch platten (Sound transmission in plates)", *Acoustica*, 2:1–17.

107. Schoenberg, M. (1971), "Transmission and reflection of plane waves at an elastic–viscoelastic interface", *Geophysical Journal International*, 25:35–47.

108. Schoenberg, M. (1980), "Elastic wave behaviour across linear slip interfaces", *Journal of the Acoustical Society of America*, 68(5):1516-1521.

109. Sengupta, P.R., Benerji, D.K. (1978), "Effects of couple-stresses on propagation of waves in an elastic layer immersed in an infinite liquid", *International Journal of Pure and Applied Mathematics*, 9:17-28.

110. Sengupta, P.R., Ghosh, B. (1974a), "Effects of couple stresses on the surface waves in elastic media", *Gerlands Beitrage zur Geophysik, Leipzig*, 83:309-318.

111. Sengupta, P.R., Ghosh, B. (1974b), "Effects of couple stresses on the propagation of waves in an elastic layer", *Pure and Applied Geophysics*, 112:331-338.

112. Sengupta, P.R., Sengupta, S., Sengupta, S. (1999), "A review of some problems of elasto-dynamics under the influence of gravity", *Proceedings of the Indian National Science Academy*, 65A(2):149-166.

113. Shao, G.Z., Li, Q.C., Liang, Z.Q. (2007), "A study on dispersion curves of guided wave in layered media with overlying liquid surface", *Chinese Journal Of Geophysics*, 50(3):783-789.

114. Sharma, A., Sharma, J.N., Sharma, Y.D. (2012), "Modelling reflection and transmission of acoustic waves at a semiconductor: fluid interface", *Advances in Acoustics and Vibration*, DOI:10.1155/2012/637912.

115. Sharma, J.N., Kumar, S. (2009), "Lamb waves in micropolar thermoelastic solid plates immersed in liquid with varying temperature", *Meccanica* 44:305–319.

116. Sharma, J.N., Kumar, S., Sharma, Y.D. (2008), "Propagation of rayleigh surface waves in microstretch thermoelastic continua under inviscid fluid loadings", *Journal of Thermal Stresses*, 31:18-39.

117. Sharma, J.N., Pathania V. (2003), "Generalized thermoelastic Lamb waves in a plate bordered with layers of inviscid liquid", *Journal of Sound and Vibration*, 268:897–916.

118. Sharma, J.N., Pathania, V. (2005), "Propagation of leaky surface waves in thermoelastic solids due to inviscid fluid loadings", *Journal of Thermal Stresses*, 28:485-519.

119. Sharma, J.N., Pathania, V., Gupta, S.K. (2003), "Thermoelastic Lamb waves in a transversely isotropic plate with layers of inviscid liquid", *International Journal of Engineering Science*, 41:1219–1237.

120. Sharma, J.N., Sharma, R. (2009), "Modelling of thermoelastic Rayleigh waves in a solid underlying a fluid layer with varying temperature", *Applied Mathematical Modelling*, 33:1683–1695.

121. Sharma, J.N., Sharma, R., Sharma, P.K. (2009), "Rayleigh waves in a thermo-viscoleastic solid loaded with viscous fluid of varying temperature", *International Journal of Theoretical & Applied Sciences*, 1(2):60-70.

122. Sharma, K., Bhargava, R.R. (2014), "Propagation of thermoelastic plane waves at an imperfect boundary of thermal conducting viscous liquid/generalized thermoelastic solid", *Afrika Matematika*, 25:81–102.

123. Sharma, K., Sharma, S., Bhargava, R.R. (2013), "Propagation of waves in micropolar thermoelastic solid with two temperatures bordered with layers or half-spaces of inviscid liquid", *Materials Physics and Mechanics*, 16:66-81.

124. Sharma, S., Sharma, K., Bhargava, R.R. (2013), "Effect of viscosity on wave propagation in anisotropic thermoelastic with green-naghdi theory type-ii and type-iii", *Materials Physics and Mechanics*, 16:144-158.

125. Sharma, V.D., Ram, R., Sachdev, P.L. (1987), "Uniformly valid analytical solution to the problem of a decaying shock wave", *Journal of Fluid Mechanics*, 185:153-170.

126. Sharma, Y.D., Kumar, V. (2012), "The effect of high-frequency vertical vibration in a suspension of gyrotactic micro-organisms", *Mechanics Research Communications*, 44:40– 46.

127. Simonetti, F., Cawley, P. (2004), "On the nature of shear horizontal wave propagation in elastic plates coated with viscoelastic materials", *Proceedings of the Royal Society of London-A*, 460:2197–2221.

128. Singh, D., Tomar, S.K. (2007), "Rayleigh–Lamb waves in a microstretch elastic plate cladded with liquid layers", *Journal of Sound and Vibration* 302:313–331.

129. Singh, J., Singh, B., Ailawalia, P. (2011), "Propagation of waves at an imperfectly bonded interface between two monoclinic thermoelastic half-spaces", *Journal of Theoretical and Applied Mechanics*, 41(3):77–92.

130. Singh, K., Singh, S.J., Kumar, V. (2006), "Displacement and strain fields due to axially symmetric sources in an elastic half space in welded contact with another elastic half space", *Proceedings of the National Academy of Sciences*, 76(A)-III:209-218.

131. Sokolnikoff, I.S. (1956), "Mathematical theory of elasticity", Mc Graw Hill, New York.

132. Tanuma, K., Manb, C.S., Chen, Y. (2015), "Dispersion of Rayleigh waves in weakly anisotropic media with vertically-inhomogeneous initial stress", *International Journal of Engineering Science*, 92:63–82.

133. Toupin, R.A. (1962), "Elastic materials with couple-stresses", *Archive for Rational Mechanics and Analysis*, 11:385–414.

134. Toupin, R.A. (1964), "Theories of elasticity with couple-stress", *Archive for Rational Mechanics and Analysis*, 17:85-112.

135. Vardoulakis, I., Georgiadis, H.G. (1997), "SH surface waves in a homogeneous gradient-elastic half-space with surface energy", *Journal of Elasticity*, 47:147–165.

136. Vavva, M.G., Gergidis, L.N., Protopappas, V.C., Charalambopoulos, A., Polyzos, D., Fotiadis, D.I. (2014), "A study on Rayleigh wave dispersion in bone according to Mindlin's Form II gradient elasticity", *Journal of the Acoustical Society of America*, 135 (5):3117-3126.

137. Vavva, M.G., Protopappas, V.C., Gergidis, L.N., Charalambopoulos, A., Fotiadis, D.I., Polyzos, D. (2009), "Velocity dispersion of guided waves propagating in a free gradient elastic plates: application to cortical bone", *Journal of the Acoustical Society of America*, 125(5):3414–3427.

138. Viktorov, I.A. (1967), "Rayleigh and Lamb waves: Physical theory and applications", Plenum Press, New York.

139. Vinh, P.C., Anh,V.T.N, Thanh,V.P. (2014a), "Rayleigh waves in an isotropic elastic half-space coated by a thin isotropic elastic layer with smooth contact", *Wave Motion*, 51:496–504.

140. Vinh, P.C., Linh, N.T.K. (2012), "An approximate secular equation of Rayleigh waves propagating in an orthotropic elastic half-space coated by a thin orthotropic elastic layer", *Wave Motion*, 49:681–689.

141. Vinh, P.C., Linh, N.T.K., Anh, V.T.N. (2014b), "Rayleigh waves in an incompressible orthotropic half-space coated by a thin elastic layer", *Archives of Mechanics*, 66(3):173–184.

142. Vinh, P.C., Ogden, R.W. (2004), "Formulas for the Rayleigh wave speed in orthotropic elastic solids", *Archives of Mechanics*, 56(3):247–265.

143. Voigt, W. (1887), "Theoretische Studien über die Elastizitätsverhältnisse der Kristalle (Theoretical studies on the elasticity relationships of crystals)" Abhandlungen der Gesellschaft der Wissenschaften zu Göttingen 34.

144. Wang, L., Yuan, F.G. (2007), "Group velocity and characteristic wave curves of Lamb waves in composites: Modeling and experiments", *Composites Science and Technology* 67:1370–1384.

145. Worlton, D.C. (1961), "Experimental confirmation of Lamb waves at megacycle frequencies", *Journal of Applied Physics,* 32:967–971.

146. Wu, J., Zhu, Z. (1992), "The propagation of Lamb waves in a plate bordered with layers of a liquid", *Journal of the Acoustical Society of America,* 91:861–867.

147. Wu, X., Dzenis, Y.A. (2005), "Antiplane surface acoustic waves propagating in elastic half-space coated with an anisotropic laminate", *Composites Science and Technology,* 65:1761–1768.

148. Wu, Z., Ma, X., Brett, P.N., Xu, J. (2009), "Vibration analysis of submerged rectangular microplates with distributed mass loading", *Proceedings of the Royal Society A,* 465(2104):1323-1336.

149. Yang, F., Chong, A.C.M., Lam, D.C.C., Tong, P. (2002), "Couple stress based strain gradient theory of elasticity", *International Journal of Solids and Structures,* 39:2731-2743.

150. Yang, J.F.C., Lakes, R.S., (1982), "Experimental study of micropolar and couple stress elasticity in compact bone in bending", *Journal of Biomechanics,* 15:91–98.

151. Yang, P.S., Liu, S.W., Sung, J.C. (2008), "Transient response of SH waves in a layered half-space with sub-surface and interface cracks", *Applied Mathematical Modelling,* 32:595-609.

152. Zhu, J., Popovics, J.S., Schubert, F. (2004), "Leaky Rayleigh and Scholte waves at the fluid–solid interface subjected to transient point loading", *Journal of Acoustical Society of America,* 116(4):2101-2110.